



TECHNISCHE
UNIVERSITÄT
WIEN



DIPLOMARBEIT


Cooperative Platooning

Development and Co-Simulation-Based Validation of Distributed
Model Predictive Control Methods for Safe and Efficient
Cooperative Platooning

ausgeführt zum Zwecke der Erlangung des akademischen Grades eines
Diplom-Ingenieurs

eingereicht an der Technischen Universität Wien
Fakultät für Maschinenwesen und Betriebswissenschaft

von

Sebastian Thormann 

Matrikelnummer 01325040

unter der Leitung von

Privatdoz. Dipl.-Ing. Dr.techn. Alexander Schirrer

Univ.Prof. Dipl.-Ing. Dr.techn. Stefan Jakubek

Institut für Mechanik und Mechatronik

Wien, im Dezember 2020

Eidesstattliche Erklärung

Ich habe zur Kenntnis genommen, dass ich zur Drucklegung meiner Arbeit unter der Bezeichnung Diplomarbeit nur mit Bewilligung der Prüfungskommission berechtigt bin. Ich erkläre weiters Eides statt, dass ich meine Diplomarbeit nach den anerkannten Grundsätzen für wissenschaftliche Abhandlungen selbstständig ausgeführt habe und alle verwendeten Hilfsmittel, insbesondere die zugrunde gelegte Literatur, genannt habe. Weiters erkläre ich, dass ich dieses Diplomarbeitsthema bisher weder im In- noch Ausland (einer Beurteilerin/einem Beurteiler zur Begutachtung) in irgendeiner Form als Prüfungsarbeit vorgelegt habe und dass diese Arbeit mit der vom Begutachter beurteilten Arbeit übereinstimmt.

Ich habe die Hauptergebnisse meiner Diplomarbeit am 21. Oktober 2019 als wissenschaftliche Journal-Publikation eingereicht, welche am 30. September 2020 folgend publiziert wurde:

- S. Thormann, A. Schirrer und S. Jakubek, “Safe and Efficient Cooperative Platooning”, *IEEE Transactions on Intelligent Transportation Systems*, 2020. DOI: 10.1109/TITS.2020.3024950

Wien, im Dezember 2020

Sebastian Thormann

Kurzfassung¹

Kooperatives Platooning von Last- oder Personenkraftwägen ist im Stande die Sicherheit und Effizienz auf den Straßen zu erhöhen. Während vorausschauende aber einmalige Trajektorienplanung den Treibstoffverbrauch und die Reisezeit auf freien Straßen in der Theorie verringert, verlangt dichter Verkehr nach ständiger Anpassung dieser Pläne. Es stellt sich nun die Frage, wie durch geeignete Informierung der Einzelfahrzeugregelung dennoch ein effizientes Verhalten erreicht werden kann. Zur Beantwortung dieser Problemstellung wird in dieser Arbeit ein holistisches Regelungskonzept für kooperatives Platooning entwickelt – im Rahmen des österreichischen Leitprojekts *Connecting Austria* [2]. Dieses Regelungskonzept beinhaltet einen modellprädiktiven Regler, welcher durch den Platoon-Koordinator über effiziente und gleichzeitig fahrbare Trajektorien informiert wird. Das Konzept wird in ausgewählten Szenarien mithilfe einer eigens entwickelten Co-Simulations-Umgebung mit realitätsnaher Fahrzeugdynamik evaluiert. Die Trajektorienplanung des Platoon-Koordinators wird für zwei spezifische Szenarien, welche sich aus den Anwendungsfällen im Forschungsprojekt *Connecting Austria* [2] ergeben, formuliert und implementiert: im ersten durchfährt ein Platoon eine ampelgeregelter Kreuzung; im zweiten löst sich ein Platoon vor einer Gefahrenstelle auf.

Die Hauptergebnisse dieser Diplomarbeit wurden in der Publikation [1] mit Peer-Review im Fachjournal *IEEE Transactions on Intelligent Transportation Systems* veröffentlicht, welche vom Diplomanden unter wissenschaftlicher Anleitung der Mitautoren verfasst worden ist. Diese Publikation schlägt neuartige Methoden für die verteilte modellprädiktive Regelung von kooperativen Platoons vor. Eine Sicherheitserweiterung entkoppelt die Auslegung des Folgeverhaltens von den Sicherheitsbeschränkungen und ermöglicht kooperatives Verhalten in der Form von temporär reduzierter Bremsstätigkeit zur Reduktion der Fahrzeugabstände. Fahrkorridore, welche auf Positionsfehler bezogen sind, werden verwendet um einerseits zwischen geeigneten Regelmodi zu wechseln und um andererseits das Senden von Prädiktionen an das Folgefahrzeug auszulösen. Die vorgeschlagenen Methoden bleiben auch bei realistischen Modellfehlern effektiv, sorgen für implizite Kollisionssicherheit und reduzieren den notwendigen Kommunikationsaufwand.

¹Teile dieser Kurzfassung wurden in [1] veröffentlicht (in englischer Sprache).

Abstract²

Cooperative automotive platooning can improve safety and efficiency on the road. Look-ahead control of an entire platoon allows to reduce fuel consumption and travel time in open road scenarios, but dense traffic requires continuous adaptation of far-sighted plans. To achieve efficient individual vehicle control, these control systems need to be informed appropriately. For this purpose a holistic control concept for cooperative platooning was developed in the course of this thesis for the Austrian flagship project *Connecting Austria* [2]. This holistic control concept includes a novel model predictive controller which is informed by the platoon coordinator of permitted and at the same time efficient platooning maneuvers. The platoon safety and performance is demonstrated in selected scenarios using a custom-developed vehicle dynamics co-simulation framework. Within the developed control concept, trajectory planning is proposed to recommend scenario-specific platoon trajectories. The trajectory planning task is formulated and implemented for two scenarios stemming from use-cases defined in the project *Connecting Austria* [2]: in the first a platoon is transiting a light-controlled intersection; in the second a platoon is disbanding because of a hazardous area ahead.

The main academic results devised by the degree candidate are published in the peer-reviewed paper [1] in the journal *IEEE Transactions on Intelligent Transportation Systems*, written by the degree candidate under scientific guidance of the co-authors. This publication proposes novel methods for distributed model predictive control of cooperative platoons. A safety-extension separates safety constraints from the design of the tracking control goals and enables agreed-upon behavior in terms of temporarily limited decelerations to reduce the inter-vehicle distances. Driving corridors based on position errors are utilized to select suitable control modes or trigger prediction updates to following vehicles. The proposed measures are effective with realistic model errors, provide implicit collision safety and reduce the communication effort.

²Parts of the text in this abstract have previously been published as part of [1].

Contents

1	Introduction	1
1.1	Problem Motivation	1
1.2	Problem Statement	3
1.3	Background	4
1.3.1	The History of Platooning	4
1.3.2	Fuel Savings of Truck Platoons through Slipstreaming	6
1.3.3	Truck Platooning for Sustainable Freight Transportation	8
1.3.4	Intelligent Transportation Systems	9
1.3.5	The Impact of Platooning on Road Safety	10
1.3.6	The Basic Concept of Model Predictive Control	12
1.3.7	State of the Art of Model Predictive Platoon Control	13
1.4	Research Questions	15
1.5	Project Reference	16
1.6	Publications by the Author	17
1.7	Structure of this Work	17
2	Methodology	18
2.1	Novel Distributed Model Predictive Control Methods for Cooperative Platooning	19
2.1.1	A Generic Model Predictive Controller	19
2.1.2	Modeling of a Platooning Vehicle	20
2.1.3	Reference Tracking	23
2.1.3.1	Formulation of the Cost Function for Tracking	23
2.1.3.2	Calculation of the Position Reference Sequence	24
2.1.4	A Novel Method to Guarantee Safety	24
2.1.4.1	Fail-Safe Trajectories of Platooning Vehicles	25
2.1.4.2	Safety Extension of the Local MPC	26
2.1.4.3	Interaction Between Tracking and Fail-Safe Problems	29
2.1.4.4	Consequences in the Platoon Setting	30

Contents

2.1.5	Novel Methods to Improve Efficiency	31
2.1.5.1	Deceleration Bounds and Safe Distances	31
2.1.5.2	Braking Hold-Back Strategy to Improve Efficiency	32
2.1.5.3	Corridor-Based Reference Selection & Prediction Update	34
2.1.6	Distinction from Related Work	35
2.2	Trajectory Planning by the Platoon Coordinator	35
2.2.1	Centralized Trajectory Optimization of the Platoon	37
2.2.1.1	Modeling of the Platoon	38
2.2.1.2	Iterative Optimization Scheme	39
2.2.2	Use Case 1: TrafficLightTransit	40
2.2.2.1	Optimal Drive of the Platoon	40
2.2.2.2	Auxiliary Problems: Maximal and Minimal Drive	42
2.2.3	Use Case 2: DangerSpot	42
3	Simulation and Results	46
3.1	The Platooning Co-Simulation Framework	47
3.1.1	Basic Functioning of a Cooperative Platooning Co-Simulation Study	50
3.2	Co-Simulation Based Validation	52
3.2.1	Scenario 1: Safe Emergency Braking Capabilities	54
3.2.2	Scenario 2: Communication Loss During Active Braking Hold-Back	57
3.2.3	Evaluation of the Centralized Platooning Trajectory Optimization	58
3.2.3.1	Slow-Down when Approaching an Intersection	58
3.2.3.2	Simultaneous Start-Up at the Stopping Line	59
3.2.3.3	Platoon Dissolution at a Construction Site	61
3.2.3.4	Catch-Up for Platoon Formation	61
3.2.4	Scenario 3: Validation of Corridor-Based Situation-Aware Platoon Control with Efficient V2V Communication	66
3.3	Conclusion and Future Work	70
A	Implementation Details	82

Auf dass wir uns im Miteinander selbst erkennen dürfen!

*

May we be allowed to discern our selves within togetherness!

1 Introduction

Electronically controlling a group of vehicles in close formation, which is called *platooning*, is the main topic of this thesis. While the proposed methods and simulation approaches may be applied to automotive vehicles in general, this work concentrates in particular on platoons of heavy-duty vehicles (HDVs), as illustrated in Figure 3.5.

The outline of this introductory chapter is as follows. In Section 1.1, the problem addressed in this work is motivated and its basic context is set. The aim of this work is then defined in Section 1.2 and selected background information is presented in Section 1.3. Based on this, three research questions are formulated in Section 1.4. This chapter is concluded by the project reference of this work, the mentioning of the author's publications, and the structure of the remaining chapters in Section 1.5, 1.6, and 1.7, respectively.

1.1 Problem Motivation ¹

Safety of individual road passenger transportation is significantly lower than in passenger transportation by railway [4] and aviation [5] as pointed out in [6] for the EU and in [7] for the USA. In fact, globally, road fatalities are the leading cause of death for people aged 5-29 years according to [8]. As a result of broad efforts, the number of fatal crashes on EU roads fell remarkably until 2012, making EU roads the safest in the world [9]: with an average of 174 fatal road accidents per million inhabitants worldwide, this ratio amounts to 106 in the USA, 93 in Europe, and only 50 in the EU. [10] argues that on-board safety systems were vital to improve safety in Sweden since 1990. However, the number of crashes in the EU stagnated in recent years [9].

¹Parts of the text in this section have previously been published as part of [1].

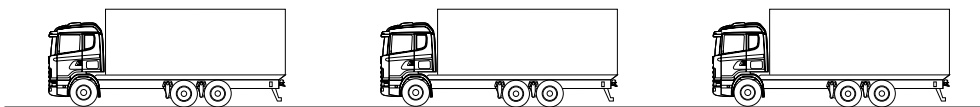


Figure 1.1: An HDV platoon of three vehicles, adapted from [3].

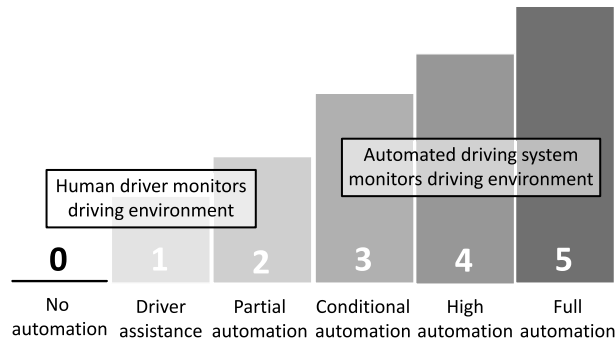


Figure 1.2: Levels of automated driving as defined in SAE 3016, taken from [15].

To further improve road safety, highly promising advanced automation technologies become available. Positive impacts of automation on safety will be visible already with a broad adoption of partial automation (SAE level 2) as argued in [11]. The organization SAE International defines automation levels (SAE levels from 0 to 5, see Figure 1.2) in [12]. At SAE level 2 the advanced driver assistance system (ADAS, see [13], [14] for a survey) executes the longitudinal and lateral dynamic driving tasks, whereby the human driver monitors the environment, supervises the dynamic driving task, and takes over immediately when required. In order to further increase traffic flow, conditional automation (SAE level 3) is deemed necessary [11], where the ADAS additionally monitors the environment and guarantees a certain lead time for the driver in case of deactivation.

The control of the longitudinal dynamics by ADAS, referred to as cruise control, is typically separated into two hierarchical levels, wherein the upper-level controller computes the desired acceleration set point for the lower-level controller which, in turn, computes the throttle input, as detailed in [16]. Adaptive cruise control (ACC) uses speed measurements of the controlled vehicle as well as measurements of the inter-vehicle distance and the relative speed with respect to the preceding vehicle to keep a certain spacing policy. Cooperative ACC (CACC) includes feed-forward information of the preceding vehicle's acceleration via V2V communication to reduce delays in detecting the acceleration, as experimentally evaluated in [17].

Grouping vehicles into closely-spaced platoons is a means to increase traffic flow and reduce fuel consumption due to aerodynamic drag reduction, as experimentally validated in [18], [19]. Aerodynamic drag reduction is especially relevant for heavy-duty vehicles (HDVs), see [20] for an overview on HDV platooning. Cooperative platooning emphasizes the aspect of communication between vehicles (V2V) and the infrastructure (V2I/I2V) to enhance predictions made by the individual vehicle and thus enable more profound control actions.

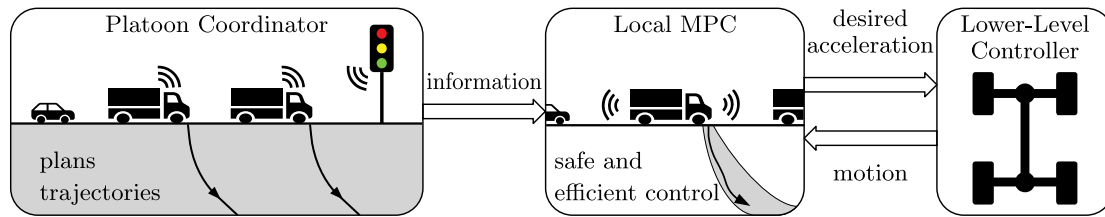


Figure 1.3: Platoon control architecture composed of the platoon coordinator, the local MPCs, and individual low level controllers.

Model Predictive Control (MPC) is a well-suited means to incorporate fuel reduction as an objective and consider safety-relevant constraints. The basic concept of MPC is to use a dynamic model to predict the behavior of the controlled system and recurrently optimize the control input in order to obtain an optimal predicted system response, as detailed in [21].

1.2 Problem Statement ²

A three-layer control architecture for cooperative platooning, as illustrated in Figure 1.3, is considered:

- The *platoon coordinator* provides planned trajectories and context information, using available traffic and platoon data.
- The *local MPC* of the individual vehicle calculates the desired acceleration based on the provided information from the platoon coordinator, local measurements, and possibly V2V communication. Thereby, the local MPC executes the longitudinal dynamic driving task of the automated vehicle.
- The *lower-level controller* tracks the desired acceleration by control of the drive train.

Aim of this work

The aim of this work is to design the local MPC of the considered control architecture based on a preferably simple model to realize distributed cooperative platooning, which guarantees safety and enhances efficiency robustly in a realistic setting.

²This problem statement is based on [1].

1.3 Background

The term platoon originally comes from the designation of a military subunit typically consisting of twelve to twenty soldiers [22]. In reference to a military platoon where the soldiers move in a row, a vehicle platoon refers to a group of vehicles that move in close formation. Usually automotive vehicles are meant, although the term is also used for aircraft [23] or watercraft [24] in the literature.

A truck platoon (or HDV platoon) is a convoy consisting of two or more trucks driving behind each other in the same direction whereby the inter-vehicle distances within the platoon are electronically controlled, as defined in [25]. In the context of control theory a platoon is also called a vehicle string, where the vehicles are typically regarded as physically uncoupled and properties of vehicle strings with infinite length are often studied. Apart from the academic use, vehicle platooning usually refers to the platooning of passenger cars or HDVs with only a few vehicles.

1.3.1 The History of Platooning

The idea of an automated highway was first presented at the World's Fair in New York in 1939. There an installation entitled Futurama and the accompanying book *Magic Highways* [26] illustrated Norman Bel Geddes vision of the future, commissioned by General Motors. Especially the concept of a network of expressways was deemed crucial to connect the nation. Even the positive effects of semi-automated driving on road capacity and road safety were part of this vision. Figure 1.4 shows a section of Futurama in which the automated highway is separated from the pedestrians walking above. The depicted platoons were supposed to be realized via automated radio control.

Until the 1990s, research on platooning has been mainly theoretical. Starting with the 1960s, attention was gained from the control community. In 1953, one of the first works regarding the dynamics of a string of vehicles [27] analyzed the movement of a string initially at rest where a simple driver model was used. An optimal control approach was proposed in 1966 in [28] where an optimal linear feedback controller is derived which regulates the positions and velocities of the platooning vehicles in a centralized fashion. One of the main topics within the control literature on platooning up to the present time, the string stability property, was originally defined in 1974 in [29] (building on the early work [30]) which is that “a string of vehicle is stable with a feedback control structure, if, for any set of bounded initial disturbances to all the vehicles, position fluctuations of all the vehicles remain bounded and these fluctuations approach zeros as time approaches infinity”.

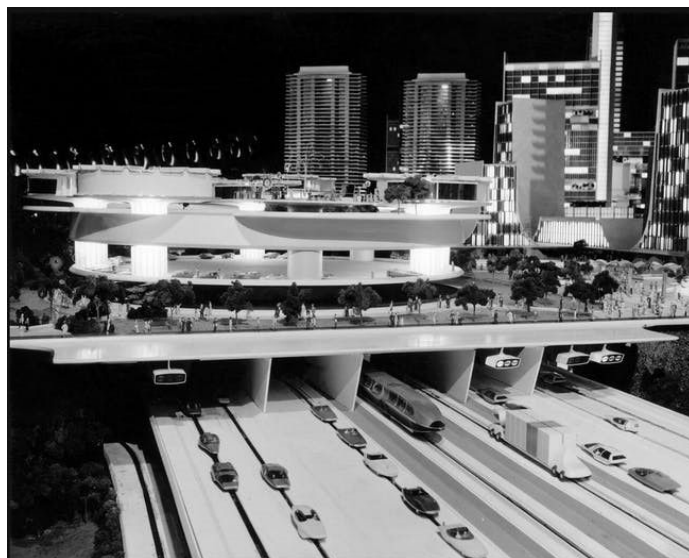


Figure 1.4: Installation at the World's Fair in 1939 named Futurama which envisions a future automated highway, taken from [26].

Starting with the 1990s, research projects and trials were conducted in the United States, Europe, Asia and Australia to evaluate the benefits and feasibility of truck platooning. Major technical progress was achieved through the partners for advanced transit and highways (PATH) program in San Diego, USA, beginning in 1986 which continues to this day. In [31], the history and major milestones of this program are outlined. The first successful vehicle-platooning experiments were conducted 1992 and a four-vehicle platoon was demonstrated for visitors in 1994. These vehicles were equipped by throttle and brake actuators, forward ranging radars, wireless LAN communication systems, and control computers. In 1997, an eight-vehicle platoon was showcased where one vehicle was able to change the position in the platoon by change of lanes, see Figure 1.5. Fully-automated HDV platooning was implemented in 2003 with a platoon of three transit buses and two tractor-trailer trucks. The fuel consumption and emission reduction potentials were experimentally investigated for inter-vehicle distances as short as 3 meters. In addition, the buses were capable of docking at bus stations. Over the course of PATH the concept of an automated highway system (AHS) was developed.

Many other research projects contributed to the public attention of truck platooning, see [32] for an informative survey. An early demonstration of truck platooning using tow-bar technology was achieved within the European project Promote Chauffeur I, as reported in 1999 in [33]. The German project KONVOI studied the impact (driver acceptance, traffic flow and environment) as well as the legal and economic implication of



Figure 1.5: Eight-car platoon demonstration of the National Automated Highway Systems Consortium in San Diego, California, in 1997 taken from [31].

platoons from 2005 to 2009, see [34]. The European SARTRE project demonstrated a platoon consisting of both passenger cars and trucks on the motorway, as stated in [35]. The recent European project COMPANION developed co-operative mobility technologies for supervised vehicle platooning from 2013 to 2016 wherein the creation, coordination, and operation of such platoons is explicitly taken into account, as presented in [36]. One of the partners in this project, the vehicle manufacturer Scania, is currently working on bringing the first HDV platoons to the market.

1.3.2 Fuel Savings of Truck Platoons through Slipstreaming

Platooning takes advantage of the unrecovered flow behind each vehicle. This phenomenon is referred to as drafting or slipstreaming, where following vehicles face a reduced air pressure, as detailed in [37]. An exemplary air velocity distribution for HDV platoons with different inter-vehicle distances is shown in Figure 1.6, which is the result of extensive Computational Fluid Dynamics (CFD) simulations. The aerodynamic drag accounts for up to one fourth of the fuel consumption of HDVs, as stated in [38], and fuel costs account to more than 35% of the operating costs of HDVs, as reported in [39]. Hence, reducing the aerodynamic drag force

$$F_{\text{drag}} = \frac{1}{2} c_{\text{drag}}(d) \rho A v^2 \quad (1.1)$$

is an essential factor for sustainable freight transport. The force F_{drag} depends on the aerodynamic drag coefficient c_{drag} , the air density ρ , the frontal area of the vehicle A ,

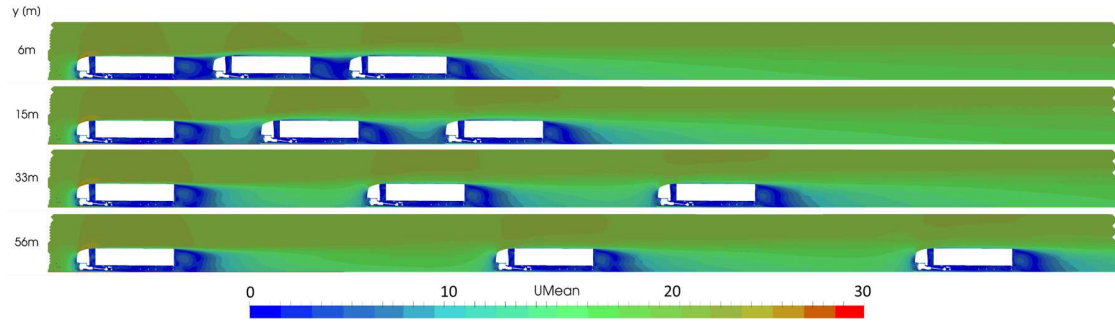


Figure 1.6: Air velocity distribution of an HDV platoon of three vehicles with varying inter-vehicle distances calculated via CFD simulations within the project Connecting Austria, adapted from [40]. Note how slipstreaming is especially pronounced for small inter-vehicle distances.

and the flow speed of the air relative to the vehicle which is approximated in (1.1) by the velocity of the vehicle v . Since the coefficient $c_{\text{drag}}(d)$ depends on the inter-vehicle distance d due to slipstreaming, platooning reduces fuel consumption significantly under ideal conditions. In [18] it was experimentally validated that drag is reduced by more than 40% for the second vehicle of an HDV platoon with two vehicles driving at 80 km/h with an inter-vehicle distance of 10 m. Similar results are reported in [19] where a reduction in fuel consumption of up to 10% is shown.

These promising results attracted great interest in HDV platooning. However, this theoretical potential is not reached under real conditions. The WABCO test runs conducted in 2017 for European type HDVs resulted in a fuel reduction of 2.8% and 7.2% for the leading and following vehicle, respectively, of a platoon of two vehicles driving at 85 km/h with an inter-vehicle spacing of 10 m, as reported in [25]. It was shown that short inter-vehicle distances under 20 m are necessary to gain (small) lead vehicle savings, while fuel savings of the following vehicle remain high even for 50 m. The author of [25] concluded that based on these results already today truck drivers are saving fuel and that getting closer does not seem to have a noticeable positive effect on the fuel savings. Tests conducted on public roads have reported the neutralization of the platooning benefits due to traffic interference and road slopes, as stated in [41]. The results of the recent German project EDDI in 2018 were obtained on highways under practical operation, which show an average fuel reduction of 1.3% and 3.5% for the leading and following vehicle, respectively, of a platoon of two vehicles driving at 80 km/h with an inter-vehicle spacing of 15 m, as reported in [42].

In conclusion, the fuel savings for HDVs purely through dense driving is small, but also not negligible when facing the high cost volume of fuel in the haulage sector.

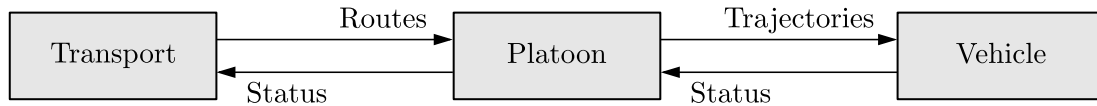


Figure 1.7: Layered freight transportation-system architecture, adapted from [20].

1.3.3 Truck Platooning for Sustainable Freight Transportation

While the resulting fuel savings through slipstreaming are small, taking a broader perspective on HDV platooning shows new opportunities for sustainable freight transportation. In recent literature, a new focus on cooperative platooning with macroscopic considerations is emerging. Exploiting preview information of the road slope, an HDV can save up to 3.5%, as experimentally validated in [38]. This is achieved by planning the velocity profile along the route with consideration of the road topography. In [43] a fuel saving potential of up to 12% compared to standard platoon control (without road slope consideration) of the following vehicles is shown. This far-sighted planning for automotive control operations with consideration of external factors is often referred to as look-ahead control. Here, efficient maneuvers are planned beforehand and are subsequently used as references for the control systems. Another variant of look-ahead control or eco-driving control is particularly relevant in urban areas where preview information on speed limits, green light phases, or surrounding traffic is exploited to plan efficient maneuvers, as presented in [44]. This methodology is closely related to green light optimal advisory (GLOSA) systems where a scalar reference velocity or a velocity profile is recommended to vehicles which approach a traffic light controlled intersection. In [45] it is shown that the application of a GLOSA system can reduce the fuel consumption as well as CO₂ emissions by up to 11.5%.

At this point it becomes apparent that platooning can be seen as a middle layer in a freight transportation system between an upper transport layer, where the distribution of goods is planned, and a lower vehicle layer, where the real-time control of individual vehicles is realized. The platoon coordinator is thus informed of the route assigned by the transport layer and, in turn, plans trajectories for the individual controlled vehicle. This concept of a layered transportation-system architecture is proposed in [20] and is illustrated here in Figure 1.7. While the broad cyber-physical system perspective taken in [20] or [46] includes the transport layer, logistical problems are not considered in this work.

1.3.4 Intelligent Transportation Systems

The novel control methods proposed below in this work (in response to the problem statement in Section 1.2) are developed with the prospect of intelligent transportation systems (ITS) wherein platooning is one component. Numerous agencies are working with ITS across the World such as, e.g. the European Road Transport Telematics Implementation Coordination Organization (ERTICO). ITS can be grouped into five categories regarding public transportation, traveler information, transportation management, transportation pricing, and automated transportation, according to [47]. An informative summary of ITS is found in [48]:

ITS aim at enhancing safety, operational performance, mobility, environmental benefits, and productivity by expanding economic and employment growth. ITS encompass the full scope of information technologies used in transportation, including control with dynamic feedback, computation and communication, as well as the algorithms, databases, models and human interfaces.

Traffic efficiency is an important aspect of ITS. The growth in road passenger and road freight transport in the European Union is estimated to increase by 30% and 55%, respectively, by 2050, as stated in [49]. Road congestion costs in the European Union are equivalent to 1% of the gross domestic product (GDP) and are predicted to increase by 50% by 2050 if no changes are made, as reported and stated in [50]. Automotive platooning is a promising means to face this future challenge. According to [51] platooning for passenger cars can potentially increase the road capacity by 200%.

Closely related to ITS is the notion of cooperative intelligent transport systems (C-ITS) where the emphasis is laid on the cooperation of multiple ITS sub-systems. The European Standards Organization ETSI standardizes V2V and V2I/I2V communication means. These standards define messages with the wireless communication protocol IEEE 802.11p and an access layer technology named ITS-G5 for the European protocol stack, as defined by ETSI EN 302 571 in [52]. By splitting the high-rate data stream into lower-rate data streams which are transmitted over a number of subcarriers, the IEEE 802.11p protocol enables the communication between high-speed vehicles and between the vehicles and the roadside infrastructure. An overview on this standard for vehicular communication is given in [53]. Two message types have to be generated by participants of C-ITS:

- Cooperative Awareness Message (CAM)
- Decentralized Environmental Notification Message (DENM)

CAMs periodically convey critical vehicle state information in support of safety and traffic efficiency application. These messages enable the tracking of vehicle movement. DENM disseminates event-triggered critical information in a geographical region.

Several infrastructure services based on vehicle-to-everything (V2X) communication are defined in ETSI TS 103 301 regarding intersection information, topology, in-vehicle information, signal control, infrastructure notification, and infrastructure awareness. These implement dedicated messages, such as the Signal Phase and Timing (SPAT) message for the intersection information service, which informs on the traffic light state and the remaining time until the traffic light changes. Harmonization of the C-ITS-based services for the release 1 (which is often referred to by the notion of the *Day 1* services) across Europe was achieved in particular through the C-ROADS project, see [54] for an Austrian perspective. Typical use cases are dynamic speed limit information or road works warnings. Note that platoon management is not included in the Day 1 services. The first platooning-related messages for Austrian C-ITS applications are defined in the ECo-AT release 4 specified in [55] of 2018 which covers the use cases

- platoon support information for automated vehicles and
- situation-based distance gap for automated vehicles.

While the C-ROADS project is concerned with the infrastructure-side harmonization of C-ITS, the CAR 2 CAR Communication Consortium takes a vehicle-centered perspective. The C-ITS services and use cases are categorized depending on their technology readiness levels in the categories:

- Day 1 (awareness driving via status data),
- Day 2 (sensing driving via sensor data), and
- Day 3+ (cooperative driving via intention and coordination data).

The C-ITS roadmap of this vehicle-centered perspective is given in [56].

However, further harmonization activities beyond Day 1 are necessary to address advanced use cases such as those covered in Section 1.3.3.

1.3.5 The Impact of Platooning on Road Safety

The impact of platooning on road safety has both positive and negative aspects. Of course, the reduction of inter-vehicle distances, which is one main goal of platooning, produces inherent safety issues regarding collisions within the platoon that need to be dealt with specifically. Therefore, the demands on the vehicle safety systems are generally higher. ACC systems with collision avoidance have been commercially available for years. However, these ADAS still depend on the human driver in complex scenarios until full automation (SAE level 5) is feasible for entire routes. The risk of accidents in situations

1 Introduction

where safety systems fail or responsibility is returned to the driver is therefore one relevant aspect of platooning safety.

In contrast, over 90% of road accidents are caused by human errors, as reported in [57] for the United States. With regard to HDV accidents on motor- and expressways in Austria, as reported by Statistik Austria for 2014-2018 and presented in [40], 62% are caused by inattention, distraction, fatigue, sleepiness, and substance impairment; 21% are caused by inadequate inter-vehicle distances or speeds; 9% are caused by right of way violations and overtaking maneuvers; only 4% are caused by technical defects. The use of ADAS can therefore make a significant contribution to road safety especially in the main application area of HDV platooning. The KONVOI project claimed to have demonstrated safe platooning in mixed traffic, but no details on the results are publicly available. “On the basis of the real traffic drives it could be shown, that a safe operation of platoons is possible.”, see [34]. However, the question arises here as to which additional advantages platooning can realize over ADAS which focus on the ego vehicle alone. The main potential lies in the interaction of cooperative platooning vehicles which enables precautionary measures in the sense of timely adjustments regarding speeds and inter-vehicle distances, as discussed in [48]. This will require corresponding test runs in the future.

In regard to HDV platooning of vehicles with driver assistance (SAE level 1) the Austrian Road Safety Board (KFV) defined a set of criteria for operation within the project Connecting Austria, as presented in [40]:

- Minimum of two lanes;
- dissolution of platoons: 1000 m ahead of tunnels, 1600 m ahead of construction sites, 1000 m ahead of hazard points such as accident black spots, 1000 m ahead of motorway junctions, motorway stations and rest areas;
- route has only bends with curve radius > 1000 m;
- sufficient length of acceleration and deceleration lanes.

According to these criteria, 43.6% of the analyzed route length (Austrian motorways) is suitable for platooning, with stretches of 3.37 km on average. The Swiss federal office for roads (ASTRA) has a similar view, according to which truck platooning is limited due to the high number of tunnels and road accesses in Switzerland, as published in [58]. From this can be concluded that only few application areas of platooning with low levels of automation exist. Mercedes-Benz Trucks has concluded in 2019 that there is no business case for truck platooning, also because of such criteria; it now plans to refocus its resources on developing autonomous, self-driving technologies in its trucks, as stated in [59].

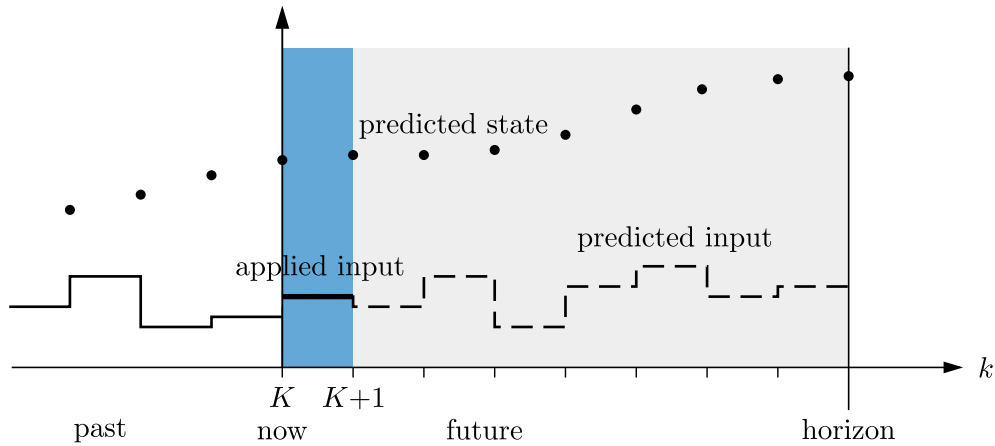


Figure 1.8: Basic concept of model predictive control in a time-discrete.

In summary, it can be said that the impact of platooning on road safety is closely related to the safety of automotive automation in general. An additional potential through cooperative platooning can be identified, but its quantity needs to be determined.

To ensure safety in the context of platoon control systems, safety-related constraints on the system states can be formulated. Model predictive control (MPC) can specifically consider and obey constraints and is thus a suitable control approach in this context.

1.3.6 The Basic Concept of Model Predictive Control

The basic concept of model predictive control (MPC) is to choose the currently applied control input based on the solution of a recurrent optimization problem, involving a dynamic model of the controlled system (the prediction model). With this optimization problem, the future input (from current time up to a specified time horizon) to the prediction model is sought, which minimizes a given cost function involving cost terms on predicted values of the inputs, states or outputs of the system while meeting given constraints. The cost function is formulated in such a way that it quantifies the attainment of specified control goals, such as accurate reference tracking or efficient actuation. Limitations of the controlled system (e.g. physical limits) or limitations of the prediction model (e.g. validity range of a linearization) are directly incorporated by the formulation of constraints. The solution of this optimization problem at one time instant is called the prediction of the MPC at this time instant.

In most cases, a time-discrete formulation is used which is illustrated in Figure 1.8. Let the current point in time be t_K . Let the running index k run from K to the prediction horizon, such that N sampling points of the future inputs u_k and future states x_k are

1 Introduction

considered each. The generic MPC problem is then to

$$\begin{aligned} & \text{minimize} && J(u_K, \dots, u_{K+N-1}, x_{K+1}, \dots, x_{K+N}) \\ & \text{such that} && \forall k \in \{K, \dots, K+N-1\}, \\ & && x_{k+1} = f(x_k, u_k), \\ & && x_{k+1} \in \mathcal{X}, \\ & && u_k \in \mathcal{U}, \\ & \text{by finding} && u_K, \dots, u_{K+N-1}, x_{K+1}, \dots, x_{K+N}, \\ & \text{given} && x_K, \end{aligned} \tag{1.2}$$

with the cost function J , the prediction model given in the form of a state transition function f , and constraints on states and inputs formulated via sets \mathcal{X} and \mathcal{U} , respectively.

In a so-called receding-horizon strategy, only the optimal value of u_K is applied as the current control input to the actual system. When transitioning to the next time step, the time horizon of the optimization problem is moved, i.e. $K \rightarrow K+1$. Hence, the names moving horizon control and MPC are often used synonymously. The model predictive controller (MPC) recurrently solves the optimization problem on-line, whereby the current measurement of the controlled system x_K is used to determine the initial conditions for the prediction model during each time step, i.e. $x_{K+1} = f(x_K, u_K)$. Thus, the arising control law depends on an assessment of the current system state x_K via the cost function J , which effectively closes the feedback-loop. Since solving the optimization problem can be arbitrarily complex depending on its mathematical structure, often linear or linearized models as well as linear or quadratic cost terms are used which leads to well-tractable optimization problems in the form of linear- or quadratic-programming problems.

1.3.7 State of the Art of Model Predictive Platoon Control³

Major challenges regarding the longitudinal control of automotive platoons include: obtaining fuel efficient behavior even in mixed traffic, dealing with partial information and communication constraints, guaranteeing safe operation, and achieving string stability. An overview on active research regarding these challenges with focus on variants of MPC is given in the following.

Look-ahead control (LAC) is an MPC variant which incorporates knowledge of future

³The text in this section has previously been published as part of the publication [1].

1 Introduction

disturbances, in particular the road topography ahead, to further reduce fuel consumption and travel time. This optimization problem is either treated in a centralized fashion as in [60] or a distributed control setting is considered where often only a single speed-profile is optimized as evaluated in [61] based on [38]. In [43] a two-layer predictive control architecture is proposed, where the upper layer (platoon coordinator) plans a single speed-profile for the distributed MPCs which guarantee safety; [62] adds gear shift management.

Distributed Model Predictive Control (DMPC) splits the overall optimization problem into local MPC problems to reduce the communication effort and computational complexity. The inherent degree of decentralization of optimal controllers for spatially invariant systems is shown in [63] and a neighbor communication scheme is derived based on this in [64], using dual decomposition. In [65] a DMPC algorithm for heterogeneous platoons with unidirectional topologies is proposed. Communication of predictions and bounds regarding the local control actions are proposed in [66] to achieve robust DMPC. In contrast, [67] argues in favor of centralized optimization based on wireless broadband communication (i.e. LTE) in real-time.

Guaranteeing the *safe operation* of a platoon requires the feasibility of a collision-free braking maneuver at any time. A simple formula for calculating the critical headway distance of a vehicle conservatively is given in [68], whereas [69] proves and implements a closed form solution of the safe inter-vehicle distance assuming a double integrator with input delay. In [70] a pursuit-evasion game is formulated to calculate safe sets of platoons considering nonlinear dynamics. In [71] it is argued that the consideration of the worst-case behavior of the predecessor in an open-loop optimal control setting (i.e. emergency braking maneuver at any time) is too conservative because all possible disturbance realizations have to be coped with. Instead, non-conservative closed-loop minimax MPC settings can be formulated, but they lead to intractable optimization problems [72]. A modified, tractable formulation is shown in [73] based on communication.

String stability is an important requirement of vehicle following control systems, where disturbances of states are not amplified along the “string” of vehicles. In fact, string instability of human-controlled vehicles can cause the emergence of traffic jams. Various definitions of string stability are proposed in literature, as discussed in [15]. Cooperative adaptive cruise control (CACC) achieves string stability even for tightly spaced platoons by including feed-forward information of the preceding vehicle’s acceleration. This is experimentally evaluated in [17] and extended with the consideration of event-triggered communication in [74]. In the DMPC setting, string stability can be enforced by explicit constraints, e.g., with respect to the amplification of accelerations as in [75], [76] or with

respect to the amplification of position errors as in [77].

1.4 Research Questions

Based on the aim of this work to design a MPC for distributed cooperative platooning (Section 1.2) and under consideration of the respective state of the art (Section 1.3.7), the following research questions are formulated.

Research questions

1. How to safely enable reduced inter-vehicle distances of a platoon based on cooperative behavior?
2. How to incorporate V2V/V2I communication to allow for situation-aware distributed control?
3. How to design a simulation framework for validation and demonstration of the elaborated platooning control concept?



Figure 1.9: Connecting Austria's cooperate design, composed from [78].

1.5 Project Reference

The holistic cooperative platooning control concept was developed within the Austrian flagship project *Connecting Austria* in the course of this thesis, see Figure 1.9 for an illustration on the project's cooperate design. Its abstract quoted from the project website [2] reads:

The flagship project Connecting Austria brings technology leaders and end-users together to demonstrate and evaluate four specific use cases for semi-automated and energy-efficient truck platoons. Key objectives is the evidence-based evaluation of energy-efficient truck platoons as a pre-requisite for competitive strength of Austrian industries such as logistics, telematics and infrastructure providers, automotive suppliers, as well as vehicle development and cooperative research.

The national flagship project's unique contribution is its specific focus on infrastructure issues and on parameterized traffic perspectives when evaluating energy-efficient and semi-autonomous truck platoons. This particularly includes platoons at intersections before entering motorways and after leaving motorways.

Connecting Austria leverages Austrian strategic strengths as pioneer in C-ITS infrastructure and continues international success stories such as ECO-AT (Austrian part of the C-ITS Corridor), co-ordination activities in C-

Roads, as well as the pioneering role in vehicle-expertise. [...]

1.6 Publications by the Author

This thesis is based on the following journal publication, which was written by the degree candidate under scientific guidance of its co-authors:

- S. Thormann, A. Schirrer, and S. Jakubek, “Safe and Efficient Cooperative Platooning,” *IEEE Transactions on Intelligent Transportation Systems*, 2020. DOI: 10.1109/TITS.2020.3024950

Two conference publications are partly based on this thesis work and were written in collaboration with the degree candidate while working on this thesis:

- A. Schirrer, T. Haniš, M. Klaučo, S. Thormann, M. Hromčík, and S. M. Jakubek, “Safety-extended Explicit MPC for Autonomous Truck Platooning on Varying Road Conditions,” *IFAC World Congress 2020*, 2020
- C. Kalteis, S. Thormann, A. Schirrer, and S. Jakubek, “Efficient Methods to Assess Linear and Non-Linear Automotive Platoon Control Stability and Performance,” *XI International Conference on Structural Dynamics*, 2020

In addition, the degree candidate participated in the editorial process of an upcoming textbook presenting the results of the project Connecting Austria:

- A. Schirrer, A. Gratzner, S. Thormann, W. Schildorfer, M. Neubauer, and S. Jakubek, Eds., *Energy-Efficient and Semi- Automated Truck Platooning*. 2021

1.7 Structure of this Work

The remainder of this thesis is structured as follows. In Chapter 2, novel distributed model predictive control methods for cooperative platooning are proposed and the use-case specific trajectory planning problems are formulated. This chapter forms the methodological basis for the treatment of the first and second research question stated in Section 1.4. In Chapter 3, a cooperative platooning simulation framework is presented which is, in turn, utilized to validate the methods and control structures proposed in Chapter 2. This chapter, as well as this thesis, is concluded by the answers to the research questions including a short discussion and possible directions for future work.

2 Methodology

A holistic concept for cooperative platoon control and its co-simulation-based validation, illustrated in Figure 2.1, was developed over the course of this thesis. Each platooning vehicle is controlled by a *local MPC*, which sets the desired acceleration of the *lower-level controller*. This MPC is specifically formulated such that a safe stop is always possible. Available information from the platoon coordinator as well as communicated predictions and agreements from the preceding and the following platooning vehicle are exploited for improved efficiency.

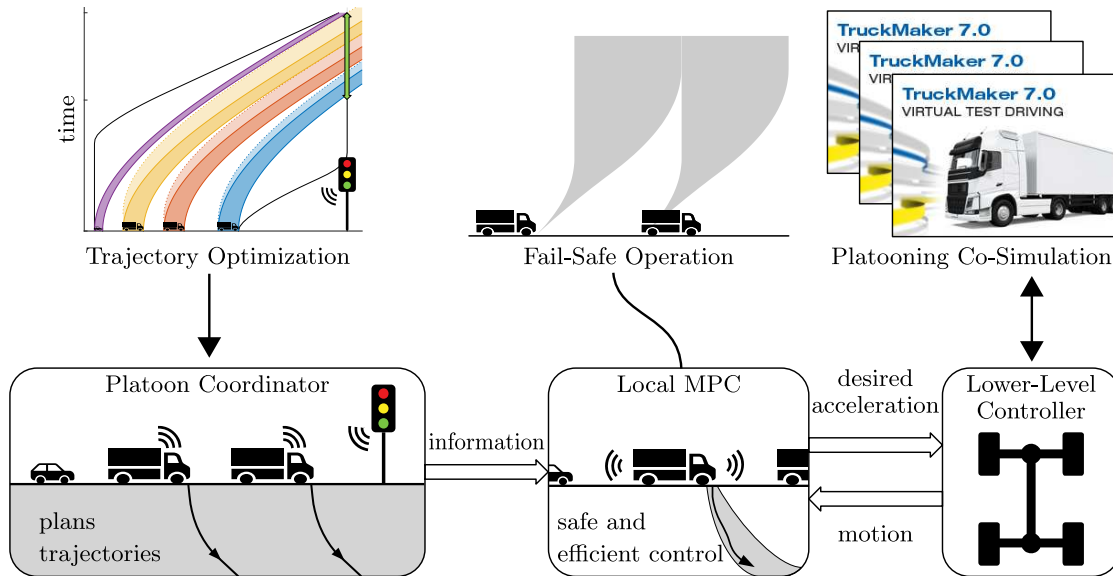


Figure 2.1: Holistic concept for cooperative platoon control.

The *platoon coordinator* is understood to be an abstract entity that issues recommendations for actions to the platooning vehicles based on additional knowledge. Given the use case of a platoon at a signaled intersection, it is assumed that the platoon coordinator receives information of the next green phase via infrastructure-to-vehicle (I2V) communication. By carrying out a centralized but simplified *trajectory optimization* where time consumption and actuation effort is minimized the platoon coordinator is able to plan and recommend efficient motion trajectories for crossing the intersection. In

turn, the local MPCs track these planned trajectories in a safe manner, enabling group maneuvers such as a simultaneous start-up.

However, the boundary conditions of such traffic optimizations are only partly known. For example, if non-platooning vehicles are present and their future behavior is uncertain, then continuous adaption of these planned trajectories is necessary. Utilizing event-triggered vehicle-to-vehicle (V2V) communication to enable cooperative behavior, the platoon efficiently adapts to the sudden presence of a non-platooning vehicle and thus realizes situation-awareness.

The proposed concepts and control structures are validated and tested by a *platooning co-simulation* of high-fidelity vehicle dynamics. While it is a pronounced goal to use simple and generic models for the design of the MPC to focus on the development of novel control methods, this simulation framework examines the control performance and robustness in a more realistic setting. Additionally, this co-simulation framework can be connected to a force-feedback wheel to experience the closed-loop platooning behavior.

2.1 Novel Distributed Model Predictive Control Methods for Cooperative Platooning¹

In this section, a local MPC for the ego vehicle is proposed which incorporates novel DMPC methods for cooperative platooning based on the stated research questions in Section 1.4.

2.1.1 A Generic Model Predictive Controller

A generic MPC is presented in the following to introduce notation used throughout this work. In this work, a discrete linear time-invariant prediction model of the state-space form

$$\mathbf{x}_{k+1} = \mathbf{A} \mathbf{x}_k + \mathbf{B} \mathbf{u}_k, \quad (2.1)$$

with state vector \mathbf{x}_k , control input vector \mathbf{u}_k , system matrix \mathbf{A} , and input matrix \mathbf{B} , is assumed. Integer number subscripts $k \in \mathbb{Z}$ refer to the sampling time instant $t = kT_S$ of the subscripted quantity throughout this work, where T_S denotes the uniform sampling time.

The recurring optimization problem is formulated from the current point in time $t_K = KT_S$ with index $K \in \mathbb{N}$ up to the control horizon t_{K+N-1} , such that the set of

¹The results presented in this section have previously been published as part of the publication [1].

$N \in \mathbb{N}^+$ sampling points,

$$\mathcal{K}(t_K) = \{K, K + 1, \dots, K + N - 1\}, \quad (2.2)$$

is considered. To shorten the notation, a future sample q_k with $k > K$ of a physical quantity q refers to its prediction $q_k := q_{k|K}$ made at t_K . Past samples with $k < K$ and the current sample q_K refer to measurements of q .

The future input values \mathbf{u}_k at the sampling points specified by $\mathcal{K}(t_K)$ are stacked into a vector, which is referred to as the input sequence

$$\mathbf{U} = \left[\mathbf{u}_K^T \quad \mathbf{u}_{K+1}^T \quad \cdots \quad \mathbf{u}_{K+N-1}^T \right]^T. \quad (2.3)$$

The current state \mathbf{x}_K is considered to be known. The future states, which are determined by \mathbf{x}_K and the future inputs \mathbf{U} via the state equation (2.9), are stacked into the state sequence

$$\mathbf{X} = \left[\mathbf{x}_{K+1}^T \quad \mathbf{x}_{K+2}^T \quad \cdots \quad \mathbf{x}_{K+N}^T \right]^T. \quad (2.4)$$

The generic MPC problem at time t_K is that of finding the optimal input sequence \mathbf{U}_* and the optimal state sequence \mathbf{X}_* minimizing the cost function J_K ,

$$(\mathbf{U}_*, \mathbf{X}_*) = \arg \min_{\mathbf{U}, \mathbf{X}} J_K(\mathbf{U}, \mathbf{X}; \mathbf{x}_K) \quad (2.5a)$$

$$\text{s.t. } \mathbf{x}_{k+1} = \mathbf{A} \mathbf{x}_k + \mathbf{B} \mathbf{u}_k, \quad \forall k \in \mathcal{K}(t_K) \quad (2.5b)$$

$$\mathbf{u}_k \in \mathcal{U}_k, \quad (2.5c)$$

$$\mathbf{x}_{k+1} \in \mathcal{X}_{k+1}, \quad (2.5d)$$

whereby only the first component in the optimal solution \mathbf{U}_* is applied to the system, according to the receding horizon principle. Problem-specific formulations of the cost function J_K , the allowed input set \mathcal{U}_k , and the allowed state set \mathcal{X}_{k+1} are defined later. The prediction model (2.5b) is defined in the following section.

2.1.2 Modeling of a Platooning Vehicle

Each vehicle (within and outside the platoon) is identified by an index $i \in \mathbb{Z}$, whereby the notation $p^{(i)}$ is used to refer to the i -th vehicle's absolute front bumper position p . Its length is denoted by $L^{(i)}$ as depicted in Fig. 2.2.

When the focus is laid on an individual vehicle (the *ego vehicle*), then its index i , the predecessor's index $i-1$, and the follower's index $i+1$, are abbreviated as ego, pre, and

2 Methodology

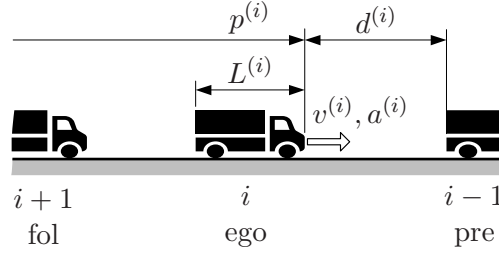


Figure 2.2: Geometric specifications of a vehicle with a follower and a predecessor.

fol, respectively. Whenever unambiguous, the ego vehicle's index is dropped throughout this work. The inter-vehicle distance between the ego vehicle and its predecessor is given by

$$d^{\text{ego}} = p^{\text{pre}} - p^{\text{ego}} - L^{\text{pre}}. \quad (2.6)$$

The longitudinal kinematics of the ego vehicle relating its position p , velocity v , and acceleration a is given by the first-order system of differential equations

$$\dot{p} = v \quad \text{and} \quad \dot{v} = a, \quad (2.7)$$

where the time derivative of a quantity p is denoted by \dot{p} .

With state vector $\mathbf{x} = [p \ v]^T$ and control input $u := a$, the state-space form of (2.7) is given by

$$\dot{\mathbf{x}} = \begin{bmatrix} 0 & 1 \\ 0 & 0 \end{bmatrix} \mathbf{x} + \begin{bmatrix} 0 \\ 1 \end{bmatrix} u. \quad (2.8)$$

A discrete-time model is obtained for uniform sampling time T_S and zero-order hold of the input u in the form

$$\mathbf{x}_{k+1} = \mathbf{A} \mathbf{x}_k + \mathbf{B} u_k. \quad (2.9)$$

Integer number subscripts $k \in \mathbb{Z}$ refer to the sampling time instant $t = kT_S$ of the subscripted quantity throughout this work.

The acceleration and the velocity of the ego vehicle is constrained by

$$a_{\min,k} \leq u_k \leq a_{\max,k} \quad (2.10a)$$

$$v_{\min} \leq v_k \leq v_{\max}, \quad (2.10b)$$

where (2.10a) could depend on the velocity (due to power constraints of the engine) and may require iterative (SQP) solution of the MPC problem.

Also, the control actions are robustified by considering dynamic restrictions of the low

2 Methodology

level controlled vehicle. For this purpose, it is assumed that acceleration a is built up through first-order dynamics (see Remark 1) with time constant $\tau \geq 0$ (a vehicle-specific tuning parameter),

$$\tau \dot{a} + a = \nu \quad (2.11)$$

and that the reference acceleration ν is bounded analogously to (2.10a), giving the dynamic constraint

$$a_{\min,k} \leq \nu_k \leq a_{\max,k}. \quad (2.12)$$

Applying the backward Euler discretization method to (2.11) yields

$$\nu_k = (1 + \alpha)u_k - \alpha u_{k-1} \quad \text{with} \quad \alpha = \tau/T_S, \quad (2.13)$$

so that (2.12) can be rewritten in terms of u_k .

Remark 1 *Ref. [16, ch 5.3] argues that low level controllers for cruise control track a desired acceleration with first-order dynamics. Ref. [81] additionally considers an input delay. In this work, no explicit model of the (uncertain) closed loop dynamics of the low level controlled vehicle is used to prevent the MPC from inverting these dynamics. However, the dynamic constraints (2.12)-(2.13) are a simple yet effective means to incorporate vehicle-specific knowledge and have been observed to robustify the control design.*

The constraints on the ego vehicle (2.10) are formulated as corresponding input/state sets

$$\mathcal{U}_{\nu,k} = \{u_k : a_{\min,k} \leq \nu_k(u_k, u_{k-1})\}, \quad (2.14a)$$

$$\mathcal{U}_{a,k} = \{u_k : a_{\min,k} \leq u_k \leq a_{\max,k}\}, \quad \text{and} \quad (2.14b)$$

$$\mathcal{X}_{v,k} = \{\mathbf{x}_k : v_{\min} \leq v_k \leq v_{\max}\}. \quad (2.14c)$$

where the virtual output ν_k is defined above in (2.13).

To clarify the notation when multiple constraints are utilized in the MPC problem, the allowed input set \mathcal{U}_k in (2.5c) respectively the allowed state set \mathcal{X}_{k+1} in (2.5d) are defined by intersecting the considered constraint sets. The constraints (2.14a) and (2.14b) are thus applied together by defining the allowed input set as $\mathcal{U}_k = \mathcal{U}_{\nu,k} \cap \mathcal{U}_{a,k}$.

2.1.3 Reference Tracking

A simple reference tracking scheme is used which serves as an interface for environment information. This information includes local distance and velocity measurements of the predecessor, recommended maneuvers provided by the platoon coordinator, and communicated predictions from the predecessor.

2.1.3.1 Formulation of the Cost Function for Tracking

Using a linear quadratic tracking objective as in [82, ch 4.4], the cost function is of the general form

$$J_K = \underbrace{\tilde{\mathbf{x}}_{K+N}^T \mathbf{P} \tilde{\mathbf{x}}_{K+N}}_{\text{terminal cost}} + \sum_{k \in \mathcal{K}(t_K)} \underbrace{(\tilde{\mathbf{x}}_k^T \mathbf{Q} \tilde{\mathbf{x}}_k + r \tilde{u}_k^2)}_{\text{stage cost}}, \quad (2.15)$$

where $\tilde{\mathbf{x}}_k$ and \tilde{u}_k generally denote the deviations from the state reference sequence $\mathbf{x}_{\text{ref},k}$ and the input reference sequence $u_{\text{ref},k}$,

$$\tilde{\mathbf{x}}_k = \mathbf{x}_k - \mathbf{x}_{\text{ref},k} \quad \text{and} \quad \tilde{u}_k = u_k - u_{\text{ref},k}. \quad (2.16)$$

The input reference is chosen here as

$$u_{\text{ref},k} \equiv 0. \quad (2.17)$$

The weighting matrices $\mathbf{P} = \mathbf{P}^T \succeq 0$ and $\mathbf{Q} = \mathbf{Q}^T \succeq 0$ (both symmetric and positive semi-definite) are chosen here as

$$\mathbf{Q} = \begin{bmatrix} q_p & 0 \\ 0 & 0 \end{bmatrix} \quad \text{and} \quad \mathbf{P} = \mathbf{0}. \quad (2.18)$$

Leaving the scalar weights $q_p \geq 0$ and $r \geq 0$ as tuning parameters. Consequently, the cost function (2.15) simplifies to

$$J_K = \sum_{k \in \mathcal{K}(t_K)} q_p (p_k - p_{\text{ref},k})^2 + r u_k^2. \quad (2.19)$$

The position reference sequence $p_{\text{ref},k}$ will be calculated in each time step based on information provided by the platoon coordinator and/or the preceding vehicle.

2.1.3.2 Calculation of the Position Reference Sequence

A strategy to formulate a suitable reference for the tracking cost function (2.19) is proposed in the following. First, it is assumed that a planned maneuver (planned trajectory) is available in the form of a position sequence $p_{\text{plan},k}$. To cope with situations which involve mixed traffic, i.e. interaction with individual non-controlled other vehicles, a desired minimal inter-vehicle distance d_{min} is defined. In addition, a default behavior characterized by a desired velocity v_{des} is applied if the planned maneuver cannot be tracked sufficiently closely and becomes invalid. Finally, available predictions of the predecessor motion are accounted for by modifying the reference sequence appropriately. The construction of the position reference sequence $p_{\text{ref},k}$ for an ego vehicle is detailed in Algorithm 1.

Algorithm 1 Construction of the Position Reference Sequence

```

1: get control mode decisions from Algorithm 2
2: if planned maneuver is executed then
3:    $p_{\text{ref},K:K+N} \leftarrow p_{\text{plan},K:K+N}$ 
4: else  $\triangleright$  execute default behavior:  $v_{\text{ref},K:K+N} := v_{\text{des}}$ 
5:    $p_{\text{ref},K} \leftarrow p_K$ ,
6:   for  $k \in \mathcal{K}(t_K)$  do
7:      $p_{\text{ref},k+1} \leftarrow p_{\text{ref},k} + T_S v_{\text{des}}$ .
8: if ego vehicle has predecessor then
9:   if communicated predecessor prediction is used then
10:     $p_{K:K+N}^{\text{pre}} \leftarrow p_{\text{com},K:K+N}^{\text{pre}}$ 
11:   else  $\triangleright$  use simple prediction:  $v_{K:K+N}^{\text{pre}} := v_K^{\text{pre}}$ 
12:   for  $k \in \mathcal{K}(t_K)$  do
13:     $p_{k+1}^{\text{pre}} \leftarrow p_k^{\text{pre}} + T_S v_k^{\text{pre}}$ .
14:   for  $k \in \mathcal{K}(t_K)$  do  $\triangleright$  “cut-off” reference
15:     $p_{\text{ref},k} \leftarrow \min(p_{\text{ref},k}, p_k^{\text{pre}} - L^{\text{pre}} - d_{\text{min}})$ ,
16: return  $p_{\text{ref},K:K+N}$   $\triangleright$  position reference sequence

```

2.1.4 A Novel Method to Guarantee Safety

In this section, a method is proposed that extends the local MPC of the ego vehicle to ensure vehicle safety with respect to emergency braking. First, the concept of fail-safe trajectories is presented. Building on this, a safety-extended MPC is proposed and its properties investigated. This formulation effectively separates the collision safety from designing the tracking control specifications. It will be shown that this concept is also helpful in fault cases such as communication loss.

2.1.4.1 Fail-Safe Trajectories of Platooning Vehicles

As a fundamental safety requirement, a safe emergency braking maneuver that brings the ego vehicle to a full stop without collision must be possible at any time. This requirement is formulated by requiring the existence of fail-safe trajectories.

Definition 1 *A trajectory $p(t \geq t_K)$ is fail-safe at time t_K , if it guides the ego vehicle to standstill at time t_{stop} , i.e.*

$$\dot{p}(t) \equiv 0, \quad p(t) \equiv p(t_{\text{stop}}) \quad \forall t \geq t_{\text{stop}}, \quad (2.20)$$

and avoids collisions for all permitted control actions of its predecessor and its follower, such that

$$\underline{p}(t) \leq p(t) \leq \bar{p}(t), \quad \forall t \geq t_K \quad (2.21)$$

holds, where $\underline{p}(t)$ and $\bar{p}(t)$ are bounding trajectories concerning the follower respectively the predecessor which fulfill

$$\underline{p}(t) \geq p^{\text{fol}}(t) + L, \quad \text{and} \quad (2.22a)$$

$$\bar{p}(t) \leq p^{\text{pre}}(t) - L^{\text{pre}}, \quad (2.22b)$$

with braking trajectories $p^{\text{fol}}(t)$, $p^{\text{pre}}(t)$ of the following an preceding vehicles, respectively.

In this work, the following two assumptions are taken:

Assumption 1 *A lower bounding trajectory concerning the predecessor $\bar{p}(t)$ fulfilling (2.22b) is known to the ego vehicle.*

A conservative choice of $\bar{p}(t)$ can be calculated via (2.7) by considering an immediate emergency braking maneuver of the predecessor with acceleration trajectory

$$a^{\text{pre}}(t) = \begin{cases} \underline{a}_{\text{min}}^{\text{pre}} & v^{\text{pre}}(t) \geq 0 \\ 0 & \text{else,} \end{cases} \quad (2.23)$$

where $\underline{a}_{\text{min}}^{\text{pre}}$ is a guaranteed lower acceleration limit of the predecessor which is known to the ego vehicle.

Assumption 2 *The follower avoids collisions with the ego vehicle, so that $\underline{p}(t) \leq p(t)$ holds in (2.21) and does not need to be considered by the ego vehicle.*

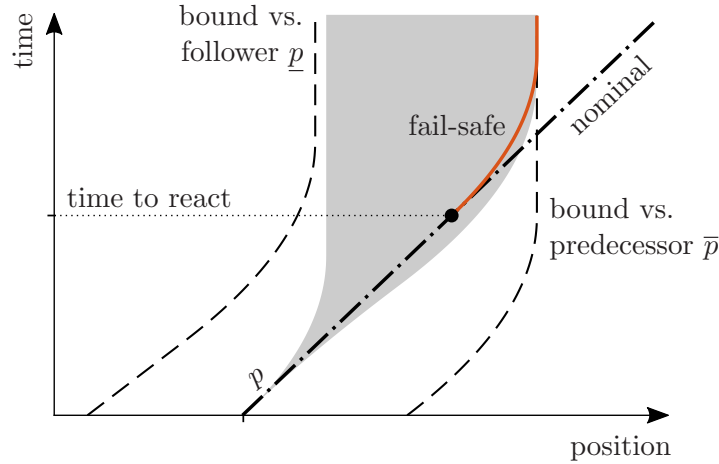


Figure 2.3: Fail-safe trajectories of the ego vehicle.

Fig. 2.3 illustrates this fail-safe trajectory concept. Fail-safe trajectories of the ego vehicle are located inside the indicated fail-safe region (gray area), which is determined by the dynamic capabilities of the ego vehicle, constrained by the bounding trajectory concerning the predecessor $\bar{p}(t)$ (dashed curve to the right of the gray area). If the ego vehicle continues to track a nominal trajectory (dash-dotted line) without state information of its predecessor and follower past the initial time, then there is a limited time left to react. From that time on, the ego vehicle would need to diverge from the nominal trajectory (at the circle-shaped marker) and apply the fail-safe trajectory (solid red curve), i.e. initiate an emergency braking maneuver, to safely avoid collision with its predecessor. These considerations constitute the basic idea of the safety-extension proposed in the following.

The non-collision requirement (2.21), given Assumption 2, is utilized to formulate the state set

$$\mathcal{X}_{p,k} = \{ \mathbf{x}_k : p_k \leq \bar{p}_k + s - d_{\text{buffer}} \}, \quad (2.24)$$

where the scalar slack variable $s \geq 0$ and the buffer distance $d_{\text{buffer}} \geq 0$ are added for practical settings to cope with model errors and uncertainties. Note that d_{buffer} tightens (negative sign) the non-collision requirement, while s softens (positive sign) it.

2.1.4.2 Safety Extension of the Local MPC

Inspired by the discussion above, a local safety-extended MPC formulation is proposed in the following which effectively separates the design of safety aspects from tracking control design through two coupled optimization problems: the (optimistic) *tracking*

problem and the (pessimistic) *fail-safe problem*.

This safety extension is illustrated in Fig. 2.4, where the optimized ego vehicle's position trajectories are shown for both problems. The tracking problem (bold solid line) is formulated as presented in Section 2.1.1 to 2.1.2 with a reference trajectory (dashed line), without considering safety aspects versus unexpected/failing behavior. In contrast, the fail-safe problem (thin solid line) only seeks to keep the ego vehicle within the fail-safe region. These two optimization problems are coupled, such that their solutions are equal during the first n_{tol} samples. Hence, at least the time period $T_{\text{tol}} = n_{\text{tol}}T_S$ would be left to react and thus diverge from the optimized trajectory of the tracking problem, which is referred to as tolerance time T_{tol} .

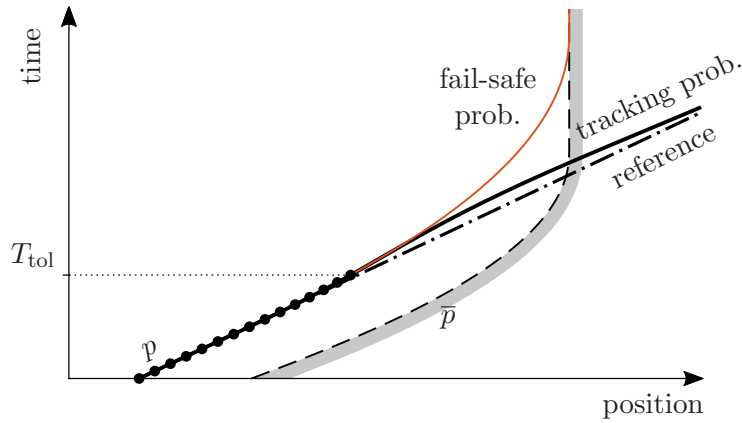


Figure 2.4: The local safety-extended MPC with tolerance time T_{tol} tracks a reference trajectory.

In Fig. 2.4 it can be seen that the long tolerance time T_{tol} (circle-shaped markers indicate coupling) forces the safety-extended MPC to initiate braking towards the end of that time period even for the tracking trajectory to retain safety. In turn, if the MPC problem is re-solved with updated neighbor information (and no emergency braking of the predecessor has occurred), then unnecessary braking will be avoided.

Technically, the augmented input (state) sequence \hat{U} (\hat{X}) is formulated by concatenating the fail-safe input (state) sequence U^{fs} (X^{fs}), such that

$$\hat{U} = \begin{bmatrix} U \\ U^{\text{fs}} \end{bmatrix} \quad \text{and} \quad \hat{X} = \begin{bmatrix} X \\ X^{\text{fs}} \end{bmatrix} \quad (2.25)$$

hold. Quantities of the fail-safe problem are denoted by the superscript fs. The coupled

2 Methodology

problem at time t_K is to solve

$$\min_{\widehat{\mathbf{U}}, \widehat{\mathbf{X}}} \left(J_K + \varepsilon J_K^{\text{fs}} + r_s s \right) \quad (2.26a)$$

$$\text{s.t. } \forall k \in \mathcal{K}(t_K), \forall j \in \{K, K+1, \dots, K+n_{\text{tol}}\}, \quad (2.26b)$$

$$\left. \begin{aligned} \mathbf{x}_{k+1} &= \mathbf{A} \mathbf{x}_k + \mathbf{b} u_k, \\ u_k &\in \mathcal{U}_k, \mathbf{x}_{k+1} \in \mathcal{X}_{k+1}, \end{aligned} \right\} \text{tracking prob.} \quad (2.26c)$$

$$\left. \begin{aligned} \mathbf{x}_{k+1}^{\text{fs}} &= \mathbf{A} \mathbf{x}_k^{\text{fs}} + \mathbf{b} u_k^{\text{fs}}, \\ u_k^{\text{fs}} &\in \mathcal{U}_k^{\text{fs}}, \mathbf{x}_{k+1}^{\text{fs}} \in \mathcal{X}_{k+1}^{\text{fs}}, \end{aligned} \right\} \text{fail-safe prob.} \quad (2.26d)$$

$$\mathbf{x}_K^{\text{fs}} = \mathbf{x}_K, u_j = u_j^{\text{fs}}, \dots \text{ coupling} \quad (2.26e)$$

$$s \geq 0, \dots \text{ slack} \quad (2.26f)$$

whereby only the optimal value of u_K is applied to the system. Here, the state/input sets can be formulated as

$$\mathcal{X}_{k+1} = \mathcal{X}_{v,k+1}, \quad (2.27a)$$

$$\mathcal{X}_{k+1}^{\text{fs}} = \mathcal{X}_{k+1} \cap \mathcal{X}_{p,k+1}, \quad (2.27b)$$

$$\mathcal{U}_k = \mathcal{U}_{a,k}, \quad (2.27c)$$

$$\mathcal{U}_k^{\text{fs}} = \mathcal{U}_{a,k} \cap \mathcal{U}_{v,k}, \quad (2.27d)$$

from the definitions in (2.14) and (2.24). The cost function in (2.26a) is composed of: the tracking term $J_K(\mathbf{U}, \mathbf{X}, \mathbf{x}_K)$ from (2.19), the shaping term $\varepsilon J_K^{\text{fs}}$, and the slack term $r_s s$. Therein, the parameter $\varepsilon \geq 0$ is chosen sufficiently small (i.e. $\varepsilon J_K^{\text{fs}} \ll J_K$), and the slack cost $r_s \geq 0$ is chosen sufficiently large.

Note that the coupled problem (2.26) is a quadratic program (QP), if the proposed quadratic cost terms (2.19), (2.28) are used and no velocity dependence for the constraints (2.10a), (2.12) is formulated.

Remark 2 *The solution of (2.26) regarding the fail-safe problem, e.g. \mathbf{U}^{fs} , is not unique in general, since multiple fail-safe position sequences p_k^{fs} may exist. Shaping can be accomplished via $\varepsilon J_K^{\text{fs}}$ with $\varepsilon > 0$ and*

$$J_K^{\text{fs}} = \sum_{k \in \mathcal{K}} \left(l_{\text{stop}}^{\text{fs}} p_k^{\text{fs}} + \left(u_k^{\text{fs}} \right)^2 \right), \quad (2.28)$$

where the weight $l_{\text{stop}}^{\text{fs}}$ affects the point in time when standstill is reached in the fail-safe

problem.

Remark 3 *Tuning for the actual vehicle dynamics and the maximal velocity is necessary for the parameters τ , d_{buffer} , q_p , r because of the idealized MPC design model (2.9). While the parameters τ and d_{buffer} are used to accommodate for model errors, the tracking behavior is determined by q_p and r . The prediction length N must be large enough so that a standstill is feasible in the fail-safe problem. Note that the concrete values of the parameters ε , r_s , and $l_{\text{stop}}^{\text{fs}}$ do not significantly affect the behavior of the safety-extended MPC.*

2.1.4.3 Interaction Between Tracking and Fail-Safe Problems

To study the interaction between the stated tracking problem and the fail-safe problem, the optimization problem of the safety-extended MPC (2.26) of the ego vehicle with the parameter values in Table 3.1 is calculated once for a varied initial inter-vehicle distance d and tolerance time T_{tol} . The position reference sequence in (2.19) is calculated via Algorithm 1, without a planned maneuver and without consideration of the predecessor. The maneuver is defined by $v_{\text{des}} = 80 \text{ km/h}$ with the ego vehicle and its predecessor in a steady motion.

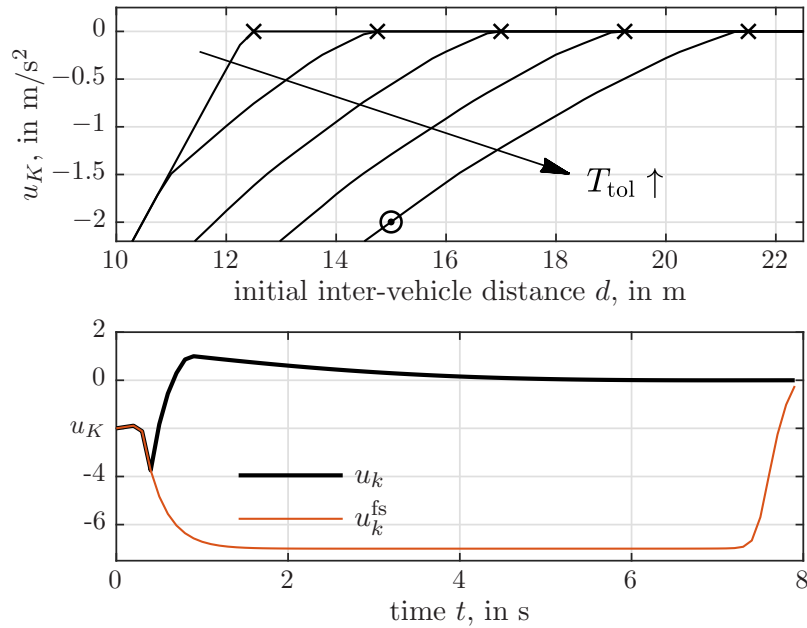


Figure 2.5: Control input u_K calculated by the safety-extended MPC for varied parameters, top. Tracking and the fail-safe trajectory for $d = 15 \text{ m}$, $T_{\text{tol}} = 0.5 \text{ s}$, bottom.

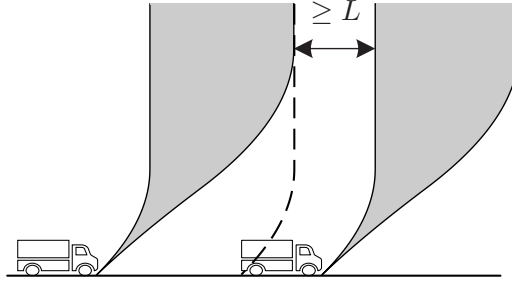


Figure 2.6: Separated fail-safe regions in the platoon setting.

In Fig. 2.5, top, five curves for $T_{\text{tol}} \in \{0.1, \dots, 0.5\text{s}\}$ depict the calculated control input u_K versus the initial inter-vehicle distance d . The interaction between the tracking problem and the fail-safe problem occurs below a parameter-dependent critical d (indicated by cross-shaped markers), which is an indicator for the achievable minimal inter-vehicle distance in steady state motion. Note that no interaction would occur for $T_{\text{tol}} = 0\text{s}$, so that $u_K = 0$ would hold independent of d .

For the parameter case $d = 15\text{m}$, $T_{\text{tol}} = 0.5\text{s}$ (indicated by the circle-shaped marker), the solution of the tracking and the fail-safe problems are shown in Fig. 2.5, bottom. The input sequences u_k and u_k^{fs} coincide from 0s to $T_{\text{tol}} = 0.5\text{s}$ because of the coupling (2.26e).

2.1.4.4 Consequences in the Platoon Setting

To extend the safety properties from the single-vehicle context to safe platooning, it will be assumed that each vehicle realizes safety with respect to its preceding vehicle (Assumption 2). Starting at the platoon leader, suitable worst-case preceding bounds of the non-platoon vehicle are required, and the leader establishes and communicates worst-case bounds of its deceleration to its follower. Each platoon vehicle, in turn, utilizes the received bounds to realize its fail-safe behavior, and transmits its own worst-case bounds to its follower.

As a result, each vehicle remains within its fail-safe trajectory region if necessary, and the fail-safe regions of different platoon vehicles are separated at least by the vehicle length, as illustrated in Fig. 2.6. Consequently, the platoon as a whole is safe with respect to the modeled worst-case scenario.

2.1.5 Novel Methods to Improve Efficiency

To improve efficiency of the local MPC control actions with respect to the global platooning objectives, systematic formulations of “agreed-upon” behavior within the platoon are developed below. First, a method to guarantee restricted decelerations and communicate these bounds within the platoon is outlined which improves platooning efficiency in terms of spacing. Second, nominal driving corridors are designed as a means to incorporate planned trajectories from the centralized platoon coordinator, efficiently switch to suitable control modes given a surrounding traffic situation and communicate predictive information only if necessary, yielding a highly flexible and efficient control architecture for situation-aware platooning.

2.1.5.1 Deceleration Bounds and Safe Distances

Studying the behavior of the safety-extended local MPC in Section 2.1.4, it becomes evident that inter-vehicle distances can be reduced if the tolerance time T_{tol} is reduced, or if the predecessor’s worst-case deceleration bounds are *increased* (i.e., if the preceding vehicle guarantees less severe deceleration) when the ego vehicle’s braking deceleration remains unchanged.

To motivate the braking hold-back strategy below, safe distances are studied in the platoon setting. The safe distance d_{safe} (cf. [69]) between two vehicles is defined as the minimum inter-vehicle distance $d(t_K)$, such that no collision occurs in the future (i.e. $t \geq t_K$) if the ego vehicle reacts appropriately to an emergency braking maneuver of the predecessor. A closed form solution of d_{safe} is presented in [69] assuming:

Assumption 3 *The relevant worst-case scenario for the ego vehicle is a simplified emergency braking maneuver wherein*

- the predecessor decelerates with $\underline{a}_{\text{min}}^{\text{pre}}$ as given in (2.23),
- the ego vehicle decelerates with \bar{a}_{min} after a delay Δ , such that

$$a(t) = \begin{cases} \bar{a}_{\text{min}} & (t \geq \Delta \wedge v(t) \geq 0) \\ 0 & \text{else} \end{cases} \quad \text{holds.} \quad (2.29)$$

Example 1 *Given a platoon of three vehicles driving at 80 km/h and given Assumption 3 holds (delay $\Delta = 0.5$ s). How to reduce the safely realizable platoon length by means of agreed-upon individual deceleration bounds $a_{\text{HB}}^{(i)}$?*

If the platoon vehicles are ordered from the weakest deceleration capabilities at the leading vehicle to the strongest possible deceleration at the platoon tail, then smaller safe inter-vehicle distances d_{safe} can be realized (cf. [70]). Therefore, the braking capabilities of the platoon leader should be limited as far as possible, such that $a_{\text{HB}}^{(1)}$ is preferably large (close to zero); the braking capabilities of the platoon tail (last vehicle of the platoon) should not be limited, such that $a_{\text{HB}}^{(3)} = \bar{a}_{\text{min}}^{(3)}$. In contrast, it is not trivial to find the optimal value of the deceleration bound for the inner vehicle $a_{\text{HB}}^{(2)}$. For this example, the resulting safe distances for a varied value of $a_{\text{HB}}^{(2)}$ are given in Table 2.1.

Table 2.1: Safe distances for a varied guaranteed bound $a_{\text{HB}}^{(2)}$. Here, $a_{\text{HB}}^{(1)} = -3 \text{ m/s}^2$ and $a_{\text{HB}}^{(3)} = -7 \text{ m/s}^2$ are used.

$a_{\text{HB}}^{(2)}$	$d_{\text{safe}}^{(2)}$	$d_{\text{safe}}^{(3)}$	$d_{\text{safe}}^{(2)} + d_{\text{safe}}^{(3)}$
-3 m/s^2	11.11 m	0.66 m	11.77 m
-4.2 m/s^2	1.3125 m	1.3125 m	2.625 m
-5 m/s^2	0.94 m	2.19 m	3.13 m
-6 m/s^2	0.75 m	5.25 m	6.00 m
-7 m/s^2	0.66 m	11.11 m	11.77 m

In Example 1, an optimal configuration is found at $a_{\text{HB}}^{(2)} = -4.2 \text{ m/s}^2$ which minimizes the total safe distance $d_{\text{safe}}^{(2)} + d_{\text{safe}}^{(3)}$ and thus the platoon length.

2.1.5.2 Braking Hold-Back Strategy to Improve Efficiency

Building on the observations above, a traffic-sensitive hold-back strategy is proposed as a means to trade braking aggressiveness against intra-platoon efficiency in real time. The basic idea of this hold-back strategy is that platooning vehicles (particularly the leader) can decide, based on the individual traffic in front of the platoon (and in consultation with the platoon coordinator), to limit (*hold-back*) their own braking capability temporarily and communicate these bounds to the followers to allow for smaller inter-vehicle distances. Note that each vehicle i in the platoon obeys an individual deceleration bound, referred to as the hold-back acceleration $a_{\text{HB}}^{(i)}$. In terms of inter-vehicle distances, it is advantageous if $a_{\text{HB}}^{(i)} > a_{\text{HB}}^{(i+1)}$ holds, as shown above in Example 1.

A platoon-wide hold-back time t_{HB} is defined as the *absolute* timestamp until which each vehicle guarantees a weaker braking action bounded by $a_{\text{HB}}^{(i)}$. It is realized via a countdown synchronously within the entire platoon, such that the limiting hold-back accelerations are guaranteed from current time t_K up to time t_{HB} . If the traffic situation

2 Methodology

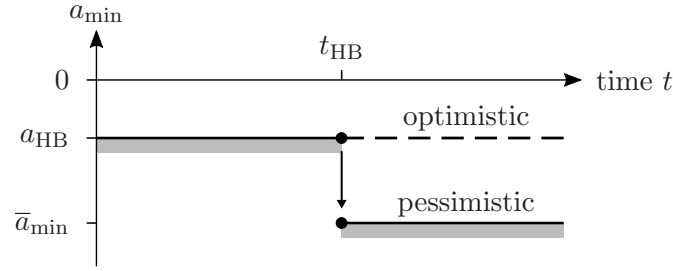


Figure 2.7: Course of the minimal agreed-upon acceleration over time of the ego and preceding vehicle, respectively, during operation of the hold-back strategy.

allows, the leader repeatedly prolongs t_{HB} via communication to the followers otherwise it elapses. Therefore the number of hold-back samples n_{HB} corresponding to t_{HB} , such that $t_{\text{HB}} = t_K + T_S n_{\text{HB}}$ holds, is locally updated from past time t_{K-1} to t_K by

$$n_{\text{HB}} \rightarrow \begin{cases} n_{\text{HB}} & \text{hold-back continued} \\ \max(n_{\text{HB}} - 1, 0) & \text{else.} \end{cases} \quad (2.30)$$

This strategy robustifies the concept against communication loss, which leads automatically to a safe expiration of the hold-back phase. Given the current value of n_{HB} , the the minimal acceleration bound $a_{\text{min},k}$ in constraint (2.14b) of the ego vehicle is defined as

$$a_{\text{min},k}^{\text{ego}} = \begin{cases} a_{\text{HB}}^{\text{ego}} & k - K < n_{\text{HB}} \\ \bar{a}_{\text{min}}^{\text{ego}} & \text{else,} \end{cases} \quad (2.31)$$

as illustrated in Fig. 2.7.

As a consequence of (2.31), the lower bound of the predecessor position $\underline{p}^{\text{pre}}(t)$ to guarantee fail-safety is changed as well, if the predecessor is part of the platoon. Instead of using the constant worst-case acceleration of the predecessor $\underline{a}_{\text{min}}^{\text{pre}}$ for the calculation of $\underline{p}^{\text{pre}}(t)$ via (2.23), the estimated sequence of the minimal acceleration

$$a_{\text{min},k}^{\text{pre}} = \begin{cases} a_{\text{HB}}^{\text{pre}} & k - K < n_{\text{HB}} \\ \underline{a}_{\text{min}}^{\text{pre}} & \text{else} \end{cases} \quad (2.32)$$

is used, similar to (2.31). This bound can be constructed by the vehicle alone even if communication to the predecessor is lost temporarily. The effects and interpretations of this hold-back scheme will be illustrated in Section 3.2.2.

2.1.5.3 Corridor-Based Reference Selection & Prediction Update

Sharing relevant information on the current traffic situation is vital to ensure high platoon control performance. In addition, it is important to avoid the transmission of unnecessary information to secure the reliability and the quality of the network, as argued in [74]. For this purpose, an efficient strategy is proposed to choose a suitable control mode (Algorithm 2) and to selectively send critical predictive information updates to follower vehicles (Algorithm 3).

For this purpose, spatial driving corridors related to the planned position sequence $p_{\text{plan},k}^{(i)}$ and the last communicated (shared) prediction sequence $p_{\text{com},k}^{(i)}$ of vehicle i are formally defined, cf. [83], as

$$\mathcal{C}_{\text{plan},k}^{(i)} = \{\mathbf{x}_k^{(i)} : |p_k^{(i)} - p_{\text{plan},k}^{(i)}| \leq \delta_p\}, \text{ and} \quad (2.33)$$

$$\mathcal{C}_{\text{com},k}^{(i)} = \{\mathbf{x}_k^{(i)} : |p_k^{(i)} - p_{\text{com},k}^{(i)}| \leq \delta_c\}, \quad (2.34)$$

where the spatial tolerances $\delta_p, \delta_c \geq 0$ are appropriately chosen.

The suitable control mode (which defines the calculation of a well-suited reference trajectory) is determined based on the ego and preceding vehicle's plan-corridors $\mathcal{C}_{\text{plan},K}^{\text{ego}}$ and $\mathcal{C}_{\text{plan},K}^{\text{pre}}$ as detailed in Algorithm 2 and consequently defines the actions taken in Algorithm 1.

A robust and efficient concept to inform a following vehicle i of the predicted actions of its predecessor $i-1$ is to send such prediction updates only selectively when the new predecessor's prediction $p^{(i-1)}$ differs significantly from its last communicated trajectory $p_{\text{com}}^{(i-1)}$. This is realized by testing if the new prediction leaves the corridor $\mathcal{C}_{\text{com}}^{(i-1)}$ which triggers the update, see Algorithm 3 for details.

Algorithm 2 Control Mode Decision

- 1: **if** $\exists p_{\text{plan},K:K+N}^{\text{ego}} \wedge \mathbf{x}_K^{\text{ego}} \in \mathcal{C}_{\text{plan},K}^{\text{ego}}$ **then**
 - 2: \triangleright planned trajectory available and valid
 - 3: decision: “execute planned maneuver”
 - 4: **else**
 - 5: decision: “execute default behavior”
 - 6: **if** $\exists p_{\text{com},K:K+N}^{\text{pre}} \wedge \mathbf{x}_K^{\text{pre}} \in \mathcal{C}_{\text{plan},K}^{\text{pre}}$ **then**
 - 7: \triangleright communicated prediction available and valid
 - 8: decision: “use communicated prediction”
 - 9: **else**
 - 10: decision: “use simple prediction”
 - 11: **return** decisions
-

Algorithm 3 Update Plan and Prediction via Communication

```

1: ▷ all quantities refer to the ego vehicle
2: if platoon coordinator updates plan then
3:   receive  $p_{\text{plan},K+1:\text{end}}$ 
4:   send  $p_{\text{com},K+1:\text{end}} \leftarrow p_{\text{plan},K+1:\text{end}}$ 
5:   if  $\exists k \in \mathcal{K} : \mathbf{x}_k \notin \mathcal{C}_{\text{com},k}$  then ▷ ego outside corridor
6:     send  $p_{\text{com},K+1:K+N} \leftarrow p_{K+1:K+N}$ 
7:     discard  $p_{\text{com},K+N+1:\text{end}}$  and  $p_{\text{plan},K+N+1:\text{end}}$ 
8:   if  $\nexists p_{\text{com},K+N+1}$  then ▷ pad communicated prediction
9:      $\Delta p \leftarrow p_{\text{com},K+N} - p_{\text{com},K+N-1}$  ▷ simple prediction
10:     $p_{\text{com},K+N+1} \leftarrow p_{\text{com},K+N} + \Delta p$ 
11: return  $p_{\text{com},K+1:\text{end}}$  and  $p_{\text{plan},K+1:\text{end}}$ 

```

Remark 4 *As will be seen in Section 3.2.4, string stability is empirically observed if sufficient predictive information of the preceding vehicle is transmitted. Additionally, it was observed that larger tolerance times improve the string stability characteristics while interactions of the tracking problem with the fail-safe problem occur, i.e., the inter-vehicle distance would fall below the safety-critical distance without the coupling (2.26e). However, it is outside the scope of this work to formally proof the string stability characteristics of this distributed MPC scheme. Further empirical string stability studies are presented in [80] in a systematic approach.*

2.1.6 Distinction from Related Work

The control architecture proposed here is similar to the one in [43], where in particular situation-awareness with regard to traffic ahead is developed. In contrast to safety constraint formulations via precomputed safe sets, as in [43], [69], or [76], here it is utilized as an extended optimization problem which enables flexible formulations of agreed-upon behavior which is exploited to allow dense spacing. The event-trigger used in [83] to selectively trigger cooperative optimization is formulated identically in this work, whereas here its integrated in a novel non-iterative optimization scheme.

2.2 Trajectory Planning by the Platoon Coordinator

To incorporate real-time infrastructure information in the distributed MPC scheme, maneuver-specific trajectory planning is used to provide recommendations for actions of the local MPC. In this work, these recommendations take the form of a planned position trajectory, a desired velocity, and a desired minimal inter-vehicle distance, as

detailed before. It is assumed that the platoon coordinator is informed about the positions and velocities of the platooning vehicles, such that the trajectory planning task can be formulated in a centralized fashion for all platooning vehicles. The transmission of recommended platooning maneuvers in the form of an explicit position trajectory serves here as a base line implementation of such an interface and may have to be adapted, for example to relative coordinates, for a suitable implementation in practice.

While the local MPC does potentially have a more detailed model of the vehicle dynamics at its disposal, the trajectory planning task of the platoon coordinator could be better informed by the infrastructure and its wider (platoon-wide) system context. This infrastructure information possibly includes speed limits, permitted inter-vehicle distances, green light information, or preview information of the road topography ahead. Additionally, the trajectory planning task is less time critical since its recommendations have only informative character. Thus trajectory planning enhances the platooning actions from a global perspective of the traffic system, while trajectory tracking control takes a local perspective of the controlled vehicle. The proposed safety extension and the corridor-based prediction update scheme ensure situation-aware actions even if the planned position trajectory is not safe or valid.

In this work, the trajectory planning task is formulated and implemented focusing on two specific platooning use cases. These use cases originate from defined use cases in the *Connecting Austria* project [2]. The trajectory planning for both use cases was implemented as a Matlab [84] functionality over the course of this thesis including a parametrization interface. Matlab is a proprietary multi-paradigm programming language and numerical computing environment developed by the Mathworks, Inc. This parametrization interface formally defines the valid domains of input parameters, serves as documentation, and provides versioning.

In the first platooning use case *TrafficLightTransit* a platoon is passing over a signaled intersection, as illustrated in Figure 2.8a. It is assumed that the platoon coordinator receives real-time information of the next green phase via infrastructure-to-vehicle (I2V) communication. By carrying out a centralized but simplified trajectory optimization where time consumption and control effort are minimized in a weighted sense the platoon coordinator is able to plan and recommend efficient motion trajectories for crossing the intersection. In turn, the local MPCs track these planned trajectories in a safe manner, enabling group maneuvers such as a simultaneous start-up.

In the second platooning use case *DangerSpot* a platoon dissolves before reaching a construction site, as illustrated in Figure 2.8b. It is assumed that the platoon coordinator is informed of the location of this danger spot and the upcoming change of the speed

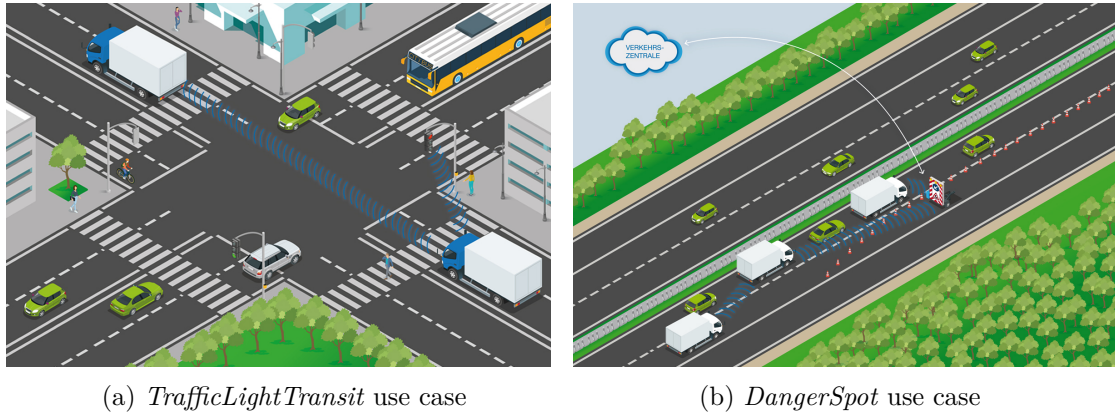


Figure 2.8: Platooning use cases originating from two use cases in the *Connecting Austria* project [2]: (a) truck platoon drives on the road approaching an intersection with traffic lights for pedestrians, prioritized public transport and other traffic participants, taken from [85]; (b) three trucks have formed a platoon and approach a hazardous location, taken from [86].

limit and permitted inter-vehicle distances sufficiently early via I2V communication. The platoon should establish these driving conditions and allow a safe hand-over to the human driver in these safe conditions. In order to allow sufficient time for the handover to the human driver, this required platoon configuration is to be maintained for a given time span before reaching the danger spot. Thus the initial and the terminal configuration of this platooning maneuver are known, so that a trajectory optimization problem for an optimal state transition can be formulated. For this optimization problem the control effort and the deviation from the terminal configuration during the handover period are minimized. Note that this platooning use case also covers generic state transition problems of the platoon including, for example, catch-up scenarios with a predefined time span, platoon dissolution before reaching a freeway exit, or the entry into a zone with a changed speed limit.

In the following, the centralized trajectory optimization problem is formulated in general and afterwards the formulation of the specific platooning use cases are detailed.

2.2.1 Centralized Trajectory Optimization of the Platoon

The centralized trajectory planning problem of the platoon coordinator can be formulated as an optimization problem, analogously to the generic MPC problem (2.5). The trajectories are planned for a platoon consisting of n vehicles, whereby the index set of

these vehicles is given by

$$\mathcal{P} = \{1, 2, \dots, n\}. \quad (2.35)$$

Solving (2.5) once with initial time t_0 at time index $K = 0$ gives the optimal input sequence \mathbf{U}_* and the optimal state sequence \mathbf{X}_* , which represent the planned trajectories for all vehicles of the platoon. The trajectories are planned from t_0 to the planning horizon t_N , such that the index set $\mathcal{K} = \{0, 1, \dots, N - 1\}$, cf. (2.2), consists of

$$N = t_N/T_S \in \mathbb{Z}^+ \quad (2.36)$$

samples.

2.2.1.1 Modeling of the Platoon

The prediction model (2.5b) for the platoon is composed of n state equations (2.9), such that

$$\underbrace{\begin{bmatrix} \mathbf{x}_{k+1}^{(1)} \\ \mathbf{x}_{k+1}^{(2)} \\ \vdots \\ \mathbf{x}_{k+1}^{(n)} \end{bmatrix}}_{\mathbf{x}_{k+1}} = \underbrace{\begin{bmatrix} \mathbf{A} & & & \\ & \mathbf{A} & & \\ & & \ddots & \\ & & & \mathbf{A} \end{bmatrix}}_{\mathbf{I}_n \otimes \mathbf{A}} \underbrace{\begin{bmatrix} \mathbf{x}_k^{(1)} \\ \mathbf{x}_k^{(2)} \\ \vdots \\ \mathbf{x}_k^{(n)} \end{bmatrix}}_{\mathbf{x}_k} + \underbrace{\begin{bmatrix} \mathbf{B} & & & \\ & \mathbf{B} & & \\ & & \ddots & \\ & & & \mathbf{B} \end{bmatrix}}_{\mathbf{I}_n \otimes \mathbf{B}} \underbrace{\begin{bmatrix} u_k^{(1)} \\ u_k^{(2)} \\ \vdots \\ u_k^{(n)} \end{bmatrix}}_{\mathbf{u}_k} \quad (2.37)$$

holds, where \mathbf{I}_n denotes the identity matrix of size n and the symbol \otimes denotes the Kronecker product.

In the following, Platoon-wide speed limits v_{\min} and v_{\max} are enforced by

$$v_{\min} \leq v_k^{(i)} \leq v_{\max}, \quad \forall i \in \mathcal{P}, \quad \forall k \in \mathcal{K}. \quad (2.38)$$

Minimal inter-vehicle distances $d_{\min}^{(i)}$ are enforced via

$$d_k^{(i)} \geq d_{\min}^{(i)}, \quad \forall i \in \mathcal{P}_{\setminus 1}, \quad \forall k \in \mathcal{K}, \quad (2.39)$$

where $\mathcal{P}_{\setminus 1}$ denotes the set of all platooning vehicles except for the first. Minimal time gaps $\Delta t_{\min}^{(i)}$ are enforced via

$$p_k^{(i-1)} - p_{k+m^{(i)}}^{(i)} \geq L^{(i-1)}, \quad \forall i \in \mathcal{P}_{\setminus 1}, \quad \forall k \in \{1, \dots, N - m^{(i)}\}, \quad (2.40)$$

where the number of shifted samples $m^{(i)}$ is given by

$$m^{(i)} = \frac{\Delta t_{\min}^{(i)}}{T_S} \in \mathbb{N}. \quad (2.41)$$

Optionally, a predictively known trajectory $p_k^{(0)}$ of a non-platooning vehicle with index $i=0$ preceding the platoon is considered. In this case the index set \mathcal{P} in (2.39)–(2.40) is modified to account for this additional vehicle, such that $\mathcal{P} = \{0, 1, \dots, n\}$ holds.

Note that no explicit formulation of the allowed input set \mathcal{U}_k in (2.5c) and the allowed state set \mathcal{X}_{k+1} (2.5d) is given throughout Section 2.2.1 to simplify the notation of the described constraints.

To plan useful trajectories for maneuvers over wide velocity ranges, individual velocity-dependent upper acceleration bounds $a_{\max}^{(i)}$ (and constant lower acceleration bounds $a_{\min}^{(i)}$) are formulated, such that a non-linear input constraint,

$$a_{\min}^{(i)} \leq u_k^{(i)} \leq a_{\max}^{(i)} \left(v_k^{(i)} \right), \quad \forall i \in \mathcal{P}, \quad \forall k \in \mathcal{K}, \quad (2.42)$$

is enforced, cf. (2.10a). Thus, a non-linear optimization problem arises.

2.2.1.2 Iterative Optimization Scheme

In contrast to the safety-extended MPC problem (2.26) being a quadratic program with linear constraints (QP), a sequential quadratic programming (SQP) method is used to deal with the non-linear acceleration constraint (2.42).

Assuming the function $a_{\max}^{(i)}(v)$ to be monotonously decreasing, a simple bound update scheme is sufficient where a sequence of QPs with iteration index j is solved. The constraint (2.42) is reformulated with time-dependent bounds as in (2.10a), such that

$$a_{\min,k}^{(i)} \leq j u_k^{(i)} \leq j a_{\max,k}^{(i)} \quad (2.43)$$

is enforced at j . Iterating from j to $j+1$, the bound is updated by

$${}_{j+1} a_{\max,k}^{(i)} = a_{\max}^{(i)} \left(j v_k^{(i)} \right), \quad (2.44)$$

whereby the initial value at $j=0$ is given by

$${}_0 a_{\max,k}^{(i)} = a_{\max}^{(i)}(v_0^{(i)}). \quad (2.45)$$

Note that (2.43)–(2.45) are enumerated over $i \in \mathcal{P}$ and $k \in \mathcal{K}$.

The iteration is terminated if the condition on the absolute error

$$\epsilon = \sqrt{\sum_{k \in \mathcal{K}} \left(j_{+1} a_{\max, k}^{(i)} - j a_{\max, k}^{(i)} \right)^2} \leq \bar{\epsilon}, \quad (2.46)$$

is fulfilled, where $\bar{\epsilon} = 0.1 \text{ m/s}^2$ is chosen.

In the following use case descriptions, the iteration index j is suppressed to simplify the notation. Except for the acceleration constraint (2.42), the trajectory planning problem remains a QP.

2.2.2 Use Case 1: TrafficLightTransit

An *optimal drive* is being sought, which leads the platoon over the intersection with efficient control actions and at the same time as early as possible during the green phase of the traffic light, as illustrated in Figure 2.9. Additionally, two auxiliary optimization problems are formulated. The *maximum drive* is the fastest possible trajectory of the platoon leader at any time until the beginning of the green phase, so that the traffic light is not run over. The *minimum drive* is the slowest possible trajectory of the platoon tail (last vehicle of the platoon) at any time until the end of the green phase, so that the traffic light is reached at latest. These trajectories are then used to formulate appropriate constraints for the optimal drive problem.

Next, the main problem of finding the optimal drive of the platoon is formulated which depends on the auxiliary problems. These are formulated afterwards.

2.2.2.1 Optimal Drive of the Platoon

The cost function of the optimal drive problem J is formulated as

$$J = w_t J_t + w_u J_u, \quad (2.47)$$

$$J_t = -\frac{1}{v_{\max}} \sum_{i \in \mathcal{P}} p_N^{(i)}, \quad (2.48)$$

$$J_u = \mathbf{U}^T \mathbf{U}, \quad (2.49)$$

where J_t is an assessment of the time efficiency, J_u are costs regarding the actuation effort, and the respective weighting parameters are given by w_t and w_u .

The velocities at the planning horizon $v_N^{(i)}$ are optionally constrained to reach the

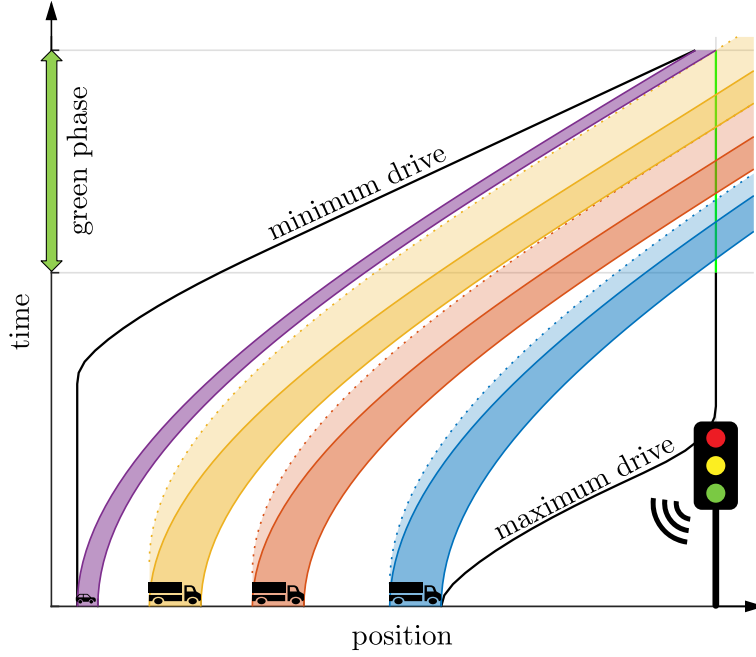


Figure 2.9: Trajectory planning for a platoon transiting a traffic light controlled intersection. The occupied space of each vehicle is depicted by individual colored faces whereby the lighter areas refer to the demanded time gaps which are velocity-dependent. Note that the minimum drive of the platoon tail is depicted here by the corresponding rear end position trajectory for illustrative reasons, in contrast to the definition given in (2.53).

uniform terminal velocity v_{end} , such that

$$v_N^{(1)} = v_N^{(2)} = \dots = v_N^{(n)} = v_{\text{end}} \quad (2.50)$$

holds.

The green time of the traffic light from t_{green} to t_{red} with the corresponding number of samples

$$N_{\text{green}} = \frac{t_{\text{green}}}{T_S} \in \mathbb{N} \quad \text{and} \quad N_{\text{red}} = \frac{t_{\text{red}}}{T_S} \in \mathbb{N} \quad (2.51)$$

is respected by using the maximal drive trajectory $p_{\text{MAX},k}$ and the minimal drive trajectory $p_{\text{MIN},k}$ from the solution of the auxiliary optimization problems (which are outlined afterwards). The position of the leader $p_k^{(1)}$ is thus bounded by

$$p_k^{(1)} \leq p_{\text{MAX},k}, \quad \forall k \in \{1, \dots, N_{\text{green}}\}, \quad (2.52)$$

while the position of the platoon tail $p_k^{(n)}$ is bounded by

$$p_k^{(n)} \geq p_{\text{MIN},k}, \quad \forall k \in \{1, \dots, N_{\text{red}}\}. \quad (2.53)$$

2.2.2.2 Auxiliary Problems: Maximal and Minimal Drive

In contrast to the optimal drive problem, the maximal and the minimal drive problem include only a single vehicle – the leader respectively the platoon tail. Moreover, the planning horizon t_N is changed to the end of the green light phase, such that $N := N_{\text{red}}$ and $t_N := t_{\text{red}}$ holds for these problems.

The cost function of the maximal drive problem J_{MAX} is formulated as

$$J_{\text{MAX}} = - \sum_{k=1}^N w_k p_k, \quad w_k = \begin{cases} 1 & k \in \{1, 2, \dots, N_{\text{green}}\} \\ w_{\text{reg}} & \text{else,} \end{cases} \quad (2.54)$$

where the small-valued weighting parameter w_{reg} for regularization is chosen as $w_{\text{reg}} = 10^{-6}$. The cost function of the minimal drive problem J_{MIN} is formulated as

$$J_{\text{MIN}} = \sum_{k=1}^N p_k. \quad (2.55)$$

Note that these cost functions are linear, so that the auxiliary problems are linear programs (LPs).

In both problems, the considered vehicle i , i.e. $i=1$ for maximal drive and $i=n$ for minimal drive, does not pass the stopping line p_{stop} before the traffic light switches to green, via enforcing

$$p_k^{(i)} \leq p_{\text{stop}}, \quad k \in \{1, \dots, N_{\text{green}}\}, \quad (2.56)$$

but reaches p_{stop} at least at the planning horizon N , via enforcing

$$p_N^{(i)} \geq p_{\text{stop}}. \quad (2.57)$$

2.2.3 Use Case 2: DangerSpot

In planning maneuvers for the *DangerSpot* use case, an efficient transition from the initial to a demanded final platoon configuration at the danger spot position p_{danger} is being sought, as illustrated in Figure 2.10. This configuration is defined by the uniform platoon velocity for manual driving v_{man} and the demanded hand-over inter-vehicle distances $d_{\text{man}}^{(i)}$. In addition, this demanded platoon configuration should already be

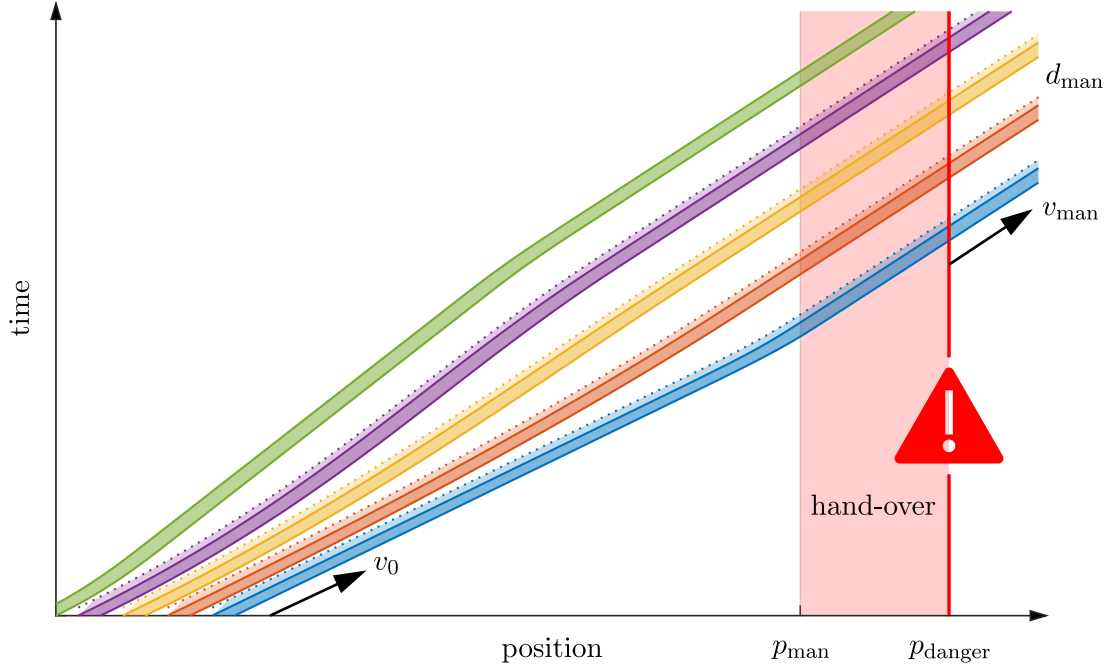


Figure 2.10: Trajectory planning for a platoon approaching a danger spot at p_{danger} , enabling a handover to the human driver with given velocities v_{man} and distances d_{man} .

kept a given hand-over period T_{man} before reaching p_{danger} .

Assuming that the velocity during the handover period T_{man} is kept constant at v_{man} , the handover distance Δp_{man} is given by

$$\Delta p_{\text{man}} = v_{\text{man}} T_{\text{man}}. \quad (2.58)$$

Thus the handover starts for every vehicle at the handover position

$$p_{\text{man}} = p_{\text{danger}} - \Delta p_{\text{man}}. \quad (2.59)$$

Since the point in time where a platooning vehicle reaches p_{man} is solution dependent, a conservative approximation assuming the vehicle drives at the speed limit v_{max} from its initial position $p_0^{(i)}$ to the handover position p_{man} is used to formulate the period of tracking of the demanded platoon configuration, such that the tracking time instants are given by

$$t_{\text{track}}^{(i)} = (p_{\text{man}} - p_0^{(i)}) / v_{\text{max}}, \quad \forall i \in \mathcal{P}. \quad (2.60)$$

2 Methodology

These tracking time instants correspond to the indices

$$k_{\text{track}}^{(i)} = \left\lfloor \frac{t_{\text{track}}^{(i)}}{T_S} \right\rfloor, \quad (2.61)$$

with sampling time T_S . Note that the floor function $\lfloor \cdot \rfloor$ is used for approximation. The index set of samples to track the demanded platoon configuration $\mathcal{K}_{\text{track}}^{(i)}$ of vehicle i is thus given by

$$\mathcal{K}_{\text{track}}^{(i)} = \left\{ k_{\text{track}}^{(i)}, \dots, N \right\}. \quad (2.62)$$

The demanded inter-vehicle distances $d_{\text{man}}^{(i)}$ for manual driving are given by the more restrictive demand of the two demands: respecting minimal time gaps $\Delta t_{\text{man}}^{(i)}$ and respecting minimal inter-vehicle distances $d_{\text{man,min}}^{(i)}$; such that

$$d_{\text{man}}^{(i)} = \max \left(v_{\text{man}} \Delta t_{\text{man}}^{(i)}, d_{\text{man,min}}^{(i)} \right), \quad \forall i \in \mathcal{P} \quad (2.63)$$

holds.

The cost function J of the *DangerSpot* trajectory optimization problem is formulated as

$$J = w_v J_v + w_d J_d + w_u J_u \quad (2.64)$$

with the tracking costs regarding the velocity

$$J_v = \frac{1}{v_{\text{scale}}^2} \sum_{i \in \mathcal{P}} \left(\sum_{k \in \mathcal{K}_{\text{track}}^{(i)}} \left(v_k^{(i)} - v_{\text{man}} \right)^2 / N_{\text{track}}^{(i)} \right), \quad (2.65)$$

the tracking costs regarding the inter-vehicle distances

$$J_d = \frac{1}{d_{\text{scale}}^2} \sum_{i \in \mathcal{P}} \left(\sum_{k \in \mathcal{K}_{\text{track}}^{(i)}} \left(d_k^{(i)} - d_{\text{man}} \right)^2 / N_{\text{track}}^{(i)} \right), \quad (2.66)$$

and the costs regarding the actuation effort

$$J_u = \frac{1}{u_{\text{scale}}^2 N} \mathbf{U}^T \mathbf{U}. \quad (2.67)$$

These cost terms are weighted by the respective weighting parameters w_v , w_d , and w_u as well as related to the individual number of tracked samples $N_{\text{track}}^{(i)} = \left| \mathcal{K}_{\text{track}}^{(i)} \right|$ and the

2 Methodology

number of overall samples N . Additionally, a scaling is used, such that each cost term is dimensionless and the cost terms are of comparable value. The dimensioned scales v_{scale} , d_{scale} , and u_{scale} define comparable values of the quantities velocity, distance, and acceleration, respectively.

A terminal constraint is used to ensure that the demanded platoon configuration is attained at least at the planning horizon t_N . Therefore, first the platoon tail has to pass the danger spot at p_{danger} via enforcing

$$p_N^{(n)} \geq p_{\text{danger}}. \quad (2.68)$$

Second, the platoon has to reach the demanded velocity v_{man} via enforcing

$$v_N^{(i)} = v_{\text{man}}, \quad \forall i \in \mathcal{P}. \quad (2.69)$$

Third, the platoon has to reach the demanded inter-vehicle distances $d_{\text{man}}^{(i)}$ via enforcing

$$d_N^{(i)} = d_{\text{man}}^{(i)}, \quad \forall i \in \mathcal{P}. \quad (2.70)$$

Exemplary results of these trajectory optimization problems are presented and discussed within the following chapter in Section 3.2.3. Next, the co-simulation-based validation approach is presented.

3 Simulation and Results

In this chapter, the methods proposed in this work are implemented and tested in a custom-developed co-simulation framework via Matlab [84] and individual trucks simulated by the simulation software Truckmaker [87] developed by IPG Automotive GmbH, see Figure 3.3. Truckmaker simulates detailed vehicle dynamics including multi-body dynamics of masses and chassis, as well as parameterized gear box, clutch, engine, and tire component models. Especially the drive train dynamics, the occurring dead times (different in acceleration vs. braking operation), as well as the dynamic response of the entire powertrain to acceleration / braking signals deviate significantly from the idealized MPC design model (2.9).

While this co-simulation-based validation approach is an appropriate means to put the robustness of the proposed control methods under realistic vehicle dynamics to test, it also serves for the purpose of demonstration. The co-simulation can be connected to a force-feedback steering wheel, making it possible to experience platoon behaviour in traffic.

Next, the implementation of the co-simulation framework is detailed. Afterwards, the results of the co-simulation-based validation are presented and finally the stated research questions are answered.

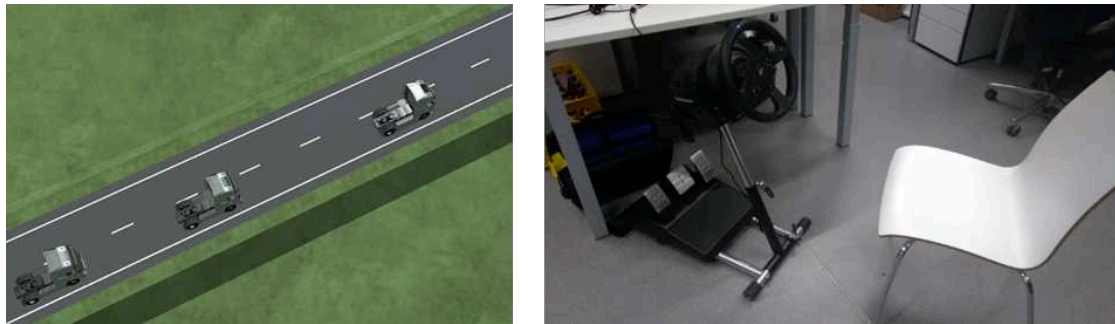


Figure 3.1: Demonstration of the proposed control methods using a force-feedback steering wheel.

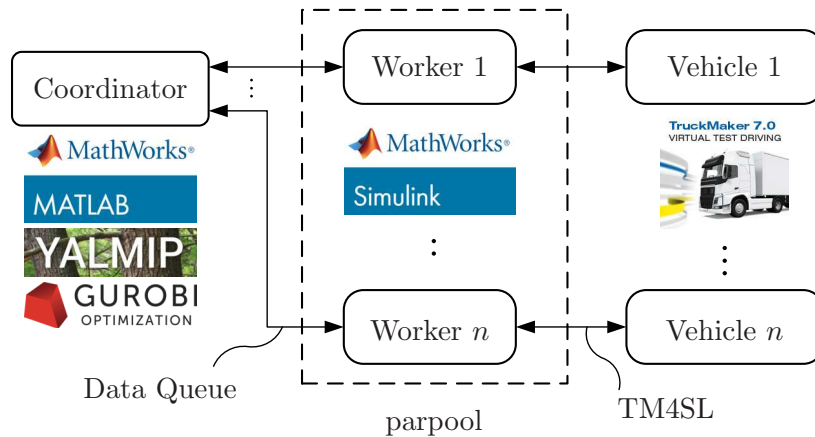


Figure 3.2: Software architecture of the co-simulation framework.

3.1 The Platooning Co-Simulation Framework

Since Truckmaker does (currently) not support the simulation of multiple vehicles, a custom-developed solution based on parallel computing is used to implement the simulation of the platoon dynamics. In addition, this approach enables decoupled development of the applied optimization problems. Simulating a coupled problem in a distributed manner while exchanging data between the simulation subsystems is referred to as *co-simulation*, as surveyed in [88].

The software architecture of the implemented co-simulation framework is illustrated in Figure 3.2. The methods and simulation studies developed in this work are implemented primarily in Matlab. Multiple instances of Truckmaker are coordinated by a central Matlab session (the coordinator), which establishes global time stepping. Also the optimization problems due to MPC and trajectory planning are managed by the central session and preferably solved by Gurobi [89] developed by Gurobi Optimization, LLC. Note that other solvers may as well be used with minor interface adaptations, but Gurobi has proven to be particularly suitable and is thus applied as the primary solver in this work. Real-time computation of the co-simulation including the MPC control computations is feasible for several trucks.

To experience the closed-loop platooning behavior, one of the platooning vehicles (the ego vehicle) can be manually driven by means of a force-feedback wheel. By running the prepared demo case

- `root/010_base/_run/run_showcase.m`

via Matlab, the user can drive the ego vehicle within a platoon on a round course which is shown in Figure 3.3. The user operates the demo run by means of the force-feedback

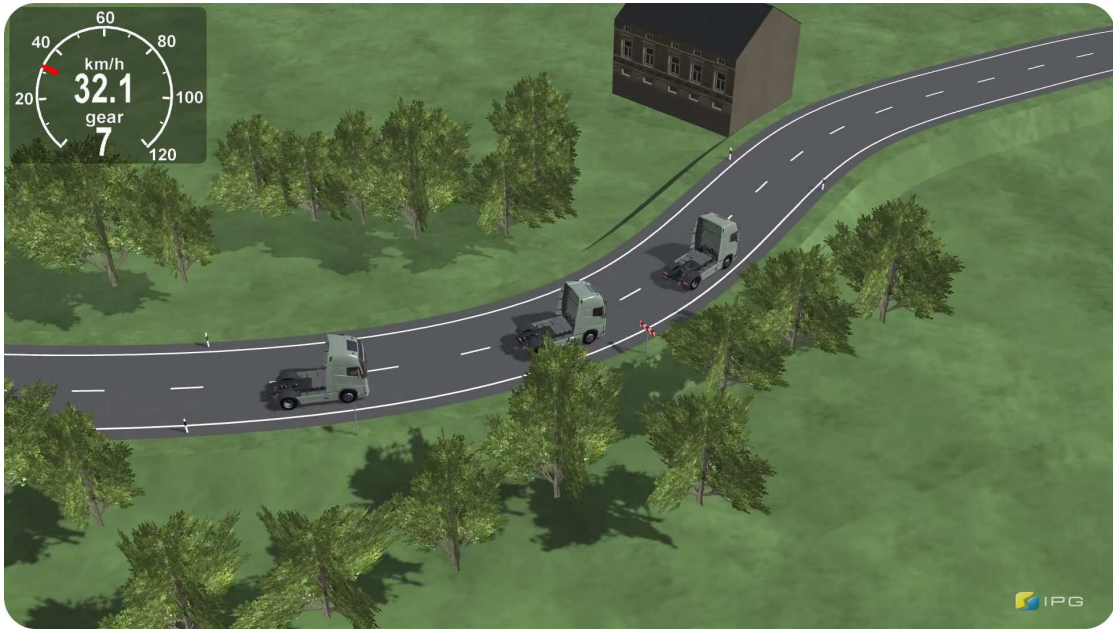


Figure 3.3: Platooning demonstration co-simulation show case of a truck platoon driving on a round course (screenshot taken from Truckmaker).

wheel of type Thrustmaster T300 RS, as shown in Figure 3.4:

- By operating the left and right wing buttons, the user can switch between automatic and manual driving mode, respectively. In automatic mode, the longitudinal dynamic driving task of the ego vehicle is executed by the safety-extended MPC proposed in this work and the lateral dynamic driving task is executed by a default controller supplied by Truckmaker. In manual mode, the user executes both driving tasks by means of the steering wheel, the gas pedal, and the brake pedal. Note that shifting is not necessary, since a vehicle with automatic gearbox is used.
- The distributed MPC is executing the default maneuver, which includes a desired velocity v_{des} and a desired minimal inter-vehicle distance d_{min} , as presented in Section 2.1.3.2. By operating the buttons \triangle and \times , the desired velocity v_{des} can be increased and decreased, respectively. By operating the buttons \square and \circ , the desired minimal inter-vehicle distances d_{min} can be increased and decreased, respectively.

The methods and simulation studies implemented are grouped into the following modules:

TruckmakerPlatoonSimulation manages the distributed co-simulation of the platoon

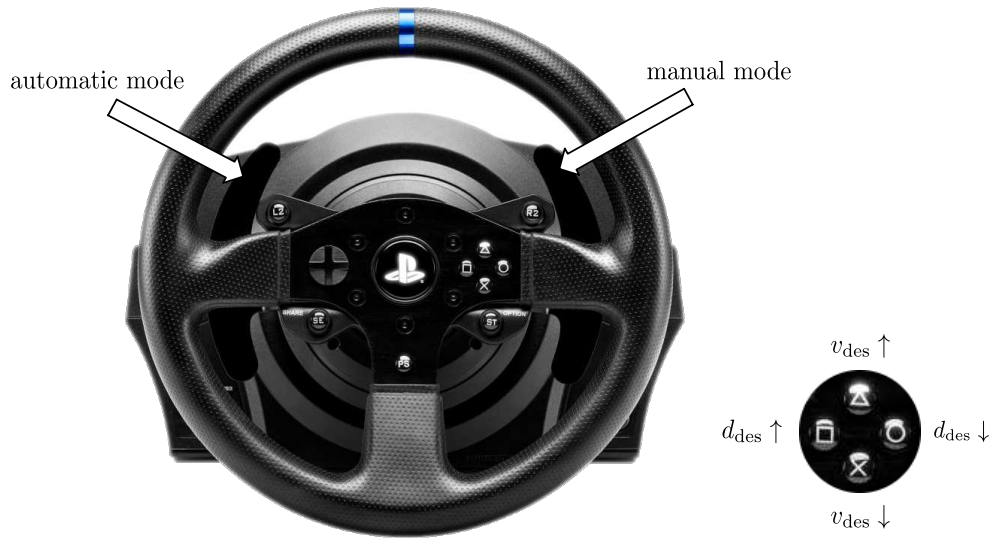


Figure 3.4: Operation of the platooning show case by means of the Thrustmaster T300 RS force-feedback steering wheel, composed from [90].

dynamics. The interface between Matlab and Truckmaker is realized via a dedicated Simulink [91] model provided by Truckmaker for Simulink (TM4SL) which is included in Truckmaker and a custom-developed interface using asynchronous function calls, as shown in Figure 3.2. Simulink is a Matlab-based graphical programming environment for modeling, simulating and analyzing multidomain dynamical systems developed by the Mathworks, Inc. These Simulink models are simulated by parallel computing on Matlab parallel pool workers (the Matlab parpool). The main Matlab class in this module is called `SysPlatoon`.

SafeMPC implements the novel methods for distributed model predictive platoon control formulated in Section 2.1. The corresponding computations are carried out by the central Matlab session. To formulate and solve the MPC problems, the Matlab toolbox Yalmip [92] developed by Johan Löfberg and the solver Gurobi have been applied. The main Matlab class in this module is called `SafeMPC`.

TrafficLightTransit/DangerSpot implements the trajectory optimizations regarding the *TrafficLightTransit/DangerSpot* use case formulated in Section 2.2/2.2. The optimization problems are purely formulated in Matlab and are either solved by Gurobi or directly within Matlab (by a solver named quadprog). A parameterization interface is implemented to support large-scale parameter studies. This interface provides inherent plausibility checks and versioning of the input and output data. The main Matlab class in this module is called `Optimize_TrafficLightTransit`

/ Optimize_DangerSpot.

3.1.1 Basic Functioning of a Cooperative Platooning Co-Simulation Study

The basic functioning of the co-simulation studies conducted below is explained in the following and outlined in Algorithm 4. Functionalities regarding the platooning co-simulation, the MPC, and trajectory planning are implemented in an object-oriented fashion with main classes `SysPlatoon`, `SafeMPC`, and `Optimize_TrafficLightTransit` / `Optimize_DangerSpot`, respectively.

Before the co-simulation starts, the *initialization* is done. Some parameters affect all modules of the co-simulation: the number of vehicles n , the sampling time T_S , and the number of time steps simulated N . Based on these parameters, the memory for the logging data, in particular the vehicle states \mathbf{x} and control inputs u , is allocated. Next, the platooning co-simulation, the MPC, and optionally the trajectory planning are initialized. Here, initialization refers to creation of the corresponding objects `platoon`, `mpc`, and `planning`, including their parameterization. The parameterization of these objects is outlined in the following section. If the co-simulation study at hand includes *trajectory planning* of the platoon coordinator, then planned trajectories p_{plan} are calculated by evaluating the method `run` of the trajectory planning object `planning`. Note that the trajectory planning task may also be executed within the run time of the co-simulation.

Afterwards, the *co-simulation time stepping loop* starts. Each time step $t_K \rightarrow t_{K+1}$ includes the evaluation of the MPC control laws, the application of the control inputs to the vehicles, the management of the Truckmaker simulations, the reading of the Truckmaker simulation results, and the management of the prediction update. Optionally also the management of the braking hold-back and an adjustment of the default maneuver may be included.

First, the *regulation* is done for each vehicle i . Therefore the MPC control law is evaluated via the method `simstep` of `mpc`. Note the difference in the evaluation between the platoon leader and the followers. Then the calculated control input $u_K^{(i)}$ is applied to the vehicle by setting the `input` property of `platoon`. Afterwards, the next time step of the corresponding Truckmaker simulation is triggered via the method `simstep`. When the regulation loop is finished, the method `endstep` waits for the completion of the current time step of all Truckmaker simulations. The reason for the separation of the simulation management into `simstep` and `endstep` is that in this way the MPC problems can be solved in parallel to the Truckmaker simulations.

Second, *measurements* of the vehicle states are read from the `output` property and written to the corresponding logging data vector $\mathbf{x}_K^{(i)}$.

Algorithm 4 Cooperative Platooning Co-simulation Study

```

1: ▷ Initialization
2: define  $n, T_S, N$ 
3: allocate  $\mathbf{x}_{1:N}^{(1:n)}, u_{1:N}^{(1:n)}$ 
4: initialize platoon from class SysPlatoon
5: initialize mpc from class SafeMPC
6:
7: ▷ Trajectory planning
8: ▷ initialize planning from class Optimize_TrafficLightTransit
9: ▷  $p_{\text{plan},(1:N)}^{(1:n)} \leftarrow \text{planning.run}()$ 
10: ▷ mpc.communicate_plan( $p_{\text{plan},(1:N)}^{(1:n)}$ )
11:
12: ▷ Co-simulation time stepping loop
13: for  $K \in \{1, 2, \dots, N\}$  do
14:   ▷ Regulate
15:   for  $i \in \{1, 2, \dots, n\}$  do
16:     if  $i > 1$  then
17:        $u_K^{(i)} \leftarrow \text{mpc}(i).\text{simstep}(k, \mathbf{x}_K^{(i)}, \mathbf{x}_K^{(i-1)})$  ▷ follower
18:     else
19:        $u_K^{(i)} \leftarrow \text{mpc}(i).\text{simstep}(k, \mathbf{x}_K^{(i)})$  ▷ leader
20:     platoon.input( $i$ )  $\leftarrow u_K^{(i)}$ 
21:     platoon.simstep( $i$ )
22:   platoon.endstep()
23:
24:   ▷ Collect measurements
25:   for  $i \in \{1, 2, \dots, n\}$  do
26:      $\mathbf{x}_{K+1}^{(i)} \leftarrow \text{platoon.output}(i).\text{state}$ 
27:
28:   ▷ Communicate
29:   mpc.update_prediction(mode)
30:   ▷ mpc.holdback_start( $n_{\text{HB}}, a_{\text{HB}}^{(1:n)}$ ) or mpc.holdback_stop()
31:   ▷ mpc.change_default_maneuver( $v_{\text{des}}^{(1:n)}, d_{\text{min}}^{(1:n)}$ )

```

Third, the V2V *communication* is done. Only the use of the method `update_prediction` of `mpc` is mandatory. Depending on the update `mode`, each vehicle may communicate its prediction to its follower (see Algorithms 2, 3):

- ``corridor'` results in the position-corridor-based prediction update described in this work above;
- ``always'` triggers the prediction update in each time step;
- ``never'` does not perform any communication; the controllers work in a decentralized fashion based only on their local measurements.

Optionally, the braking hold-back strategy can either be started/continued via the method `holdback_start` with given number of hold-back samples n_{HB} and hold-back accelerations $a_{\text{HB}}^{(i)}$ or expired via the method `holdback_stop`. Also optionally, the default maneuver may be changed during the study via the method `change_default_maneuver` with new desired velocities $v_{\text{des}}^{(i)}$ and new desired minimal inter-vehicle distances $d_{\text{min}}^{(i)}$.

Finally, post processing and plotting of the results may be done. Recall that the Algorithm 4 is written in pseudo code to clarify the basic functioning of the cooperative platooning co-simulation studies conducted in this work. While the actual implementation is considerably more complex, the most relevant functionalities are found in this outline. See Appendix A for further details regarding the implementation.

3.2 Co-Simulation Based Validation

The proposed platoon control methods are investigated with the co-simulation framework in three selected scenarios:

1. The capabilities of the safety-extended MPC are demonstrated in an emergency braking maneuver of the platoon leader.
2. A communication loss is showcased while the proposed hold-back strategy is applied.
3. The performance of the nominal driving corridor formulation is evaluated.

These scenarios consider a platoon of three trucks (tractor units *without trailers*) which are parameterized identically in TruckMaker[®]. The default model

- `Demo2AxleSemiTruck4x2_Volvo`

is used with an 8-speed automatic gearbox. This default model is based on “typical, unvalidated data for 2-axle semi-truck 4x2”. The vehicle mass is 7000 kg. The maximal torque of approximately 2200 Nm is provided for angular velocities of 1000 to 1500 rotations per minute.

Each individual truck is interfaced via a lower-level controller: a PI-acceleration con-

3 Simulation and Results



Figure 3.5: Lateral view on the HDV 3D-model used for the co-simulations, taken from Truckmaker [87].

Table 3.1: Parameters for the safety-extended MPCs

$\bar{a}_{\min}^{\text{ego}}$	-7 m/s^2	ego braking capacity
a_{\max}^{ego}	$+2 \text{ m/s}^2$	maximal acceleration
$\underline{a}_{\min}^{\text{pre}}$	-8 m/s^2	predecessor braking capacity
τ	0.2 s	time constant
L	10 m	vehicle length
T_S	0.1 s	sampling time
n_{tol}	5	tolerance samples
N	80	prediction length
q_p	1	weight on tracking
r	20	weight on acceleration
ε	10^{-6}	weight on fail-safe shaping
r_s	10^{10}	weight on slack
$l_{\text{stop}}^{\text{fs}}$	100	weight affecting standstill
d_{buffer}	1.5 m	buffer distance
δ_p, δ_c	2 m	spatial tolerances
v_{\max}	89 km/h	maximum velocity

troller in a basic, non-optimized parameter setting. The platoon drives on a straight and flat road. All vehicles are controlled by local safety-extended MPCs (2.26). The parameter values given in Table 3.1 are used in all three scenarios.

Next, the three selected co-simulation scenarios are detailed and the results are discussed in Sections 3.2.1, 3.2.2, and 3.2.4. Since trajectory planning by the platoon coordinator is only included in the third scenario where the nominal driving corridor formulation is evaluated, the trajectory planning capabilities are evaluated between the presentation of the second and third scenario in Section 3.2.3.

3.2.1 Scenario 1: Safe Emergency Braking Capabilities¹

The capabilities of the platoon under safety-extended MPC in an unforeseen emergency braking scenario is demonstrated in a detailed co-simulation in this section. In Figure 3.6, velocities, inter-vehicle distances, accelerations, and positions for each vehicle are plotted over time.

Each platoon vehicle implements a safety-extended MPC (2.26), see Table 3.1 for parameter values. The position reference sequence in (2.19) is calculated via Algorithm 1 and the prediction update is done via Algorithm 3, without a planned maneuver. The default behavior is defined by $v_{\text{des}} = 80 \text{ km/h}$, and the desired inter-vehicle spacing $d_{\text{min}} = 1.5 \text{ m}$ is used.

The platoon is initialized in tight spacing at standstill and accelerates subsequently until v_{des} is reached. The velocity trajectories coincide up to $v \approx 34 \text{ km/h}$ since all vehicles are parameterized identically, but thereafter larger inter-vehicle distances are necessary due to safety reasons. A uniform motion is subsequently realized at time $t \approx 25 \text{ s}$. At time $t = 40 \text{ s}$ the control action of the leader is abruptly overruled by an emergency braking maneuver with $a^{(1)} \approx -8 \text{ m/s}^2$. All vehicles come to a safe standstill, even though an unmodeled input delay $\Delta \approx 0.3 \text{ s}$ is present. This scenario shows that the proposed safety-extended MPC enables the separation of the tracking control design tasks and the safe operation of the platoon. In [79], the distributed platoon MPC is extended by including road friction estimates and collision safety also under varying road friction conditions is demonstrated.

¹The results presented in this section have previously been published as part of the publication [1].

3 Simulation and Results

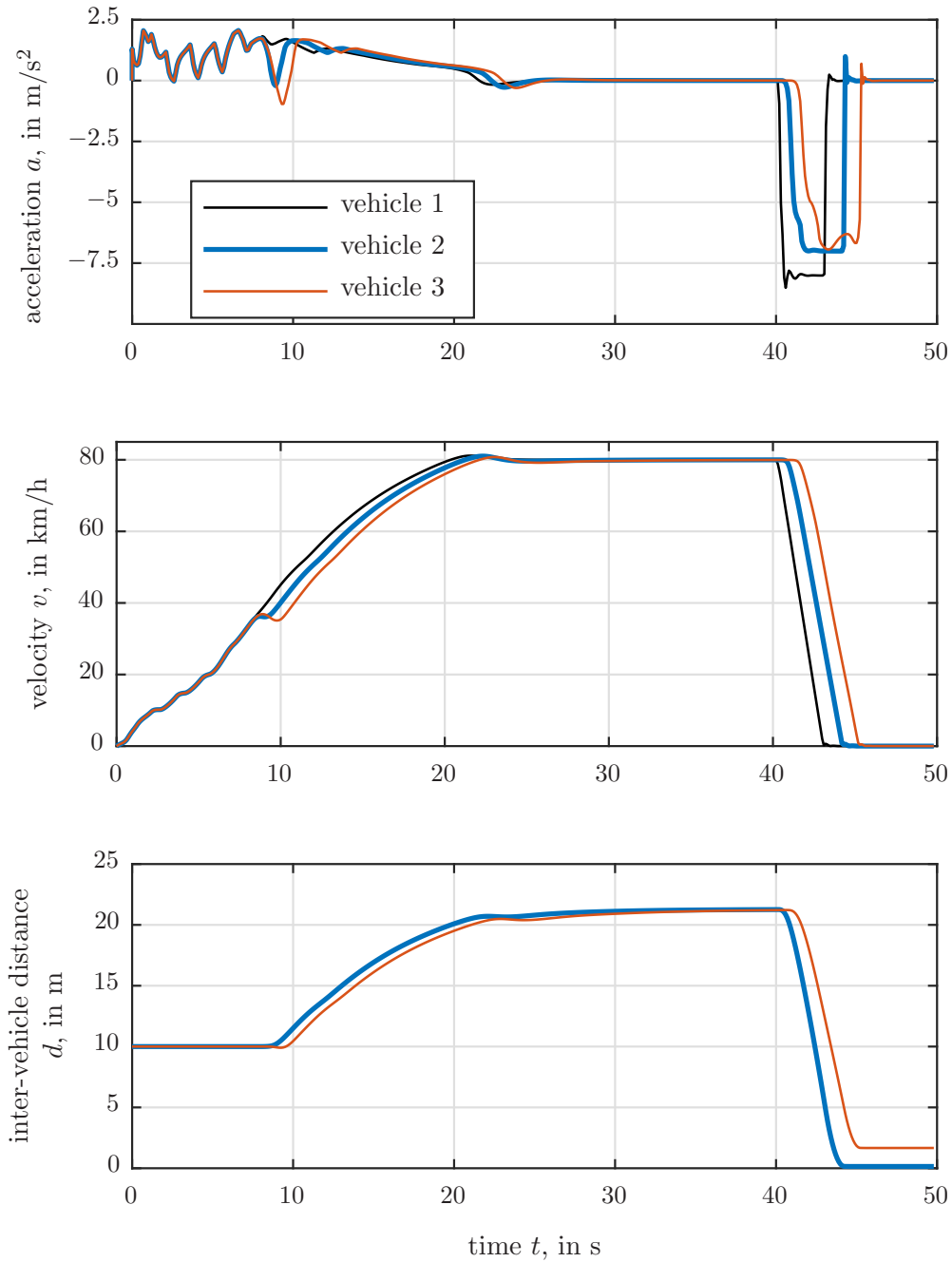


Figure 3.6: Validation of safety in the emergency braking case

3 Simulation and Results

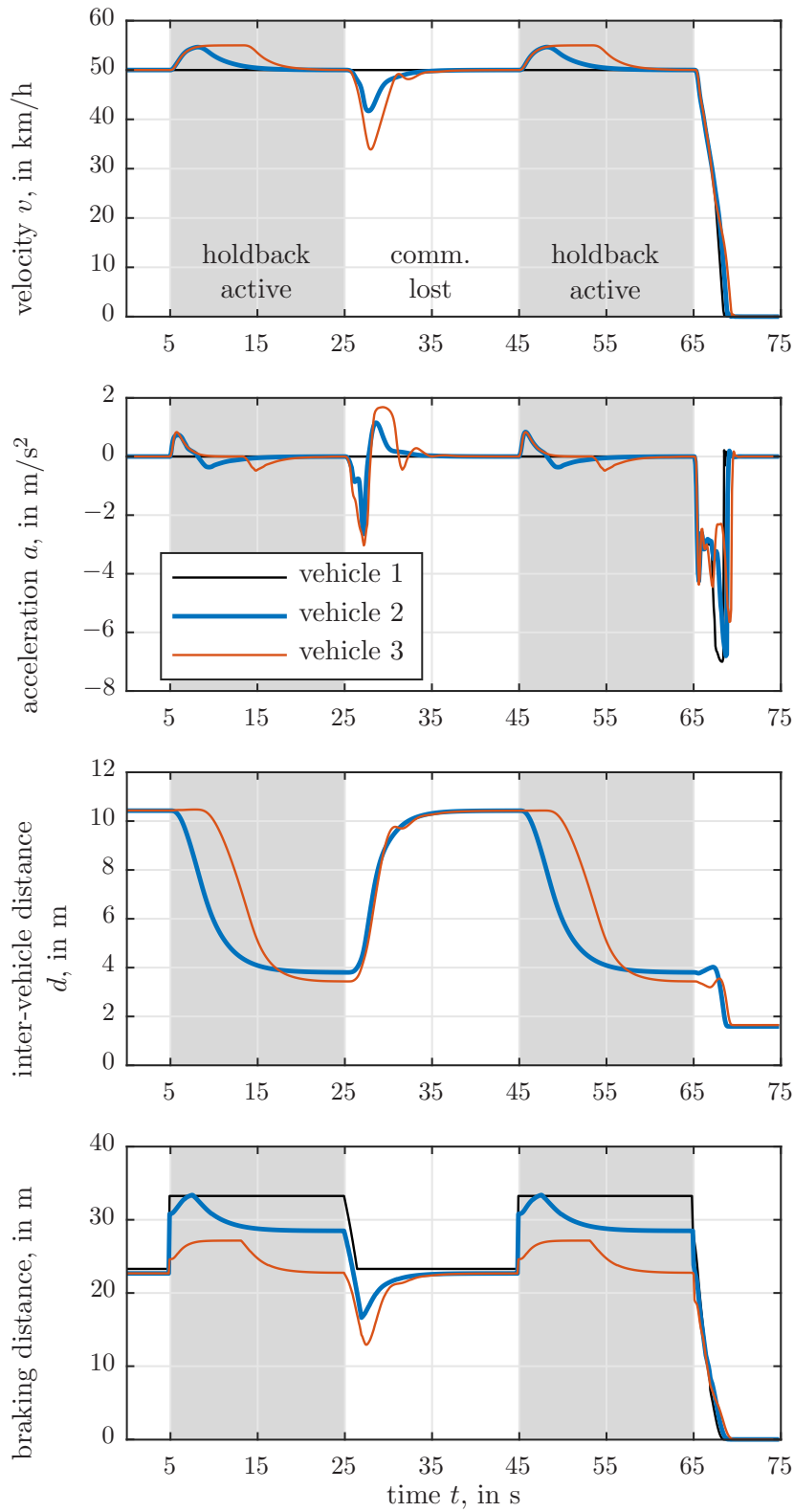


Figure 3.7: Co-simulation validation of safe braking hold-back strategy under communication loss.

Table 3.2: Hold-back operation parameters

$a_{\text{HB}}^{(1)}$	-3 m/s^2	leader hold-back acceleration
$a_{\text{HB}}^{(2)}$	-4.4 m/s^2	2nd vehicle hold-back acceleration
$a_{\text{HB}}^{(3)}$	-7 m/s^2	tail hold-back acceleration
n_{HB}	20	hold-back samples (if active)

3.2.2 Scenario 2: Communication Loss During Active Braking Hold-Back²

The dynamic platoon behavior and the operational safety accomplished by the proposed braking hold-back strategy in Section 2.1.5.2 are highlighted in the following simulation case. Initially the platoon drives in steady state at velocity $v_{\text{des}}^{(1)} = 50 \text{ km/h}$. At time $t = 10 \text{ s}$ the braking hold-back operation (see Table 3.1 and 3.2 for parameter values) is activated, but communication is lost for $t \in [30 \text{ s}, 50 \text{ s}]$, as illustrated in Figure 3.7. Subsequently, the hold-back operation is re-established at $t = 50 \text{ s}$. At $t = 70 \text{ s}$, the hold-back phase is again discontinued (let to expire). Simultaneously, a full braking maneuver of the leader according to the agreed-upon deceleration bounds is started, cf. (2.31).

In Figure 3.7, the velocities, inter-vehicle distances, accelerations, and the instantaneous braking distances, for each vehicle are plotted versus time. The instantaneous braking distances correspond to the solution of the fail-safe problem when $l_{\text{stop}}^{\text{fs}}$ in the shaping term (2.28) is chosen sufficiently high. Note that overlaps of the braking distances, e.g., between the first and second vehicle at $t \approx 7.5 \text{ s}$, do not indicate a potential collision – at equal braking distances, the vehicles are still separated by their inter-vehicle distances. Each platoon vehicle implements a safety-extended MPC (2.26), see Table 3.1 for parameter values. The position reference sequence in (2.19) is calculated via Algorithm 1 and the prediction update is done via Algorithm 3, without a planned maneuver. The default behavior is defined by $v_{\text{des}}^{(1:3)} = (50, 55, 55) \text{ km/h}$, and the desired inter-vehicle spacing $d_{\text{min}} = 1.5 \text{ m}$ is used. Thus the platoon realizes the minimal safe distances automatically, since the follower MPCs try to track a higher desired velocity. Finally, all vehicles come to a safe standstill despite the simultaneous occurrence of full braking and hold-back discontinuation.

This scenario clearly shows that the proposed hold-back strategy is capable of reducing the platoon length significantly. However, situational awareness of the platoon is required since the platoon length reduction is traded for increased braking distance.

²The results presented in this section have previously been published as part of the publication [1].

3.2.3 Evaluation of the Centralized Platooning Trajectory Optimization

Before investigating the corridor-based reference selection and prediction update proposed in Section 2.1.5.3, the capabilities of the developed trajectory optimization tools are showcased for some exemplary platooning maneuvers:

- The results of the trajectory optimization regarding the *TrafficLightTransit* use case is presented for two platooning maneuvers: In the first maneuver (Section 3.2.3.1), a platoon approaches an intersection during the red phase such that a slow down is necessary. In the second (Section 3.2.3.2), a platoon performs a simultaneous start-up at the stopping line of an intersection when it turns green.
- The results of the trajectory optimization regarding the *DangerSpot* use case is presented for two platooning maneuvers: In the first maneuver (Section 3.2.3.3), a platoon dissolves before reaching a construction site. In the second (Section 3.2.3.4), a platoon is formed by a catch-up maneuver of the platoon tail.

Note that in the following presentation of these maneuvers, only selected parameter values are given. See Appendix A for additional details.

3.2.3.1 Slow-Down when Approaching an Intersection

In this maneuver, a platoon of $n = 3$ vehicles ($i = 1, 2, 3$) initially drives in a uniform motion at velocity $v_0^{(i)} = 50$ km/h. The traffic light ahead is red with stopping line at position $p_{\text{stop}} = 180$ m. Since the green light timing information is known to the platoon coordinator, an efficient slow down can be planned. The lights will turn green and afterwards back to red at times $t_{\text{green}} = 20$ s and $t_{\text{red}} = 30$ s, respectively. The platoon formation is restricted by minimal inter-vehicle distances $d_{\text{min}}^{(i)} = 5$ m and minimal time gaps $\Delta t_{\text{min}}^{(i)} = 1.5$ s. Thus the platoon coordinator plans trajectories which preferably enable a pass-over at a high velocity in the moment the lights turn green.

The results of the trajectory optimization as formulated in Section 2.2.2 are shown in Figure 3.9 whereby details on the graphical representation are given within the caption. The time and actuation weightings are given by $w_t^{(i)} = 1$ and $w_u^{(i)} = 0.1$, respectively. The sampling time $T_S = 0.1$ s is used. This results in sequential linear programs for the minimal drive and the maximal drive problems with 300 unknown variables each, which are solved within seven iterations each. The sequential quadratic program corresponding to the optimal drive problem encompasses 1203 unknown variables and is solved within two iterations. It can be seen that all vehicles slow down but no vehicle comes to a full stop. Furthermore the platoon leader passes over the stopping line at approximately

40 km/h which results in only a small loss in time considering the given maximal velocity $v_{\max} = 50$ km/h. Thus planning this maneuver can improve the platooning efficiency due to reduced time loss of the platoon, increased traffic throughput, and reduced emissions due to reduced acceleration intensity. However, if an unknown non-platooning vehicle is waiting at the stopping line, then situational awareness is required, to efficiently adapt the maneuver to the new circumstances. Section 3.2.4 below describes such a scenario including an unknown non-platooning vehicle.

3.2.3.2 Simultaneous Start-Up at the Stopping Line

A simultaneous start-up of a platoon is a measure to increase traffic throughput by minimizing the time delays between the individual start-up actions. While this cooperative platooning functionality can be realized without incorporation of infrastructure information, an additional potential is shown here by exploiting green light information.

In this maneuver, a platoon of $n = 3$ vehicles ($i = 1, 2, 3$) is waiting at the stopping line of the first intersection at position 0 m. The stopping line of a second intersection ahead is located at position $p_{\text{stop}} = 200$ m. The green light timing information of both intersections is known to the platoon coordinator. At time $t = 0$ s the lights of the first intersection turn green. Afterwards the lights of the second intersection turn green and later back to red at times $t_{\text{green}} = 20$ s and $t_{\text{red}} = 35$ s, respectively. The platoon formation is restricted by minimal inter-vehicle distances $d_{\min}^{(i)} = 5$ m and minimal time gaps $\Delta t_{\min}^{(i)} = 2$ s. Thus the platoon coordinator plans trajectories which realize an efficient start-up at the first intersection and an efficient pass-over for the second intersection.

Two different cases are evaluated with different cost weightings: in *Case A* the time efficiency is of high priority with weighting $w_t^{(1)} = 10$ regarding the leader, while in *Case B* the actuation efficiency is more important since $w_t^{(1)} = 0$. In both cases a zero time weighting for the followers $w_t^{(2)} = w_t^{(3)} = 0$ is used. The actuation weighting is given by $w_u^{(i)} = 1$. The results of the trajectory optimization as formulated in Section 2.2.2 are shown in Figure 3.9, where the left and the right columns correspond to *Case A* and *Case B*, respectively. Details on the graphical representation of this figure are given within the caption. The sampling time $T_S = 0.25$ s is used. This results in sequential linear programs for the minimal drive and the maximal drive problems with 140 unknown variables each, which are solved for both cases within 7 and 9 iterations, respectively. The sequential quadratic programs corresponding to the optimal drive problems encompass 483 unknown variables and is solved for both cases within 6 iterations.

In *Case A*, the platoon performs a fast start-up, so that the platoon leader passes the second intersection when the green light phase starts at $t_{\text{green}} = 20$ s. All vehicles

3 Simulation and Results

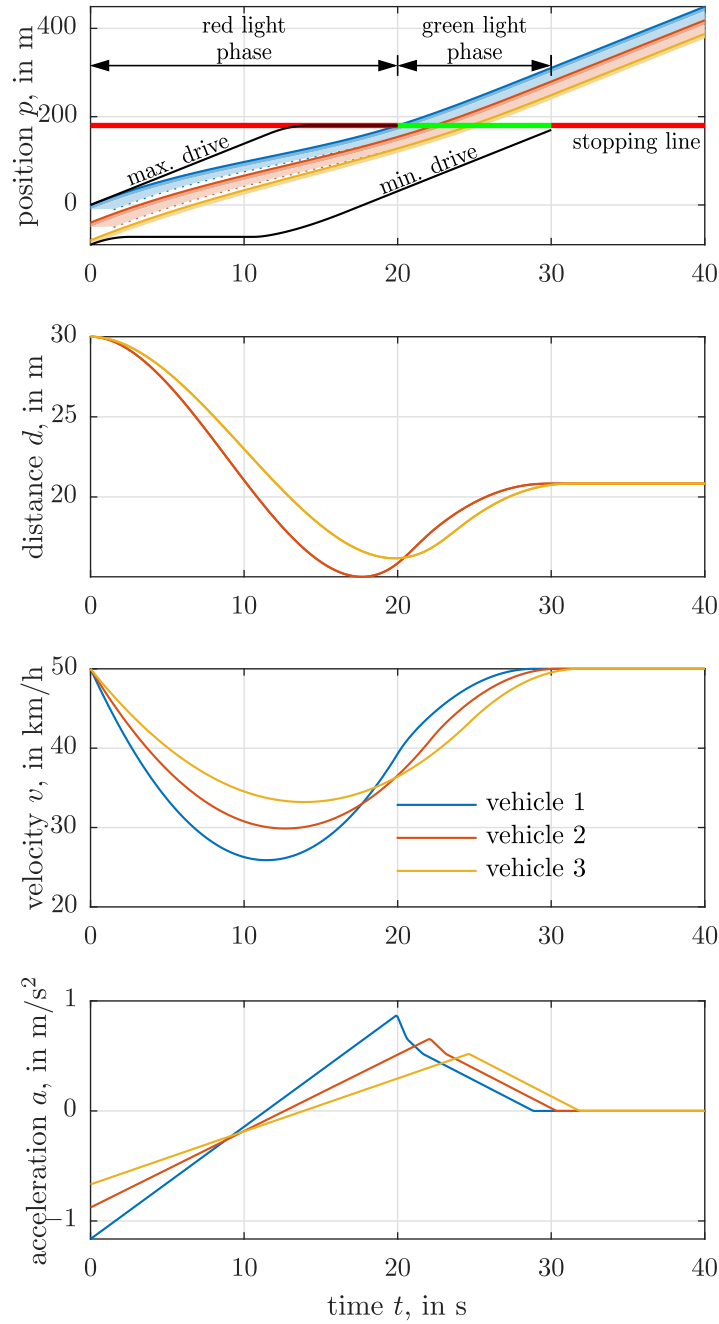


Figure 3.8: Results of the trajectory optimization of a slow-down maneuver at a traffic-light-controlled intersection. Regarding the position plot, top row: The consumed space of the individual vehicles is illustrated by dark shaded areas in the respective vehicle colors (see legend), while additional necessary space due to minimal space and time gaps is illustrated by light shaded areas. Note that the minimum drive of the platoon tail is depicted here by the corresponding rear end position trajectory for illustrative reasons, in contrast to the definition given in (2.53).

reach the maximum velocity $v_{\max} = 50 \text{ km/h}$ shortly after the pass-over. It is noteworthy that between an initial start-up phase and a terminal phase the vehicles realize identical acceleration trajectories in a time-shifted manner.

In *Case B* the accelerations are relatively small for all times, such that the maximal velocity is reached only at the end and the platoon tail performs the pass-over when the green light phase ends at $t_{\text{red}} = 35 \text{ s}$.

3.2.3.3 Platoon Dissolution at a Construction Site

In this maneuver, a platoon of $n = 5$ vehicles ($i = 1, 2, 3, 4, 5$) initially driving at $v_0^{(i)} = 80 \text{ km/h}$ approaches a construction site at position $p_{\text{danger}} = 800 \text{ m}$ where a dissolution of the platoon is mandatory because, for example, of legislative reasons, and thus required inter-vehicle distances $d_{\text{man}}^{(i)} = 50 \text{ m}$ for manual driving have to be established. Moreover a hand-over period with duration $T_{\text{man}} = 5 \text{ s}$ for the human drivers with uniform motion of the platoon at $v_{\text{man}} = 60 \text{ km/h}$ is necessary to meet this reduced speed limit. Thus the platoon coordinator plans trajectories which realize an efficient transition to this required platoon formation.

The results of the trajectory optimization as formulated in Section 2.2.3 are shown in Figure 3.11 whereby details on the graphical representation are given within the caption. The weightings are given by $w_d = 1$, $w_v = 1$, and $w_u^{(i)} = 0.1$. The sampling time $T_s = 0.5 \text{ s}$ is used. This results in a sequential quadratic program with 570 unknown variables, which is solved within 2 iterations. It can be seen that all vehicles except the platoon leader slow down immediately. Only the last two vehicles fall below $v_{\text{man}} = 60 \text{ km/h}$. All vehicles except the third (middle) vehicle realize the inter-vehicle distance requirement before realizing the velocity requirement. This observation may be interpreted given the analogy of a body where the center of mass is kept at the same position to reduce the actuation effort. All vehicles adhere to both requirements early enough so that a hand-over to the human driver is possible. Thus planning this maneuver can improve the platooning efficiency due to reduced braking actions. Note that a significantly longer transition time is necessary if a minimal velocity of $v_{\text{man}} = 60 \text{ km/h}$ is enforced. On the downside, in the illustrated maneuver, the trailing traffic may be negatively affected because of the slow-down of the platoon tail.

3.2.3.4 Catch-Up for Platoon Formation

In practice it is rarely the case that multiple HDVs take the same route. To attain high platooning efficiency given this fact, establishing platoons en-route becomes a relevant

3 Simulation and Results

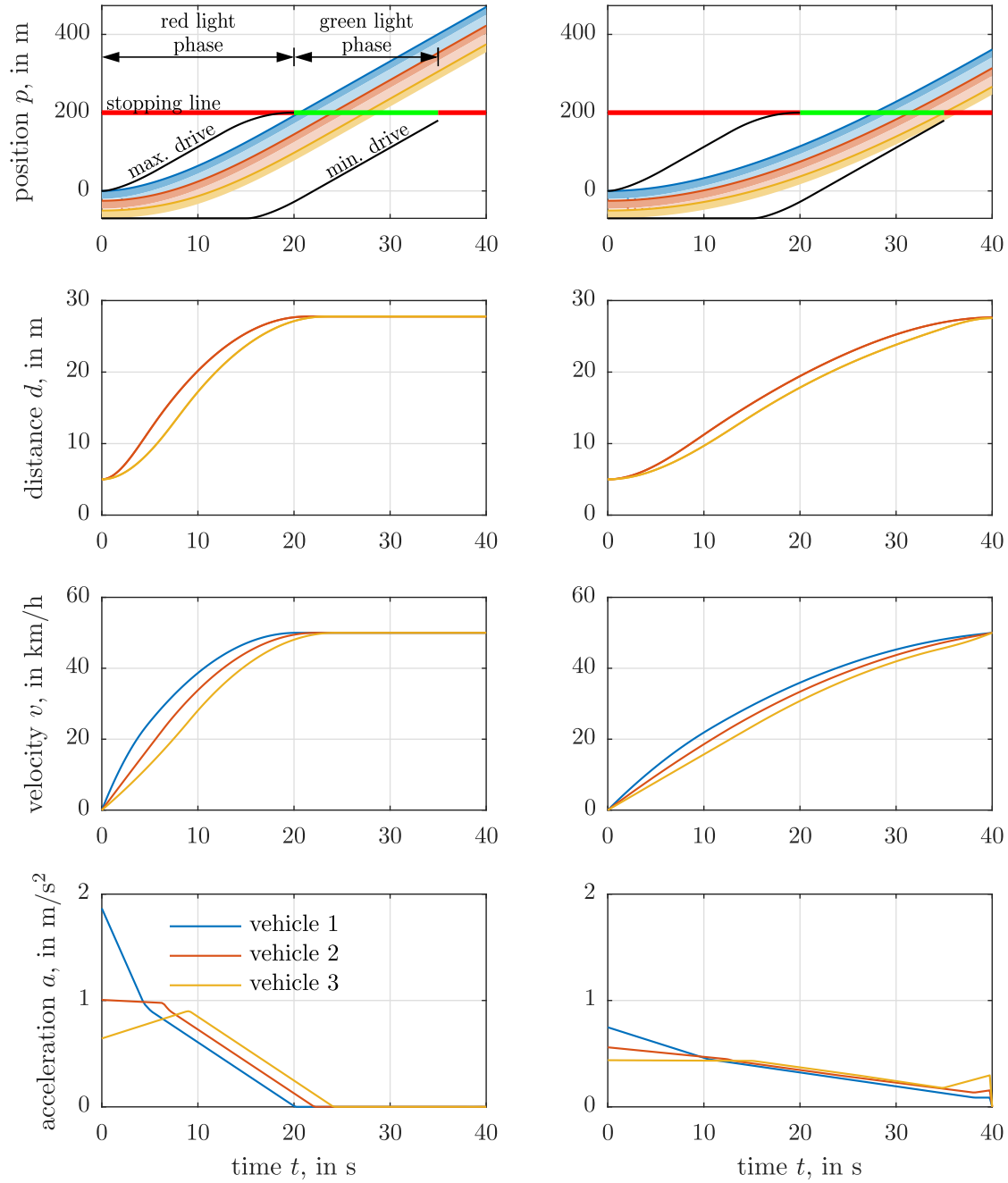


Figure 3.9: Results of the trajectory optimization of a simultaneous start-up maneuver for two cases: *Case A*, left column; *Case B*, right column. Regarding the position plot, top row: The consumed space of the individual vehicles is illustrated by dark shaded areas in the respective vehicle colors (see legend), while additional necessary space due to minimal space and time gaps is illustrated by light shaded areas. Note that the minimum drive of the platoon tail is depicted here by the corresponding rear end position trajectory for illustrative reasons, in contrast to the definition given in (2.53).

3 Simulation and Results

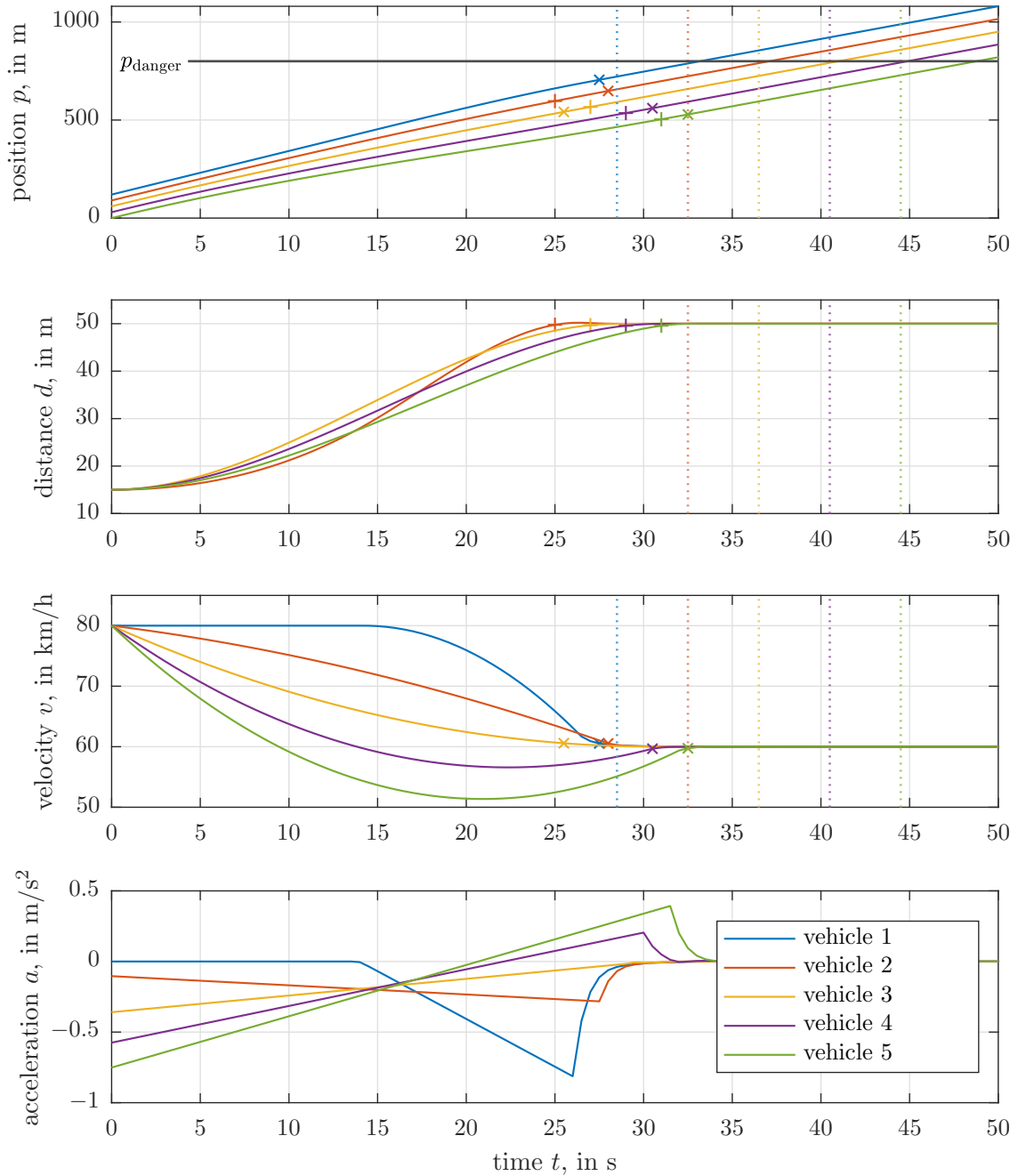


Figure 3.10: Results of the trajectory optimization of a platoon dissolution maneuver before reaching a construction site. The point in time where a vehicle adheres to the distance and velocity requirement is indicated by markers + and \times (in the respective vehicle color, see legend within plot), respectively. The point in time where a vehicle has to adhere to both requirements at latest to ensure sufficiently long hand-over duration is indicated by a dotted vertical line.

3 Simulation and Results

platooning functionality with the emergence of intelligent transportation systems. A future freight transportation system, as outlined in [20], may find a suitable single vehicle nearby and propose a catch-up maneuver which integrates this vehicle into the platoon. In this maneuver, initially a platoon of 2 vehicles is 435 m ahead of a single vehicle. To form a new platoon of $n = 3$ vehicles ($i = 1, 2, 3$), a catch-up maneuver is performed. It is assumed that a so-called overboost is permitted for this case to promote economical driving. This means that the pursuing vehicle is allowed to drive temporarily at $v_{\max}^{(3)} = 88 \text{ km/h}$ to reduce the duration of this maneuver and, in turn, enable more platoon formations of this type. The speed limit of the other (platooning) vehicles remains unchanged at $v_{\max}^{(1)} = v_{\max}^{(2)} = 80 \text{ km/h}$. To reduce the impact on the subsequent traffic, the first two vehicles are required to stay above $v_{\min} = 75 \text{ km/h}$. Here, the position p_{danger} is used differently than described above. Since the duration such a catch-up maneuver can take is practically limited, in this maneuver, a spatial limit is given with the formulation of $p_{\text{danger}} = 3000 \text{ m}$. Thus the platoon coordinator plans trajectories which realize an efficient catch-up of the new defined platoon tail, while limiting the required track length.

The results of the trajectory optimization as formulated in Section 2.2.3 are shown in Figure 3.11 whereby details on the graphical representation are given within the caption. The weightings are given by $w_d = 1$, $w_v = 1$, and $w_u^{(i)} = 0.1$. The sampling time $T_S = 0.5 \text{ s}$ is used. This results in a sequential quadratic program with 864 unknown variables, which is solved within 2 iterations. It can be seen that the permitted speed limits are fully exploited, such that the first two vehicles drive at the minimal velocity $v_{\min} = 75 \text{ km/h}$ for the most part of this maneuver while the platoon tail drives at $v_{\max} = 88 \text{ km/h}$. Furthermore, it is reasonable that the efficiency of these trajectories is satisfactory, since no actuation is planned for a large part of this maneuver. However, note that coasting of the vehicles (no actuation causes negative accelerations) is not modeled in this work, so that a zero acceleration level is likely to be suboptimal in reality. The newly formed platoon of $n = 3$ vehicles drives in a uniform motion shortly after $t = 120 \text{ s}$.

3 Simulation and Results

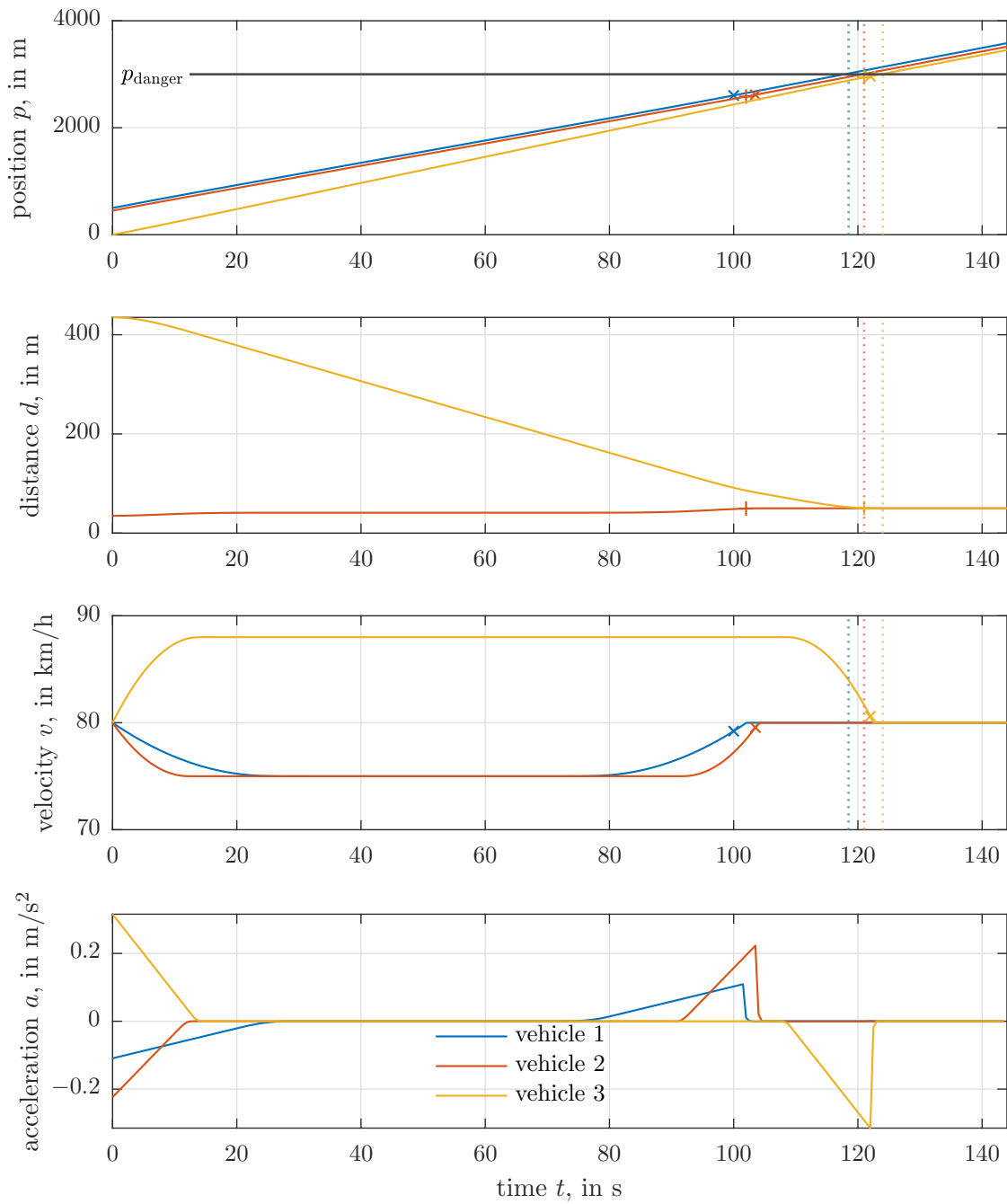


Figure 3.11: Results of the trajectory optimization of a platoon dissolution maneuver before reaching a construction site. The point in time where a vehicle adheres to the distance and velocity requirements is indicated by markers + and × (in the respective vehicle color, see legend), respectively.

3.2.4 Scenario 3: Validation of Corridor-Based Situation-Aware Platoon Control with Efficient V2V Communication³

To illustrate the safety-extended, corridor-based platoon control concept outlined in Section 2.1.5.3, a coordinated passage of the platoon over a signaled intersection is investigated. It is assumed that the platoon approaches such intersection. The traffic light is initially red and will turn green at a known time (communicated to the platoon via I2V communication, for example). Also, a set of planned trajectories p_{plan} for an efficient crossing of the intersection be available as presented in Section 3.2.3.1, created by assuming that no other traffic is present (dashed lines in Figure 3.12). The situation is now complicated by the fact that another individual vehicle (“non-platooning vehicle”) is present, waiting at standstill before the intersection and accelerating after the traffic light has turned green. Consequently, the platoon needs to appropriately react to this situation so as to safely and efficiently pass the intersection in the actual traffic situation.

Each platoon vehicle implements a safety-extended MPC, see Table 3.1 for parameter values. The position reference sequence reference in (2.19) is calculated via Algorithm 1 and the prediction update is done via Algorithm 3. The default behavior is defined by $v_{\text{des}} = 50 \text{ km/h}$, and the desired inter-vehicle spacing $d_{\text{min}} = 15 \text{ m}$ is used.

Figures 3.12 and 3.13 show the resulting platoon actions with three different intra-platoon (V2V) communication strategies. The platoon initially approaches the intersection according to the plan. However, after time $t = 15 \text{ s}$, it needs to depart from the plan in order to safely brake behind the non-platooning vehicle (see Figure 3.12, left). Only after that vehicle starts moving, the platoon can accelerate again and cross the intersection. Note that the inter-vehicle distance between the platoon leader and the “non-platooning vehicle” $d^{(1)}$ is most of the time larger than the plotting range in the Figure 3.12 and 3.13, which is indicated by the dashed continuation of the corresponding lines.

The results in Figure 3.12 detail the performance of the reduced-communication concept with a corridor width of $\delta_c = 2 \text{ m}$ referred to as *Case A*, where prediction updates of a preceding vehicle are only communicated to the ego vehicle if the current prediction deviates more than 2 m from the last communicated prediction information available to the ego vehicle. It performs equally well as *Case B* (see Figure 3.13, top) in which the predicted trajectories are sent to the respective followers in every time step, i.e. $\delta_c = 0 \text{ m}$. It is noteworthy that by sufficiently often communicating the predicted trajectories backwards along the platoon, string stability is achieved here as indicated by

³The results presented in this section have previously been published as part of the publication [1].

3 Simulation and Results

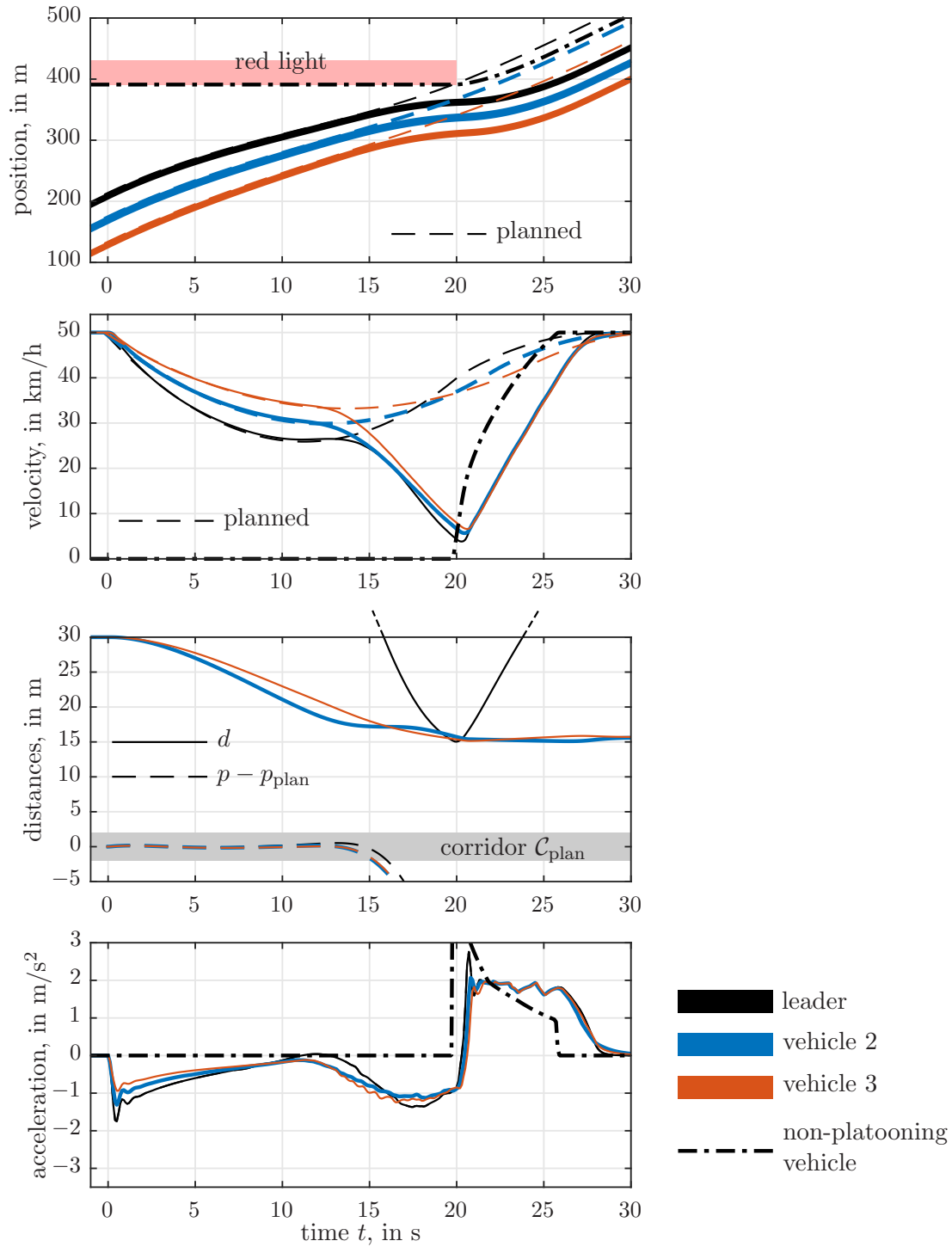


Figure 3.12: Co-simulation validation of safe corridor-based situation-aware platoon behavior in a shaped intersection crossing maneuver. The platoon safely reacts to the presence of individual vehicle in a string stable manner with low communication effort in *Case A*.

3 Simulation and Results

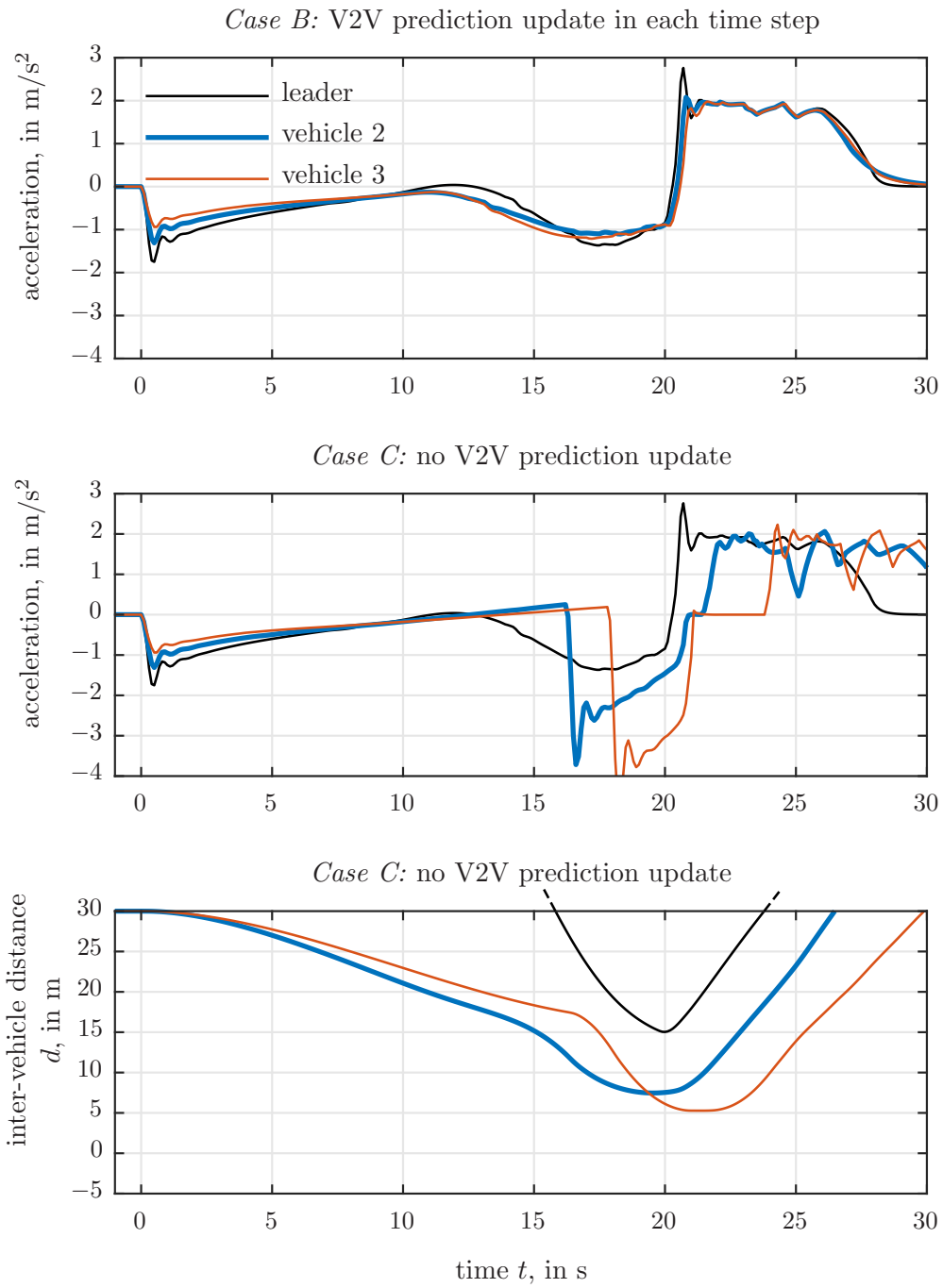


Figure 3.13: Influence of amount of communication on platoon behavior (*Case B* versus *Case C*): string-stable response with highest communication effort, collision-safe but non-string stable behavior without V2V communication.

3 Simulation and Results

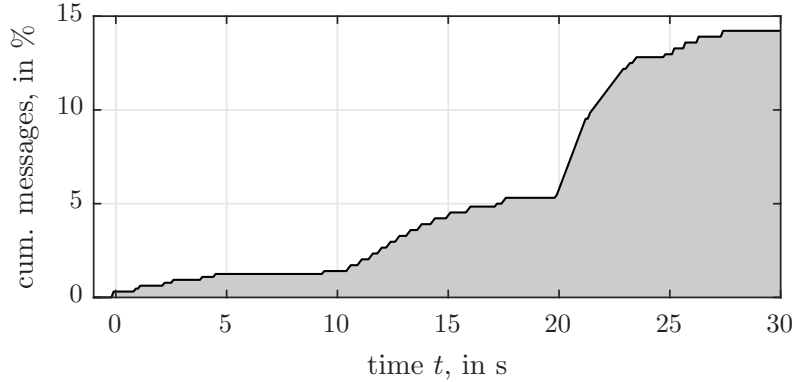


Figure 3.14: Amount of cumulated V2V messages sent in the reduced-communication strategy *Case A* (fraction of total message count in *Case B*).

the simultaneous and almost congruent deceleration patterns of all platoon vehicles for $t \in [15\text{ s}, 20\text{ s}]$ (Fig 3.12, bottom right and Figure 3.13, top). The intra-platoon distances are kept approximately constant at d_{\min} during the scenario (Figure 3.12, top right).

With the corridor widths of 2 m chosen in *Case A*, string stability can effectively be maintained and communication effort is significantly reduced: The number of sent messages (transmitting an updated prediction to the next follower) can be reduced to less than 15% compared to *Case B* where prediction updates are sent in each time step (as in Figure 3.13, top). In turn, not sending any updates of the predicted trajectories to followers as in *Case C*, i.e. $\delta_c = \infty$, still results in a collision-safe behavior (established by the safety extension of the MPCs), but string stability is lost and comfort/efficiency is degraded (see Figure 3.13, middle and bottom).

Finally, Figure 3.14 shows the ratio of messages sent from a vehicle to its follower in the reduced-communication *Case A* of Figure 3.12. The ratio is given with respect to the total message count of the outlined maneuver in *Case B* with prediction update in each time step (Figure 3.13, top), in which predicted trajectories are sent from leader and follower 1 to follower 1 and 2, respectively. Over time, it is noteworthy that as long as the communicated, correctly time-shifted predictions remain valid (i.e., sufficiently close to the newly computed predictions), no communication occurs. Once the waiting non-platooning vehicle forces the leader to deviate from the planned maneuver trajectories for $t \in [12\text{ s}, 18\text{ s}]$, prediction updates become necessary. The intense communication effort within $t \in [20\text{ s}, 23\text{ s}]$ stems from the simple constant-velocity prediction model utilized to predict the non-platooning vehicle's trajectory (which performs, however, a transient acceleration maneuver).

Further opportunities to efficiently reduce communication requirements can thus be

spotted in applying more elaborate motion prediction of individual traffic. Note that collision safety is achieved independently of V2V communication quality. In turn, V2V communication could be realized via non-critical channels which potentially benefit from parsimonious communication loads.

3.3 Conclusion and Future Work

The work presented in this thesis focuses on the development of novel methods for the distributed model predictive control of cooperative platoons.

Reducing the inter-vehicle distances increases the platooning efficiency by means of increased traffic throughput, reduced aerodynamic drag in case of heavy-duty vehicle (HDV) platoons, and last but not least increased room for cooperative maneuvers. While cooperative platooning offers the opportunity to establish agreed-upon behavior via vehicle-to-vehicle (V2V) communication, the reduction of inter-vehicle distances is a safety-critical endeavor which requires autonomous approaches. The first research question therefore addressed how inter-vehicle distances could still be reduced based on agreed-upon cooperative behavior.

Research Question & Finding 1

How to safely enable reduced inter-vehicle distances of a platoon based on cooperative behavior?

The flexible safety extension for the distributed predictive controller proposed in Section 2.1.4 accomplishes autonomous collision-free driving behavior, as validated in Section 3.2.1, while effectively separating the design of safety from the remaining control design task. Smaller inter-vehicle gaps are enabled by letting each vehicle commit to temporarily reduce (“hold back”) its braking authority if possible in the current traffic situation, as proposed in Section 2.1.5.2. This concept is formulated in a way to be robust against communication loss, as validated in Section 3.2.2.

This braking “hold-back” strategy is thus particularly effective on roads with little traffic and minimal occurrence of vulnerable road users, such as lightly frequented highways, where the braking authority of the platoon leader could be significantly reduced. However, the application of this strategy depends on the situation-aware and safety-critical monitoring of the surrounding traffic, which is beyond the scope of this thesis.

On roads with dense traffic as well as urban areas, the platooning efficiency is highly

affected by external factors. With the emergence of cooperative intelligent transportation systems (C-ITS), increasingly more traffic status information will be available for C-ITS-participating road users. Hence, the second research question addressed how such information can be exploited by a cooperative platooning control system.

Research Question & Finding 2

How to efficiently incorporate V2V/V2I communication to allow for situation-aware distributed control?

An efficient strategy to choose a suitable control mode and to selectively send critical predictive information updates to follower vehicles is proposed in Section 2.1.5.3. The decision is based on a simple yet effective definition of agreed-upon driving corridors to allow for high control performance at a drastically reduced V2V (vehicle-to-vehicle) communication demand. Traffic information from the infrastructure is used to parameterize maneuver-specific trajectory planning, presented in Section 2.2 and validated in Section 3.2.4, to recommend efficient motion profiles to the local trajectory tracking controllers.

Many simplifications have been made throughout this work regarding the considered cyber-physical system of a C-ITS-enabled cooperative platoon, which includes at least longitudinal & lateral vehicle dynamics, vehicular safety & communication systems, and traffic sensing & monitoring systems. While most of these simplifications were not further considered, more realistic vehicle dynamics can be studied via a dedicated simulation software. The third research question addressed how a simulation-based validation approach could be implemented.

Research Question & Finding 3

How to design a simulation framework for validation and demonstration of the elaborated platooning control concept?

A modular co-simulation framework for high-fidelity vehicle dynamics in a platoon setting is developed in Section 3.1. The parallel-computing-based approach enables the integration of an industry-standard vehicle dynamics software and state-of-the-art optimization problem solving. While this co-simulation framework is employed to validate and test the proposed concepts and control structures, it is also capable of demonstrating these by means of a force-feedback steering wheel.

3 Simulation and Results

Finally, possible directions for future work building on this thesis are presented. These possible directions are based in part on the fruitful comments of the reviewers to the journal publication [1], written by the degree candidate, on which this thesis is largely based:

- Further investigations on the implementation of the proposed braking “hold-back” strategy in mixed road scenarios, its impact on the overall traffic flow, and on the associated parameter choices remain open as future work.
- A quantitative assessment of further simulation studies in realistic urban and long-distance traffic settings by well-defined efficiency measures will be necessary to evaluate the real-world performance of complex platoon control concepts such as the proposed distributed MPC scheme.
- While model predictive control concepts achieve efficient, situation-aware, and safe platooning, establishing formally verified string stability properties of closed-loop platoon dynamics is difficult. The empirically observed results on the string stability properties of the prediction update method developed in this work could serve as a starting point for future work. Note that some further related numerical studies are conducted in [80].
- The proposed control system needs to be tested in experiments involving real vehicles. Here, implementation requirements such as the real-time capabilities are crucial. One step towards this goal is done in [79], where an adapted version of the proposed control system is reformulated as an parameterized optimization problem which leads to explicit model predictive control.

Bibliography

- [1] S. Thormann, A. Schirrer, and S. Jakubek, “Safe and Efficient Cooperative Platooning,” *IEEE Transactions on Intelligent Transportation Systems*, 2020. DOI: 10.1109/TITS.2020.3024950.
- [2] (2018). Connecting Austria - Austrian Lead Project, Funded by the Austrian Research Promotion Agency (FFG), [Online]. Available: <https://www.connecting-austria.at/>.
- [3] B. Besselink and K. H. Johansson, “Control of platoons of heavy-duty vehicles using a delay-based spacing policy,” *IFAC-PapersOnLine*, 12th IFAC Workshop on Time Delay Systems 2015, vol. 48, no. 12, pp. 364–369, Jan. 1, 2015. DOI: 10.1016/j.ifacol.2015.09.405.
- [4] “Report on Railway Safety and Interoperability in the EU - 2018,” European Union Agency for Railways, 2018.
- [5] “Aviation: Annual Safety Review 2018,” European Aviation Safety Agency, 2018.
- [6] “Transport safety performance in the EU: A statistical overview.,” European Transport Safety Council, Brussels, 2003.
- [7] I. Savage, “Comparing the fatality risks in United States transportation across modes and over time,” *Research in Transportation Economics*, The Economics of Transportation Safety, vol. 43, no. 1, pp. 9–22, Jul. 1, 2013. DOI: 10.1016/j.retrec.2012.12.011.
- [8] “Global status report on road safety 2018,” World Health Organization, 2018. [Online]. Available: http://www.who.int/violence_injury_prevention/road_safety_status/2018/en/.
- [9] “Road safety in the European Union – Trends, statistics and main challenges,” European Union, 2018, p. 28.
- [10] F. Gustafsson, “Automotive safety systems,” *IEEE Signal Processing Magazine*, vol. 26, no. 4, pp. 32–47, Jul. 2009. DOI: 10.1109/MSP.2009.932618.

Bibliography

- [11] “Prioritising the Safety Potential of Automated Driving in Europe | ETSC,” European Transport Safety Council, 2016. [Online]. Available: <https://etsc.eu/automated-driving-report/>.
- [12] “Taxonomy and Definitions for Terms Related to On-Road Motor Vehicle Automated Driving Systems (J3016 Ground Vehicle Standard) - SAE Mobilus,” SAE International, 2014.
- [13] A. Ziebinski, R. Cupek, H. Erdogan, and S. Waechter, “A survey of ADAS technologies for the future perspective of sensor fusion,” in *International Conference on Computational Collective Intelligence*, Springer, 2016, pp. 135–146.
- [14] R. Okuda, Y. Kajiwara, and K. Terashima, “A survey of technical trend of ADAS and autonomous driving,” in *Technical Papers of 2014 International Symposium on VLSI Design, Automation and Test*, Apr. 2014, pp. 1–4. DOI: 10.1109/VLSI-DAT.2014.6834940.
- [15] S. Feng, Y. Zhang, S. E. Li, Z. Cao, H. X. Liu, and L. Li, “String stability for vehicular platoon control: Definitions and analysis methods,” *Annual Reviews in Control*, vol. 47, pp. 81–97, Jan. 1, 2019. DOI: 10.1016/j.arcontrol.2019.03.001.
- [16] R. Rajamani, *Vehicle Dynamics and Control*. New York, NY, USA: Springer, Dec. 21, 2011, 516 pp.
- [17] J. Ploeg, B. T. M. Scheepers, E. Nunen, N. Wouw, and H. Nijmeijer, “Design and experimental evaluation of cooperative adaptive cruise control,” in *2011 14th International IEEE Conference on Intelligent Transportation Systems (ITSC)*, Oct. 2011, pp. 260–265. DOI: 10.1109/ITSC.2011.6082981.
- [18] C. Bonnet and H. Fritz, “Fuel Consumption Reduction in a Platoon: Experimental Results with two Electronically Coupled Trucks at Close Spacing,” presented at the Future Transportation Technology Conference & Exposition, Aug. 21, 2000, pp. 2000–01–3056. DOI: 10.4271/2000-01-3056.
- [19] A. A. Alam, A. Gattami, and K. H. Johansson, “An experimental study on the fuel reduction potential of heavy duty vehicle platooning,” in *13th International IEEE Conference on Intelligent Transportation Systems*, Sep. 2010, pp. 306–311. DOI: 10.1109/ITSC.2010.5625054.
- [20] A. Alam, B. Besselink, V. Turri, J. Martensson, and K. H. Johansson, “Heavy-Duty Vehicle Platooning for Sustainable Freight Transportation: A Cooperative Method to Enhance Safety and Efficiency,” *IEEE Control Systems Magazine*, vol. 35, no. 6, pp. 34–56, Dec. 2015. DOI: 10.1109/MCS.2015.2471046.

Bibliography

- [21] J. B. Rawlings and D. Q. Mayne, *Model Predictive Control: Theory and Design*. Nob Hill Pub., 2009.
- [22] *Platoon*, in *Wikipedia*. [Online]. Available: <https://en.wikipedia.org/w/index.php?title=Platoon&oldid=966838043>.
- [23] M. Chen, Q. Hu, C. Mackin, J. F. Fisac, and C. J. Tomlin, “Safe platooning of unmanned aerial vehicles via reachability,” in *2015 54th IEEE Conference on Decision and Control (CDC)*, Osaka: IEEE, Dec. 2015, pp. 4695–4701. DOI: 10.1109/CDC.2015.7402951.
- [24] C. Viel, U. Vautier, J. Wan, and L. Jaulin, “Platooning control for heterogeneous sailboats based on constant time headway,” *IEEE Transactions on Intelligent Transportation Systems*, vol. 21, no. 5, pp. 2078–2089, 2019.
- [25] S. Kallenbach, “Truck Platooning—A Pragmatical Approach,” in *Fahrerassistenzsysteme 2018*, Springer, 2019, pp. 132–157.
- [26] N. B. Geddes, *Magic Motorways*. Read Books Ltd, 1940.
- [27] L. A. Pipes, “An operational analysis of traffic dynamics,” *Journal of applied physics*, vol. 24, no. 3, pp. 274–281, 1953.
- [28] W. S. Levine and M. Athans, “On the optimal error regulation of a string of moving vehicles,” *IEEE Transactions on Automatic Control*, vol. 11, no. 3, pp. 355–361, 1966.
- [29] K.-c. Chu, “Decentralized control of high-speed vehicular strings,” *Transportation science*, vol. 8, no. 4, pp. 361–384, 1974.
- [30] R. L. Cosgriff, “Dynamics of Automatic Longitudinal Control Systems for Automobiles,” *The Ohio State University, Report. EES-202A-8*, pp. 235–351, 1965.
- [31] S. E. Shladover, “PATH at 20—History and Major Milestones,” *IEEE Transactions on Intelligent Transportation Systems*, vol. 8, no. 4, pp. 584–592, Dec. 2007. DOI: 10.1109/TITS.2007.903052.
- [32] S. Tsugawa, S. Jeschke, and S. E. Shladover, “A Review of Truck Platooning Projects for Energy Savings,” *IEEE Transactions on Intelligent Vehicles*, vol. 1, no. 1, pp. 68–77, Mar. 2016. DOI: 10.1109/TIV.2016.2577499.

Bibliography

- [33] H. Fritz, “Longitudinal and lateral control of heavy duty trucks for automated vehicle following in mixed traffic: Experimental results from the CHAUFFEUR project,” in *Proceedings of the 1999 IEEE International Conference on Control Applications (Cat. No.99CH36328)*, vol. 2, Kohala Coast, HI, USA: IEEE, 1999, pp. 1348–1352. DOI: 10.1109/CCA.1999.801168.
- [34] (2019). Research project KONVOI, TRIMIS, [Online]. Available: <https://trimis.ec.europa.eu/project/konvoi>.
- [35] T. Robinson, E. Chan, and E. Coelingh, “Operating platoons on public motorways: An introduction to the sartre platooning programme,” in *17th World Congress on Intelligent Transport Systems*, vol. 1, 2010, p. 12.
- [36] S. Eilers, J. Maartensson, H. Pettersson, M. Pillado, D. Gallegos, M. Tobar, K. H. Johansson, X. Ma, T. Friedrichs, and S. S. Borojeni, “COMPANION—Towards Cooperative Platoon Management of Heavy-Duty Vehicles,” in *2015 IEEE 18th International Conference on Intelligent Transportation Systems*, IEEE, 2015, pp. 1267–1273.
- [37] W. Hucho and G. Sovran, “Aerodynamics of road vehicles,” *Annual review of fluid mechanics*, vol. 25, no. 1, pp. 485–537, 1993.
- [38] E. Hellström, M. Ivarsson, J. Åslund, and L. Nielsen, “Look-ahead control for heavy trucks to minimize trip time and fuel consumption,” *Control Engineering Practice*, vol. 17, no. 2, pp. 245–254, Feb. 1, 2009. DOI: 10.1016/j.conengprac.2008.07.005.
- [39] “Scania Annual Report 2014,” Södertälje, 2015.
- [40] A. Schirrer, A. Gratzler, S. Thormann, W. Schildorfer, M. Neubauer, and S. Jakubek, Eds., *Energy-Efficient and Semi- Automated Truck Platooning*. 2021.
- [41] “Recent international activity in cooperative vehicle–highway automation systems,” United States. Federal Highway Administration. Office of Corporate Research., 2012.
- [42] “Final report,” research project EDDI, Germany, 2019. [Online]. Available: https://www.deutschebahn.com/resource/blob/4136370/3227eac8b688106dc68e9292f4a173e9/Platooning_EDDI_Projektbericht_10052019_DE-data.pdf.
- [43] V. Turri, B. Besselink, and K. H. Johansson, “Cooperative Look-Ahead Control for Fuel-Efficient and Safe Heavy-Duty Vehicle Platooning,” *IEEE Transactions on Control Systems Technology*, vol. 25, no. 1, pp. 12–28, Jan. 2017. DOI: 10.1109/TCST.2016.2542044.

Bibliography

- [44] A. Sciarretta, G. D. Nunzio, and L. L. Ojeda, “Optimal Ecodriving Control: Energy-Efficient Driving of Road Vehicles as an Optimal Control Problem,” *IEEE Control Systems Magazine*, vol. 35, no. 5, pp. 71–90, Oct. 2015. DOI: 10.1109/MCS.2015.2449688.
- [45] D. Eckhoff, B. Halmos, and R. German, “Potentials and limitations of Green Light Optimal Speed Advisory systems,” in *2013 IEEE Vehicular Networking Conference*, Dec. 2013, pp. 103–110. DOI: 10.1109/VNC.2013.6737596.
- [46] B. Besselink, V. Turri, S. H. Hoef, K. Liang, A. Alam, J. Mårtensson, and K. H. Johansson, “Cyber-Physical Control of Road Freight Transport,” *Proceedings of the IEEE*, vol. 104, no. 5, pp. 1128–1141, May 2016. DOI: 10.1109/JPROC.2015.2511446.
- [47] S. Ezell, “Explaining international IT application leadership: Intelligent transportation systems,” 2010. [Online]. Available: <https://itif.org/publications/2010/01/09/explaining-international-it-application-leadership-intelligent>.
- [48] A. Alam, *Fuel-Efficient Heavy-Duty Vehicle Platooning*. Stockholm: Electrical Engineering, KTH Royal Institute of Technology, 2014. [Online]. Available: <http://urn.kb.se/resolve?urn=urn:nbn:se:kth:diva-145560>.
- [49] M. Alonso Raposo, B. Ciuffo, F. Ardente, J. P. Aurambout, G. Baldini, R. Braun, P. Christidis, A. Christodoulou, A. Duboz, and S. Felici, “The future of road transport,” Joint Research Centre (Seville site), 2019.
- [50] “White Paper on Transport: Roadmap to a Single European Transport Area: Towards a Competitive and Resource-Efficient Transport System,” Publications Office of the European Union, Luxembourg, 2011.
- [51] P. Varaiya, “Smart cars on smart roads: Problems of control,” *IEEE Transactions on automatic control*, vol. 38, no. 2, pp. 195–207, 1993.
- [52] “ETSI EN 302 571 V2.1.1: Intelligent Transport Systems (ITS); Radiocommunications equipment operating in the 5 855 MHz to 5 925 MHz frequency band; Harmonised Standard covering the essential requirements of article 3.2 of Directive 2014/53/EU,” ETSI, 2017. [Online]. Available: https://www.etsi.org/deliver/etsi_en/302500_302599/302571/02.01.01_60/en_302571v020101p.pdf.
- [53] A. Festag, “Standards for vehicular communication—from IEEE 802.11 p to 5G,” *e & i Elektrotechnik und Informationstechnik*, vol. 132, no. 7, pp. 409–416, 2015.

Bibliography

- [54] A. Froetscher and B. Monschiebl, “C-roads: Elements of c-its service evaluation to reach interoperability in europe within a wide stakeholder network: Validation steps and comparative elements used in a living lab environment in austria,” in *2018 IEEE 87th Vehicular Technology Conference (VTC Spring)*, IEEE, 2018, pp. 1–5.
- [55] “ECo-AT Release 4.0 System Specification, C-ITS for Automated Driving, Functional Specification,” ECo-AT, 2018. [Online]. Available: <http://www.eco-at.info>.
- [56] “Guidance for day 2 and beyond roadmap,” CAR 2 CAR Communication Consortium, 2019. [Online]. Available: https://www.car-2-car.org/fileadmin/documents/General_Documents/C2CCC_WP_2072_RoadmapDay2AndBeyond.pdf.
- [57] N. H. T. S. Administration, “Fatal Motor Vehicle Crashes: Overview,” US Department of Transportation, 2017.
- [58] “Chancen und Risiken des Einsatzes von Abstandshaltesystemen sowie des Platoonings von Strassenfahrzeugen - Machbarkeitsanalyse,” Bundesamt für Strassen (ASTRA), 2017. [Online]. Available: https://www.astra.admin.ch/dam/astra/de/dokumente/abteilung_strassennetzeallgemein/bericht_platooning.pdf.download.pdf/170811_ASTRA_Platooning_Bericht_V5.0.pdf.
- [59] (2019). Mercedes switches focus away from platooning trials, [Online]. Available: <https://www.commercialfleet.org/news/truck-news/2019/02/04/mercedes-switches-focus-away-from-platooning-trials>.
- [60] A. Kaku, M. A. S. Kamal, M. Mukai, and T. Kawabe, “Model Predictive Control for Ecological Vehicle Synchronized Driving Considering Varying Aerodynamic Drag and Road Shape Information,” *SICE JCMSI*, vol. 6, no. 5, pp. 299–308, 2013. DOI: 10.9746/jcmsi.6.299.
- [61] A. Alam, J. Mårtensson, and K. H. Johansson, “Look-ahead cruise control for heavy duty vehicle platooning,” in *16th International IEEE Conference on Intelligent Transportation Systems (ITSC 2013)*, Oct. 2013, pp. 928–935. DOI: 10.1109/ITSC.2013.6728351.
- [62] V. Turri, B. Besselink, and K. H. Johansson, “Gear management for fuel-efficient heavy-duty vehicle platooning,” in *2016 IEEE 55th Conference on Decision and Control (CDC)*, Dec. 2016, pp. 1687–1694. DOI: 10.1109/CDC.2016.7798508.
- [63] B. Bamieh, F. Paganini, and M. A. Dahleh, “Distributed control of spatially invariant systems,” *IEEE Transactions on Automatic Control*, vol. 47, no. 7, pp. 1091–1107, Jul. 2002. DOI: 10.1109/TAC.2002.800646.

Bibliography

- [64] M. Fardad, F. Lin, and M. R. Jovanović, “On the dual decomposition of linear quadratic optimal control problems for vehicular formations,” in *49th IEEE Conference on Decision and Control (CDC)*, Dec. 2010, pp. 6287–6292. DOI: 10.1109/CDC.2010.5717487.
- [65] Y. Zheng, S. E. Li, K. Li, F. Borrelli, and J. K. Hedrick, “Distributed Model Predictive Control for Heterogeneous Vehicle Platoons Under Unidirectional Topologies,” *IEEE Transactions on Control Systems Technology*, vol. 25, no. 3, pp. 899–910, May 2017. DOI: 10.1109/TCST.2016.2594588.
- [66] D. Groß and O. Stursberg, “Distributed predictive control of communicating and constrained systems,” *ZAMM - Journal of Applied Mathematics and Mechanics / Zeitschrift für Angewandte Mathematik und Mechanik*, vol. 94, no. 4, pp. 303–316, 2014. DOI: 10.1002/zamm.201100166.
- [67] M. Mazzola, G. Schaaf, A. Stamm, and T. Kürner, “Safety-Critical Driver Assistance Over LTE: Toward Centralized ACC,” *IEEE Transactions on Vehicular Technology*, vol. 65, no. 12, pp. 9471–9478, Dec. 2016. DOI: 10.1109/TVT.2016.2617320.
- [68] A. Doi, T. Butsuen, T. Niibe, T. Takagi, Y. Yamamoto, and H. Seni, “Development of a rear-end collision avoidance system with automatic brake control,” *JSAE Review*, vol. 15, no. 4, pp. 335–340, Oct. 1, 1994.
- [69] C. M. Filho, M. H. Terra, and D. F. Wolf, “Safe Optimization of Highway Traffic With Robust Model Predictive Control-Based Cooperative Adaptive Cruise Control,” *IEEE Transactions on Intelligent Transportation Systems*, vol. 18, no. 11, pp. 3193–3203, Nov. 2017. DOI: 10.1109/TITS.2017.2679098.
- [70] A. Alam, A. Gattami, K. H. Johansson, and C. J. Tomlin, “Guaranteeing safety for heavy duty vehicle platooning: Safe set computations and experimental evaluations,” *Control Engineering Practice*, vol. 24, pp. 33–41, Mar. 2014. DOI: 10.1016/j.conengprac.2013.11.003.
- [71] S. Sadraddini, S. Sivaranjani, V. Gupta, and C. Belta, “Provably Safe Cruise Control of Vehicular Platoons,” *IEEE Control Systems Letters*, vol. 1, no. 2, pp. 262–267, Oct. 2017. DOI: 10.1109/LCSYS.2017.2713772.
- [72] J. Löfberg, *Minimax Approaches to Robust Model Predictive Control*. Linköping University Electronic Press, Apr. 11, 2003, 212 pp.

Bibliography

- [73] D. Groß and O. Stursberg, “Robust Distributed Predictive Control of Communicating and Constrained Systems,” *IFAC Proceedings Volumes*, 18th IFAC World Congress, vol. 44, no. 1, pp. 8926–8932, Jan. 1, 2011. DOI: 10.3182/20110828-6-IT-1002.03119.
- [74] V. S. Dolk, J. Ploeg, and W. P. M. H. Heemels, “Event-Triggered Control for String-Stable Vehicle Platooning,” *IEEE Trans. Intell. Transport. Syst.*, vol. 18, no. 12, pp. 3486–3500, Dec. 2017. DOI: 10.1109/TITS.2017.2738446.
- [75] R. Kianfar, P. Falcone, and J. Fredriksson, “A receding horizon approach to string stable cooperative adaptive cruise control,” in *2011 14th International IEEE Conference on Intelligent Transportation Systems (ITSC)*, Oct. 2011, pp. 734–739. DOI: 10.1109/ITSC.2011.6083088.
- [76] S. Magdici and M. Althoff, “Adaptive Cruise Control with Safety Guarantees for Autonomous Vehicles,” *IFAC-PapersOnLine*, vol. 50, no. 1, pp. 5774–5781, Jul. 2017. DOI: 10.1016/j.ifacol.2017.08.418.
- [77] W. B. Dunbar and D. S. Caveney, “Distributed Receding Horizon Control of Vehicle Platoons: Stability and String Stability,” *IEEE Transactions on Automatic Control*, vol. 57, no. 3, pp. 620–633, Mar. 2012. DOI: 10.1109/TAC.2011.2159651.
- [78] “Connecting Austria Project Folder,” research project Connecting Austria, 2019. [Online]. Available: https://assets.ctfassets.net/nzirp6tnjpw/24ryFtmwHGEiKYg0A8uoCs/aff53d411a4f16f8b0a1b7e7f1778a2b/english_folder_connecting-austria.pdf.
- [79] A. Schirrer, T. Haniš, M. Klaučo, S. Thormann, M. Hromčík, and S. M. Jakubek, “Safety-extended Explicit MPC for Autonomous Truck Platooning on Varying Road Conditions,” *IFAC World Congress 2020*, 2020.
- [80] C. Kalteis, S. Thormann, A. Schirrer, and S. Jakubek, “Efficient Methods to Assess Linear and Non-Linear Automotive Platoon Control Stability and Performance,” *XI International Conference on Structural Dynamics*, 2020.
- [81] L. Xiao and F. Gao, “Practical String Stability of Platoon of Adaptive Cruise Control Vehicles,” *IEEE Transactions on Intelligent Transportation Systems*, vol. 12, no. 4, pp. 1184–1194, Dec. 2011. DOI: 10.1109/TITS.2011.2143407.
- [82] F. L. Lewis, D. Vrabie, and V. L. Syrmos, *Optimal Control*. John Wiley & Sons, Mar. 20, 2012, 552 pp.
- [83] F. Berkel and S. Liu, “An event-triggered cooperation approach for robust distributed model predictive control,” *IFAC Journal of Systems and Control*, vol. 6, pp. 16–24, Dec. 30, 2018. DOI: 10.1016/j.ifacsc.2018.10.002.

Bibliography

- [84] *Matlab*, version 2018b, The MathWorks, Inc., 2018. [Online]. Available: www.mathworks.com.
- [85] (2017). Truck Platoon Crossing an Intersection [Digital Artwork]. Swarco Futurit Verkehrssignalsysteme GmbH, [Online]. Available: https://web.archive.org/web/20180813023156if_/http://www.connecting-austria.at/#/use-cases/traffic.
- [86] (2017). Truck Platoon Approaching a Hazardous Location [Digital Artwork]. Swarco Futurit Verkehrssignalsysteme GmbH, [Online]. Available: https://web.archive.org/web/20180813023156if_/http://www.connecting-austria.at/#/use-cases/danger.
- [87] *IPG Truckmaker*, version 7.03, IPG Automotive GmbH, 2018. [Online]. Available: <https://ipg-automotive.com/>.
- [88] C. Gomes, C. Thule, D. Broman, P. G. Larsen, and H. Vangheluwe, “Co-simulation: A survey,” *ACM Computing Surveys (CSUR)*, vol. 51, no. 3, pp. 1–33, 2018.
- [89] *Gurobi Optimizer*, version 8.1, Gurobi Optimization, LLC, 2018. [Online]. Available: www.gurobi.com.
- [90] (2020). Thrustmaster T300 RS [Photo]. Guillemot Corporation, [Online]. Available: http://www.thrustmaster.com/de_DE/produkte/t300rs.
- [91] *Simulink*, version 2018b, The MathWorks, Inc., 2018. [Online]. Available: www.mathworks.com.
- [92] J. Löfberg, “YALMIP: A toolbox for modeling and optimization in MATLAB,” in *Proceedings of the CACSD Conference*, vol. 3, Taipei, Taiwan, 2004.
- [93] L. Torvalds and J. Hamano, *Git: Fast version control system*, 2010.
- [94] J. Löfberg, *Yalmip*, version R20200116, 2020. [Online]. Available: <https://yalmip.github.io/>.

A Implementation Details

In this section, selected implementation details and important development notes are given. The version control system Git [93] is used to ensure reproducible software development. An overview on the directory structure of the software repository is shown below. Selected executable Matlab [84] scripts are located in the folder `010_base/_run` to allow for a quick start.

```
root
├── 000_tools
│   └── start_matlab.bat
├── 010_base
│   ├── _run
│   ├── DangerSpot
│   ├── SafeMPC
│   ├── TrafficLightTransit
│   └── TruckmakerPlatoonSimulation
├── 020_dev
├── 040_publications
│   └── master_thesis_thormann
```

Important notes on working with the software repository

Use the batch script `start_matlab.bat` in the tools folder to start the Matlab session to ensure:

1. The Matlab working directory should always be set to be the root path of the repository.
2. It is expected that the directory `010_base` and its subfolders are on the Matlab path.

When working on development code outside of `010_base` (i.e., in `020_dev`), add necessary folders to the Matlab path.

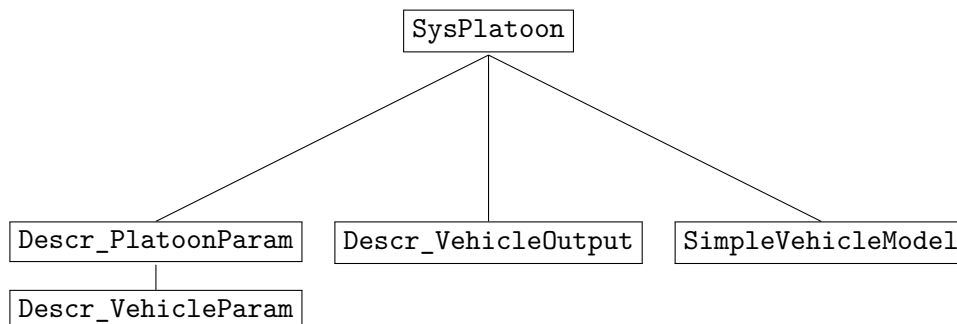


Figure A.1: Class architecture of the Matlab class `SysPlatoon`.

TruckmakerPlatoonSimulation

- The current software and hardware requirements are:
 - Matlab 2018b (including the toolbox Simulink 3D Animation)
 - IPG Truckmaker 7.0.3
 - Thrustmaster T300 RS force-feedback steering wheel (optional)
- The class architecture of the main class `SysPlatoon` is illustrated in Figure A.1.
 - The class `Descr_PlatoonParam` describes parameters of the platooning co-simulation which are not relevant to individual vehicles. Selected parameters are given in Table A.1.

Table A.1: Selected properties of the `Descr_PlatoonParam` class.

<code>n_veh</code>	Number of vehicles.
<code>Ts</code>	Sampling time, in seconds.
<code>id_ego_veh</code>	Index of vehicle which
<code>do_use_thrustmaster</code>	Enable ThrustMaster steering wheel for manual driving of the ego vehicle, if true.
<code>veh</code>	Individual vehicle parameters, see Table A.2.
<code>filename_road</code>	Road definition file (.rd5 format).

- The class `Descr_VehicleParam` describes parameters of the platooning co-simulation relevant to individual vehicles. Selected parameters are given in Table A.2.
- The class `Descr_VehicleOutput` describes the output signals which are returned in the property `output` of `SysPlatoon` when the method `endstep` is called.

Table A.2: Selected properties of the `Descr_VehicleParam` class.

<code>do_bypass_simulation</code>	Use simple linear model to bypass the TruckMaker simulation, if true
<code>bypass_tau</code>	PT1 time constant for simple bypass model, in seconds
<code>bypass_nd</code>	Dead time for simple bypass model, in samples
<code>do_display_vehicle</code>	Use IPGMovie for visualization, if true
<code>user_defined_signals</code>	Struct which defines user-defined outputs read from Truckmaker
<code>pos_0</code>	Initial position vector

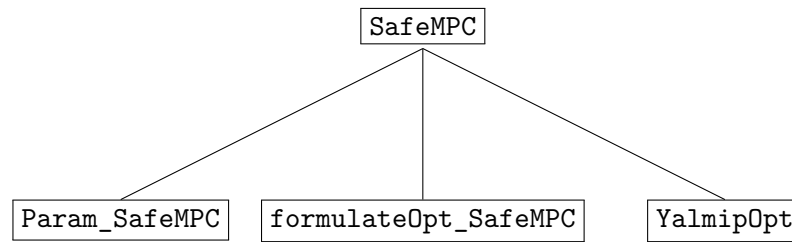


Figure A.2: Class architecture of the Matlab class `SafeMPC`.

- The class `SimpleVehicleModel` implements linear vehicle dynamics which are evaluated if the simulation of a vehicle via Truckmaker is bypassed.
- Exemplary Matlab code for the initialization of an object of the class `SysPlatoon` is given below.

```

n_veh = 3;
platoon = SysPlatoon(n_veh);
p = platoon.param;
p.Ts = 0.1;
p.id_ego_veh = 1;
p.do_use_thrustmaster = false;
p.filename_road = 'straight_road.rd5';
p.veh(1).pos_0 = 100;
p.veh(2).pos_0 = 50;
p.veh(3).pos_0 = 0;
p = platoon.init(p);
    
```

SafeMPC

- The class architecture of the main class `SafeMPC` is illustrated in Figure A.2.

A Implementation Details

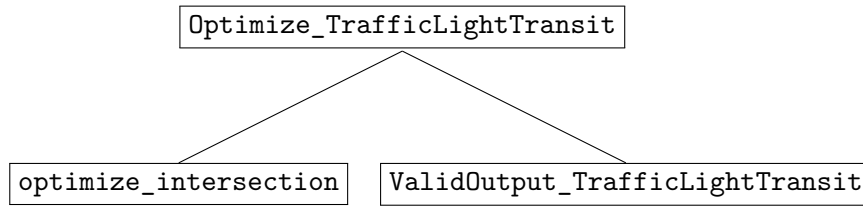


Figure A.3: Class architecture of the Matlab class `Optimize_TrafficLightTransit`.

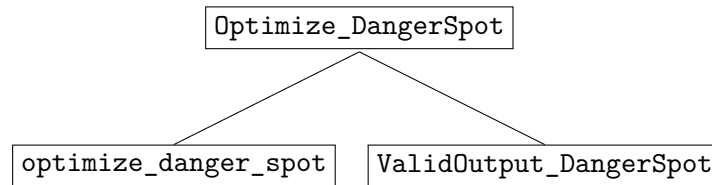


Figure A.4: Class architecture of the Matlab class `Optimize_DangerSpot`.

- The class `Param_SafeMPC` describes parameters of the safety-extended optimization problem (2.26). See Table 3.1 for an overview of these parameters.
- The function `formulateOpt_SafeMPC` formulates the safety-extended optimization problem (2.26) by Yalmip [94] and the class `YalmipOpt`.
- The class `YalmipOpt` manages the formulation of optimization problems with Yalmip.

TrafficLightTransit

- The class architecture of the main class `Optimize_TrafficLightTransit` is illustrated in Figure A.2. This class defines and validates the input parameters of the regarding trajectory optimization. See Table A.3 for an overview of its parameters.
 - The function `optimize_intersection` constructs and solves the optimization problem regarding the *TrafficLightTransit* use case formulated in Section 2.2.
 - The class `ValidOutput_TrafficLightTransit` describes valid outputs of the trajectory optimization.

DangerSpot

- The class architecture of the main class `Optimize_DangerSpot` is illustrated in Figure A.4. This class defines and validates the input parameters of the regarding trajectory optimization. See Table A.4 for an overview of its parameters.

Table A.3: Input Parameters for the trajectory planning tool for the *TrafficLightTransit* use case.

Symbol	Description	Input parameter
	Version of the input data	<code>this_version</code>
n	Number of platooning vehicles	<code>n_veh</code>
$L^{(i)}$	Lengths of vehicles	<code>L_veh</code> (vector)
$p_0^{(i)}$	Initial position of platooning vehicles	<code>x0</code> (vector)
$v_0^{(i)}$	Initial velocity of platooning vehicles	<code>v0</code> (vector)
$d_{\min}^{(i)}$	Minimal inter-vehicle distances	<code>d_min</code> (vector)
$\Delta t_{\min}^{(i)}$	Minimal time gaps	<code>t_min</code> (vector)
$a_{\max}^{(i)}$	Maximal accelerations	<code>amax</code> (lookup table)
$a_{\min}^{(i)}$	Minimal accelerations	<code>amin</code> (lookup table)
p_{stop}	Position of the stopping line	<code>x_signal</code>
t_{green}	Time when switch to green occurs	<code>t_signal_green_start</code>
t_{red}	Time when switch to red occurs	<code>t_signal_green_end</code>
t_0	Initial time	<code>t0</code>
t_N	Planning horizon	<code>t_end</code>
T_S	Sampling time	<code>t_sampling</code>
w_t, w_u	Cost function weighting	<code>obj</code> (struct)
v_{\min}, v_{\max}	Speed limits	<code>bnds</code> (struct)
$p_k^{(0)}$	Optionally, trajectory of a preceding vehicle	<code>front_vehicle</code> (struct)
	Plots results, if true	<code>do_show_plots</code>

A Implementation Details

Table A.4: Input Parameters for the trajectory planning tool for the *DangerSpot* use case.

Symbol	Description	Input parameter
	Version of the input data (decimal number)	<code>this_version</code>
n	Number of platooning vehicles	<code>n_veh</code>
$L^{(i)}$	Lengths of vehicles (vector)	<code>L_veh</code>
$p_0^{(i)}$	Initial position of platooning vehicles (vector)	<code>x0</code>
$v_0^{(i)}$	Initial velocity of platooning vehicles (vector)	<code>v0</code>
$d_{\min}^{(i)}$	Minimal inter-vehicle distances (vector)	<code>d_min</code>
$\Delta t_{\min}^{(i)}$	Minimal time gaps (vector)	<code>t_min</code>
$a_{\max}^{(i)}$	Maximal accelerations (lookup table)	<code>amax</code>
$a_{\min}^{(i)}$	Minimal accelerations (lookup table)	<code>amin</code>
v_{\min}, v_{\max}	Speed limits (struct)	<code>bnds</code>
p_{danger}	Danger spot absolute position	<code>x_danger</code>
v_{man}	Desired velocity in handover period	<code>v_man</code>
T_{man}	Duration of handover period	<code>delta_t_man</code>
Δt_{man}	Minimal time gap within platoon during handover period	<code>t_min_man</code>
$d_{\text{man}}^{(i)}$	Desired spatial distance in handover period	<code>d_man</code>
t_0	Initial time	<code>t0</code>
t_N	Planning horizon	<code>t_end</code>
T_S	Sampling time	<code>t_sampling</code>
w_v, w_d, w_u	Cost function weightings	<code>obj</code>
$v_{\text{scale}}, d_{\text{scale}}, u_{\text{scale}}$	and cost function scales (struct)	
	Time tolerance for reaching the tracking goals: <code>tol_track_v, tol_track_v</code>	<code>delta_t_error_limit</code>
	Velocity tracking tolerance	<code>tol_track_v</code>
	Distance tracking tolerance	<code>tol_track_d</code>
	Plots results, if true	<code>do_show_plots</code>

A Implementation Details

- The function `optimize_danger_spot` constructs and solves the optimization problem regarding the *DangerSpot* use case formulated in Section 2.2.
- The class `ValidOutput_DangerSpot` describes valid outputs of the trajectory optimization.